Collinsville: Sediment Dispersion Modeling Report

PREPARED FOR

LS Power Grid California, LLC

DATE

14/11/2024

REFERENCE

0712968

DOCUMENT DETAILS

The details entered below are automatically shown on the cover and the main page footer. PLEASE NOTE: This table must NOT be removed from this document.	
DOCUMENT TITLE	Collinsville: Sediment Dispersion Modeling Report
DOCUMENT SUBTITLE	
PROJECT NUMBER	0712968
Date	14/11/2024
Version	Draft
Authors	Brooke Frazier, Audrey Bourne, Tayebeh Tajalli Bakhsh, Venkat Kolluru
Client name	LS Power Grid California, LLC

DOCUMENT HISTORY

				ERM APPROVAL TO ISSUE		
VERSION	REVISION	AUTHOR	REVIEWED BY	NAME	DATE	COMMENTS
Draft Version 1.0	0	Brooke Frazier, Audrey Bourne, Tayebeh Tajalli Bakhsh, Venkat Kolluru	Venkat Kolluru, Tayebeh Tajalli Baksh	Michele Barlow	25/03/2024	Task 2 (cable trenching)
Draft Version 2.0	0	Brooke Frazier, Audrey Bourne, Tayebeh Tajalli Bakhsh, Venkat Kolluru	VK, TT, MB	MB	31/10/2024	Task 4 add on
Draft Version 2.1	1	BF, VK	TT, VK		13/11/2024	Edits on the results presentations
Draft Version 2.2	2	BF			14/11/2024	Addressing comments

SIGNATURE PAGE

Collinsville: Sediment Dispersion Modeling Report

0712968

Michele Barlow
Partner in Charge

Venkat Kolluru, PhD
Technical Consulting Director, Engineering

Tayebeh Tajalli Bakhsh, PhD
Principal Consultant, Project Manager

Environmental Resources Management (ERM)
1340 Treat Boulevard
Suite 550
Walnut Creek, CA 94597
T +1 650 704 9378

CONTENTS

LIST OF TABLES

LIST OF FIGURES

ACRONYMS AND ABBREVIATIONS

Acronyms	Description
2-D	two-dimensional
3-D	three-dimensional
µm	micrometer
DEM	Digital elevation model
ERM	Environmental Resources Management, Inc.
ft	feet
FVCOM	Finite Volume Coastal Ocean Model
GEBCO	General Bathymetric Chart of the Oceans
GEMSS®	Generalized Environmental Modelling System for Surface waters
GIFT	Generalized Integrated Fate and Transport Module
IFC	International Finance Corporation
kg/m³	kilogram per cubic meter
km	kilometer
kV	kilovolt
m	meter
m²	square meter
m³	cubic meter
m/hr	meter per hour
m³/hr	cubic meter per hour
mm	millimeter
mg/L	milligram per liter
m/s	meter per second

Acronyms	Description
N/A	Not Applicable
NAVD 88	North American Vertical Datum of 1988
NOAA	National Oceanic and Atmospheric Administration
PPT	parts per thousand
SF Bay	San Francisco Bay
SFBOFS	San Francisco Bay Operational Forecast System
tons/hr	tons per hour
TSS	total suspended solids
USGS	United States Geological Survey
UTM	Universal Transverse Mercator

EXECUTIVE SUMMARY

LS Power Grid California, LLC (LS Power) proposes to install a submarine power cable crossing the Sacramento River near its confluence with the San Francisco Bay (SF Bay), California. The Submarine Cable layout is part of an approximate 8.4 kilometers (5.2 miles) double circuit 230 kilovolt (kV) transmission line that passes through Solano, Sacramento, and Contra Costa counties which will be linked with a new 500/230 kV substation in Solano County. The proposed Submarine Cable route will be approximately 6.9 kilometers (4.3 miles) in length and travel from Collinsville to Old Town Pittsburg. LS Power intends to install the land to water cable transitions using a clamshell bucket for excavation and backfilling associated with cable burial at the northern transition area. At the southern transition area, the excavation and backfilling will be completed using a long reach excavator. Additionally, a jet sled that is designed to simultaneously lay and bury the cable through a one-pass process is intended to be used for cable installation across the river.

Fourteen scenarios were selected to simulate the disturbed and resuspended sediment behavior due to the above activities during two extreme hydrodynamic conditions in Suisun Bay (minimum and maximum ambient current conditions). They included the following operations:

- Cable installation across the Sacramento River using a jet sled (two scenarios);
- Excavation associated with cable burial at the northern site location using an in-river transition approach in regions R1 and R2 (four scenarios);
- Backfilling associated with cable burial at the northern site location using an in-river transition approach in regions R1 and R2 (four scenarios);
- Excavation associated with cable burial at the southern site location using an open trenching approach (two scenarios); and
- Backfilling associated with cable burial at the southern site location using an open trenching approach (two scenarios).

Comprehensive modeling was performed to predict total suspended solids (TSS) concentrations in the water column across all scenarios. Depositional thickness assessments focused specifically on the cable burial and the R2 northern site location scenarios, where excavation and backfilling operations could impact sediment distributions. For other scenarios, during the excavation and backfilling operations at the northern R1 and southern site locations, sheet piles or silt curtains effectively contained dispersed sediments within enclosed areas. This sediment containment management strategy ensured that the dispersed sediment settled within the designated areas, preventing any increase in TSS levels or bed deposition in the other regions of Suisun Bay.

Sediment dispersion modeling of excavating, backfilling, and trenching activities for cable installation simulated:

- the resuspension of approximately 71 cubic meters (m^3) of sediment volume due to excavation and 1784 m^3 of sediment volume during backfilling at the northern transition area over nearly 1.5 days;

- 15 m^3 of sediment volume due to excavation and 367 m^3 of sediment volume during backfilling at the southern transition area over nearly 1.3 days; and
- 9987 m^3 of sediment volume with one pass of trenching over 1 day for cable installation across the river.

Across all scenarios, TSS concentrations peaked near the bed during the initial stages of each operation, and returned to zero or below 10 mg/L within 20 to 30 hours post-operation. This rapid decline demonstrates the effectiveness of LS Power's sediment management strategy, which successfully minimizes TSS levels around the project footprint in Suisun Bay, ensuring minimal impact on surrounding water quality.

The maximum depositional thickness during cable burial was minimal, measuring less than 0.1 mm. For excavation and backfilling operations, depositional thickness is not a concern in most scenarios, as the majority of sediment remains effectively contained within the sediment control measures. However, in the R2 scenarios (i.e., excavation and backfilling at the in-river transition structure), some sediment has dispersed through the southern open boundary, resulting in a minor deposition outside the designated semi-enclosed sheet pile containment area.

1. INTRODUCTION

LS Power Grid California, LLC (LS Power) proposes to install a submarine power cable crossing the Sacramento River near its confluence with the San Francisco Bay (SF Bay), California. The Submarine Cable layout is part of an approximate 8.4 kilometers (5.2 miles) double circuit 230 kV transmission line that passes through Solano, Sacramento, and Contra Costa counties which will be linked with a new 500/230 kV substation in Solano County. The proposed Submarine Cable route will be approximately 6.9 kilometers (4.3 miles) in length and travel from Collinsville to Old Town Pittsburg, as shown in Figure 1-1. The excavating and backfilling associated with cable burial at the northern site location will use an in-river transition approach (Figure 1-2) and the southern site location will use an open trenching approach (Figure 1-3).

FIGURE 1-1: SUBMARINE CABLE ROUTE

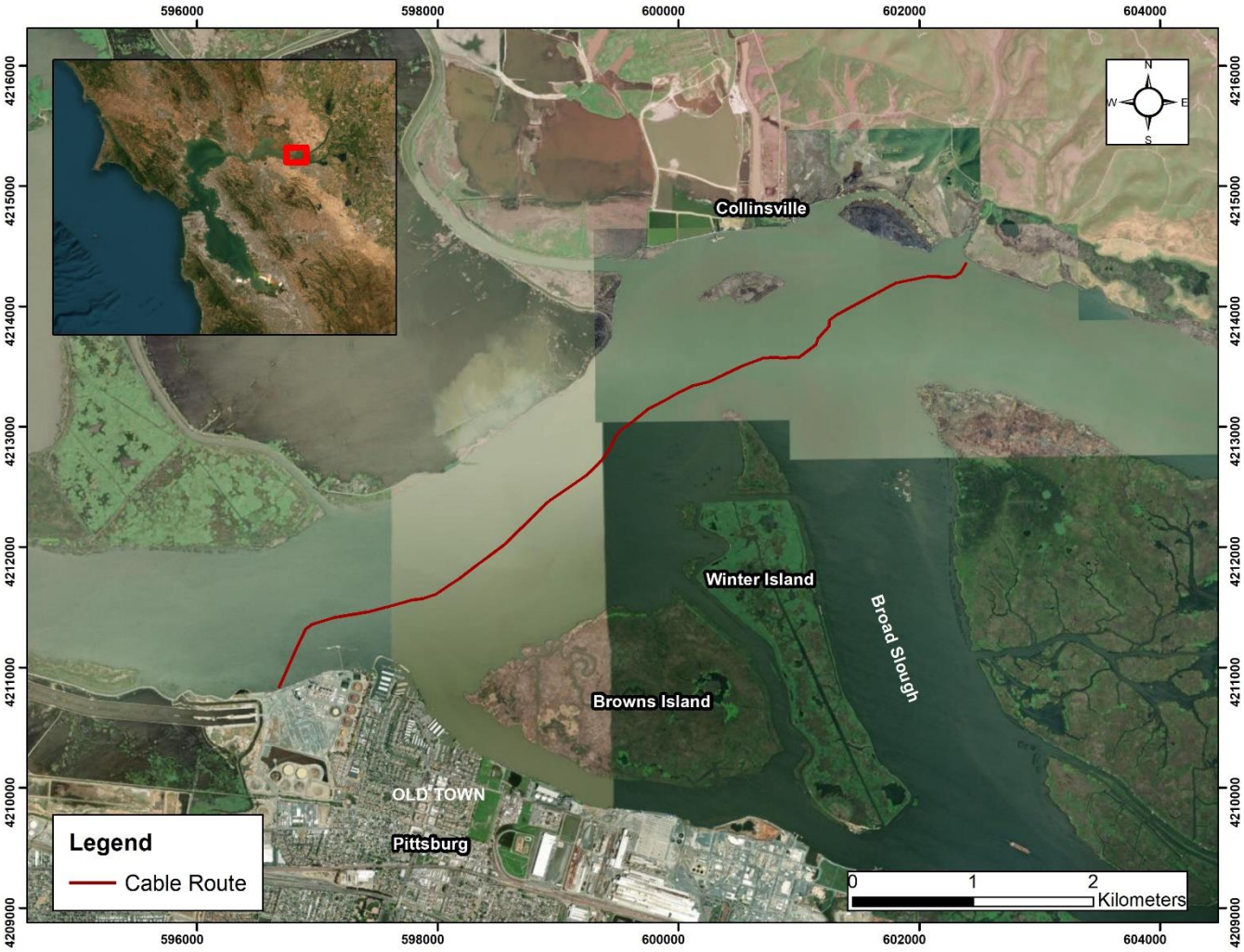

FIGURE 1-2: NORTHERN SITE LOCATION

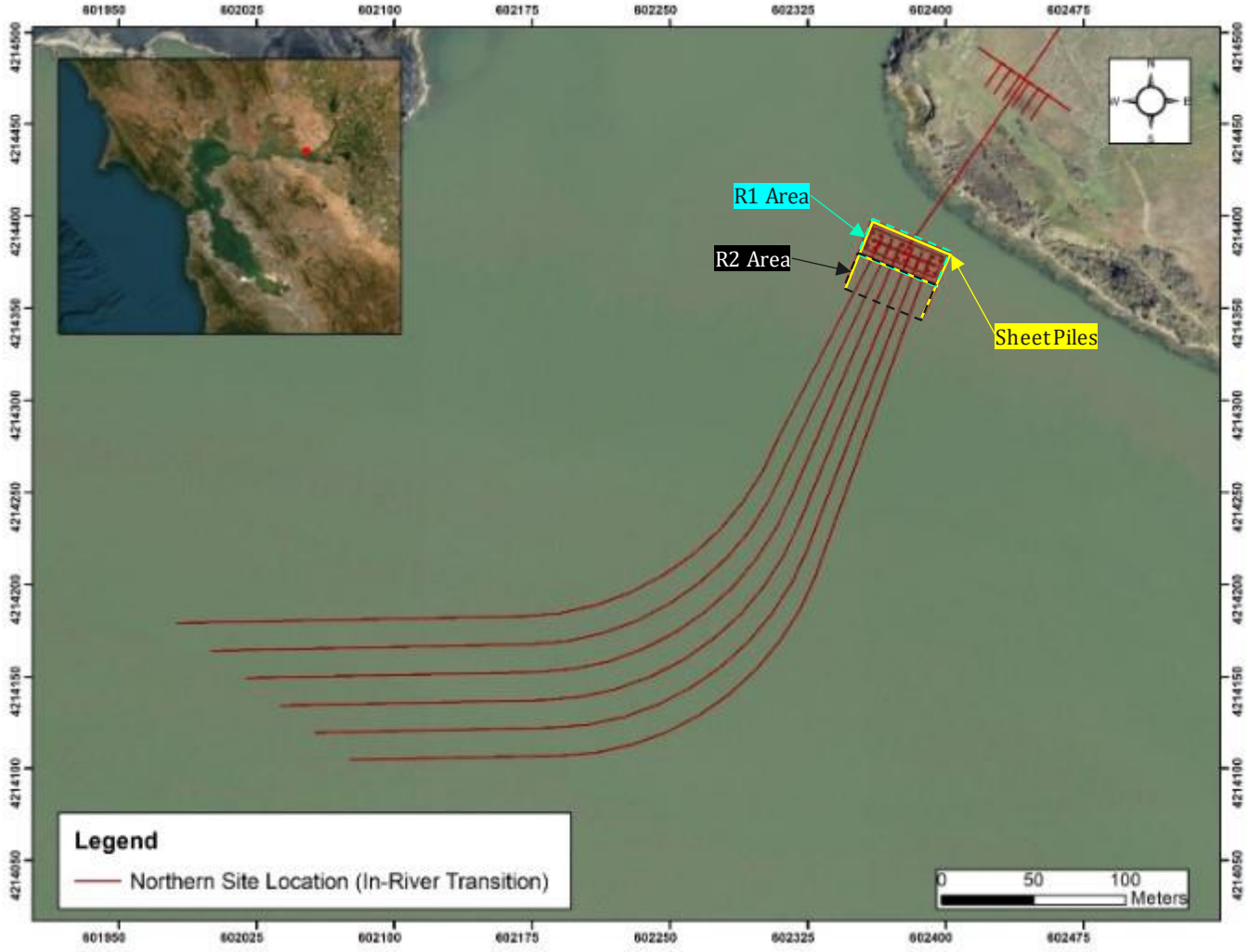

Source: LS Power, 2024

FIGURE 1-3: SOUTHERN SITE LOCATION

Source: LS Power, 2024

To proactively manage environmental impacts from sediment disturbance during excavation, backfilling, trenching, and installation activities, thorough assessments are essential. Recognizing this need, LS Power engaged ERM to conduct sediment dispersion modeling, predicting sediment plume spread in the water column and assessing related TSS levels and bed deposition. This modeling will support LS Power's comprehensive evaluation of potential impacts on water quality and the benthic environment, ensuring that the planned submarine cable installation methods are properly managed with appropriate mitigation measures if warranted.

Modeling was performed to predict the following:

- TSS concentrations in the water column, and
- Riverbed accumulation (depositional thickness) of the resuspended particles on the riverbed.

This report outlines the modeling methodology and presents the results of the modeling effort in comparison with existing regulations. Table 1-1 describes the modeling scenarios, locations, activities, and hydrodynamic conditions considered for this study.

TABLE 1-1: SUMMARY OF MODELING SCENARIOS

Scenario Number	Site	Activity	Simulation Duration	Hydrodynamic Conditions
1	Across the river (jet sled)	Cable installation across the Sacramento River	1 day	Minimum
2				Maximum
3	Northern site location (in-river transition)	Sheet piles installation and confined excavation (2026) in region R1 to install J-Tubes	3 days	Minimum
4				Maximum
5		Backfilling region R1 after installation of J-Tubes	3 days	Minimum
6				Maximum
7		Removal of southern sheet piles in the front of the J-Tubes (region R1) and excavation (2027) in region R2 to thread cables through the J-Tubes	3 days	Minimum
8				Maximum
9		Backfilling region R2 after installation of cables and removal of all sheet piles	3 days	Minimum
10				Maximum
11	Southern site location (open trenching)	Excavation	3 days	Minimum
12				Maximum
13		Backfill	3 days	Minimum
14				Maximum

2. INSTALLATION PROCESS

LS Power provided details of the installation method for all cables, as well as a proposed schedule and timeframe for the installation process.

2.1 NORTHERN SITE LOCATION IN-RIVER TRANSITION

Excavation and backfilling associated with cable burial at the northern site location is intended to be an in-river transition, which will consist of sheet piling (installation and removal), excavation, and backfilling in two regions (R1 and R2, Figure 1-2). Installation of sheet piles and confined excavation to install J-Tubes, followed by backfilling, is intended to occur in region R1 during the year 2026. Removal of the southern sheet piles in the front of the J-Tubes in region R1 and excavation to thread the cables through the J-Tubes, followed by backfilling, is intended to occur in region R2 during the year 2027. Sheet pile walls are developed using interlocking thin piles,

usually made of steel, which serve as temporary or in some cases permanent, retaining walls. They can also act as a containment curtain for the construction site (Steel Piling Group 2018). A clamshell bucket will be used for excavation and backfilling activities in both regions R1 and R2. Table 2-1 presents the excavation process characteristics, which were held consistent across the two regions. For both regions R1 and R2, it was assumed that the volume for backfilling is equal to the excavated volume.

TABLE 2-1: IN-RIVER TRANSITION DIMENSIONS AND DETAILS

Parameter	Value	Source
Excavation Depth, m	2.13	LS Power
Excavation Length, m	45.7	LS Power
Excavation Width, m	18.3	LS Power
Excavated Volume[a], m^3	1,783.7	Calculated by ERM
Excavation Rate, m/hr	0.763	Calculated by ERM
Volumetric Excavation Rate, m^3/hr	3.06	Calculated by ERM

Note: m = meter; m/hr = meter per hour; m^3/hr = cubic meter per hour.
[a] Volume calculated using unrounded and precise values

Based on LS Power input, the sheet piles installation and confined excavation in region R1 for J-Tube installations would take place from July to November, during 12 hours a day operation. Thus, the entire installation process would take around one and a half days (35.3 hours) to complete based on the trenching rate, operational schedule, and area of excavation. After the installation of J-Tubes in region R1, backfilling will also take place between July and November during 12 hours a day operation, with the entire installation process taking around an additional one and a half days (35.33 hours) to complete.

2.2 SOUTHERN SITE LOCATION OPEN TRENCHING

The installation in the southern area will leverage open trenching, using a Cat® 340 LRE (long reach excavator) or similar from the shoreline. Open trenching at the southern end for all four cables will be conducted within a silt curtain. For each of the four cables, an individual trench will be dredged, resulting in a total of four trenches for the entire southern site operations. The silt curtains are vertical, flexible structures that extend downward from the water surface to a specified water depth and have traditionally been defined as impermeable devices for control of suspended solids and turbidity in the water column generated by dredging and dredged material disposal operations (Francingues and Palmero 2005). For the present proposed operation, the silt curtains will be laid out such that they touch the bottom of the sediment bed. It is assumed that there will not be any leakage of sediments from the bottom of the silt curtains. Table 2-2 presents the excavation process characteristics. The excavation length and width are for one individual trench and the volume presented is for the total amount of sediment to be removed from all four trenches.

TABLE 2-2: OPEN TRENCHING DIMENSIONS AND DETAILS

Parameter	Value	Source
Excavation Depth, m	1.83	LS Power
Excavation Length for One Trench, m	9.14	LS Power
Excavation Width for One Trench, m	5.48	LS Power
Total Excavated Volume[a], m^3	366.99	Calculated by ERM
Excavation Rate, m/hr	0.191	Calculated by ERM
Volumetric Excavation Rate, m^3/hr	0.765	Calculated by ERM

Note: m = meter; m/hr = meter per hour; m^3/hr = cubic meter per hour.
[a] Volume calculated using unrounded and precise values.

For the proposed schedule at the southern end, LS Power indicated that the installation of the cables would take place from July to November during 12 hours a day operation. Thus, the entire installation process would take around one day and 7.2 hours (31.2 hours) to complete based on the installation rate, operational schedule, and area of excavation.

2.3 ENTIRE CABLE ROUTE

The method of installation across the Sacramento River was decided to be a jet sled, which is designed to simultaneously lay and bury the cable through a one-pass process. The jet sled works in soft materials such as sand, silt, and soft clay. Table 2-3 below presents the trenching volume, speed, and other installation process characteristics.

TABLE 2-3: JET SLED/TRENCH DIMENSIONS AND DETAILS

Parameter	Value	Source
Trench Width, m	0.326	Kokosing 2023
Trench Depth, m	4.6	LS Power
Trenching Rate, m/hr	300	LS Power
Volumetric Trenching Rate, m^3/hr	445.8	Calculated by ERM

Note: m = meter; m/hr = meter per hour; m^3/hr = cubic meter per hour.

For the proposed schedule, LS Power indicated that the installation of the cable would take place from June to December during 24 hours a day operation. This indicated the entire installation process would take around one day (24 hours) to complete based on the installation rate, operational schedule, and estimated cable route length.

3. SEDIMENT DEPOSITION MODELING

3.1 MODELING SOFTWARE

The behavior (advection, dispersion, and deposition) of disturbed and resuspended sediments was quantified using three-dimensional (3-D) hydrodynamic computer modeling techniques. Modeling was performed using GEMSS® (Generalized Environmental Modelling System for Surface waters) and its particle deposition module, GIFT (Generalized Integrated Fate and Transport). GIFT is a 3-D particle-based model that uses Lagrangian algorithms in conjunction with currents, specified mass load rates, release times and locations, particle sizes, settling velocities, and shear stress values (see Appendix A for details).

Disturbed and resuspended sediment will vertically descend through the water column (settle) due to its higher density compared with ambient water. However, this settling process can be slow if sediment particles are small and their settling velocities are low. Disturbed and resuspended sediment will also migrate horizontally due to advection by local and regional currents. The dispersion of sediment is fundamentally a 3-D phenomenon requiring 3-D hydrodynamic fate and transport modeling. Scenario selection and simulation design, modeling grids, and environmental data used in the 3-D hydrodynamic computer modeling techniques are discussed in this section. For more details on modeling software, see Appendix A.

Information required for this modeling included:

- Excavation and Backfilling Data
    - Areas of excavation
    - Excavation/backfilling methods and equipment
    - Proposed schedule
    - Number of hours per day for excavation/backfilling
    - Rate of excavation and backfilling
- Trenching Data
    - Cable route
    - Trenching methods and equipment
    - Proposed schedule
    - Number of hours per day for excavation
    - Rate of trenching
- Sediment Data
    - Sediment density along the route
    - Sediment properties (grain size distribution)
- Hydrodynamic and Geophysical Data
    - Current speed and direction

- Bathymetry
- Water properties (salinity and temperature)

3.2 ENVIRONMENTAL DATA

Model inputs were assembled and formatted for use with the GIFT model. The environmental data used by the model included sediment properties, bathymetry, currents, water temperature, and salinity data. LS Power was able to provide the results of a geotechnical survey completed for the project location (LS Power Grid California, LLC 2022). The results included sediment properties at six locations in the area of the project. Spatially and temporally varying currents, water temperature, and salinity data were used to characterize the area in which the discharges will occur and to determine appropriate simulation periods to represent the range of potential results.

3.2.1 SEDIMENT CHARACTERISTICS

LS Power provided grain size properties at six sediment core locations along the cable route (Figure 3-1). This included information about the cores including wet and dry densities, as well as the grain size properties. Based on the data provided by LS Power (LS Power Grid California, LLC 2022), ERM represented displaced sediment particles during the installation of the submarine power cable across the river, by defining six different grain size classes (Table 3-1). These particle sizes were determined by using the provided sieve analysis to determine the percent of sediment passing each sieve (Figure 3-2). This allowed for percentages of the core to be assigned specific size ranges. From the ranges, the midpoint was determined for each sieve and was used for the particle size distribution setup. Densities for each material type were derived from general densities. For each of the releases, the specific densities were set to be the individual core densities. The settling velocities for the various materials' particle sizes were computed by the model.

ERM represented displaced sediment particles during excavation and backfilling activities at the northern and southern site locations by defining six different grain size classes (Table 3-1) using the same process as described above on core data from the closest sediment core location to the areas. Sediment core locations V-9 and V-2 (Figure 3-1) were the closest core data for the northern and southern site locations, respectively.

FIGURE 3-1: SEDIMENT CORE LOCATIONS, AND SOIL TYPE

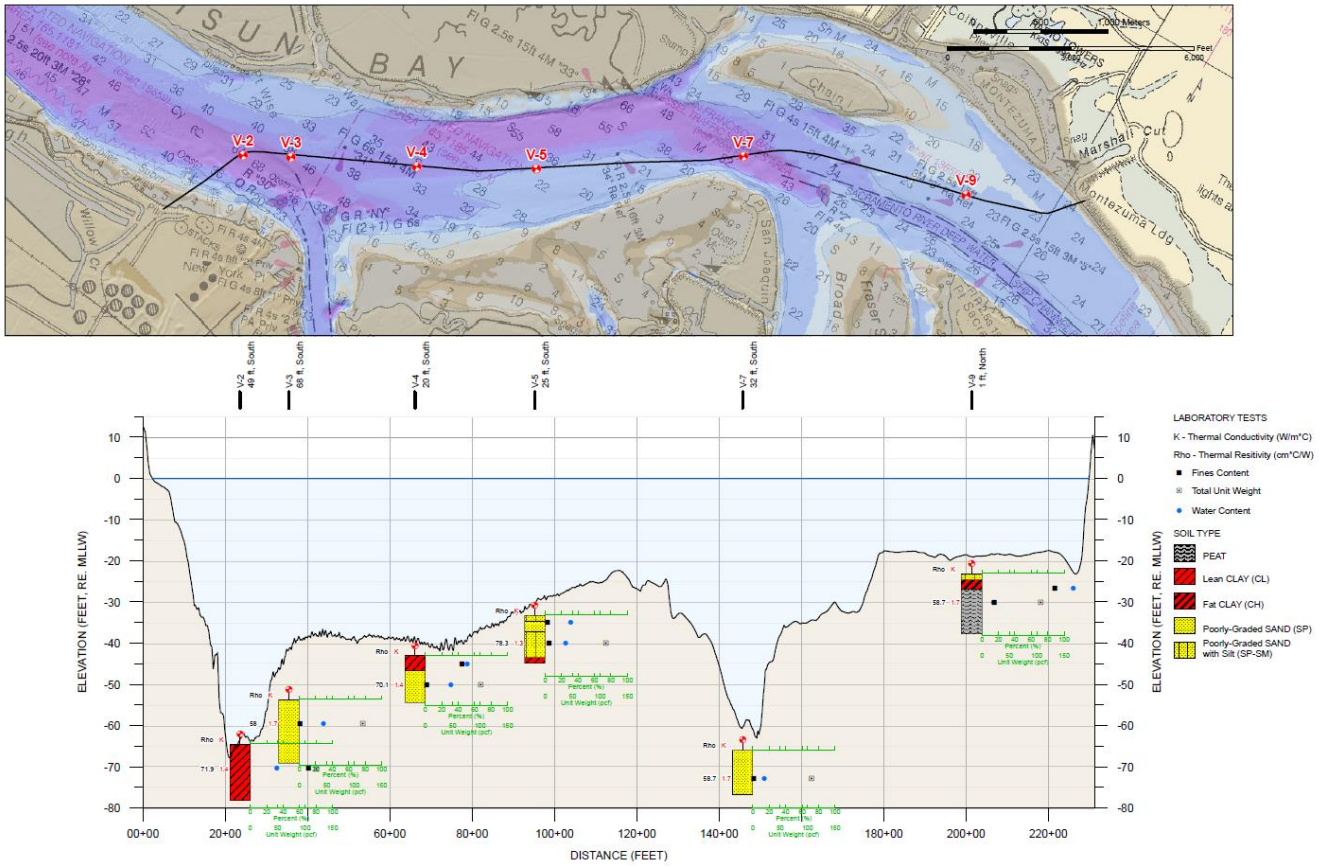

Source: LS Power Grid California, LLC, 2022

FIGURE 3-2: GRAIN SIZE CURVE FOR EACH SEDIMENT CORE

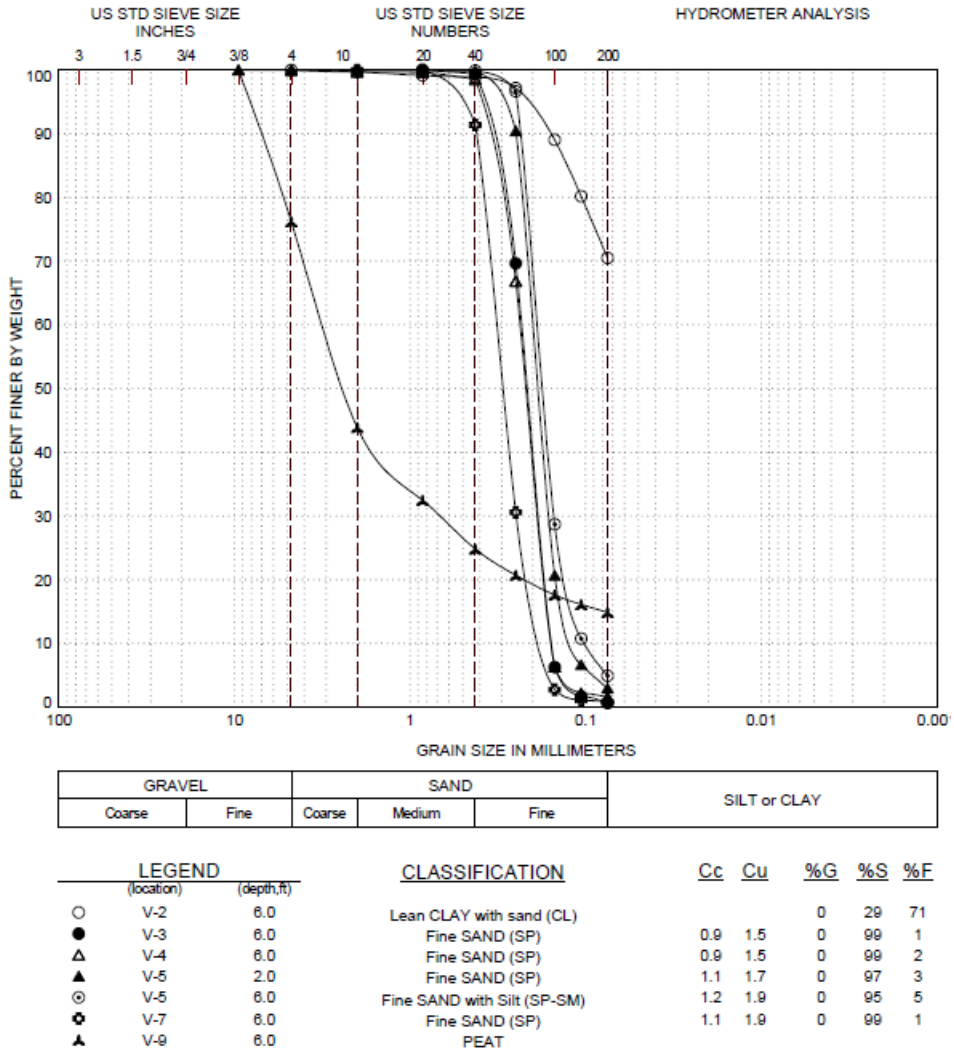

Source: LS Power Grid California, LLC, 2022

TABLE 3-1: REPRESENTATIVE GRAIN SIZE DISTRIBUTION OF BED SEDIMENT ALONG THE CABLE ROUTE

Grain Size Class	Grain Size(s) (µm)	Density (kg/m³)
Sand – Coarse	3,555	1,750
Sand – Medium	890, 1770	1,575
Sand – Fine	112.5, 225, 450	1,500
Silt	25	1,736
Clay	2	1,760
Peat	7,225	1,100

Note: µm = micrometer, kg/m³ = kilograms per cubic meter.

3.2.2 BATHYMETRY

The primary spatial dataset is bathymetric data, used to describe the depth and shape of the bed. Bathymetric data are used to develop the lower boundary of the modeling grid. For the study area, bathymetric data was developed using two different sources: an underwater survey completed by eTrac (eTrac, 2023) for LS Power, and a digital elevation model (DEM) of San Francisco Bay from the United States Geological Survey (Fregoso et al 2021). The eTrac survey was completed in September 2023 using 100 feet (ft) by 100 ft soundings. The DEM has a 1 m resolution and provides data from bathymetric surveys collected from 2005 to 2020 of the San Francisco Bay.

3.2.2.1 CABLE ROUTE

The data from each bathymetric source was combined to make a single raster grid for model use; Figure 3-3 depicts the final bathymetry used as input for the model grid. To combine the two sources the United States Geological Survey (USGS) DEM was used to fill the gaps found in the eTrac survey data to ensure bathymetry was populated for the entire domain of the model grids (description of grids in Section 3.4).

FIGURE 3-3: FINAL GENERATED BATHYMETRY FOR THE STUDY AREA, IN UTM 10N, NAVD 88

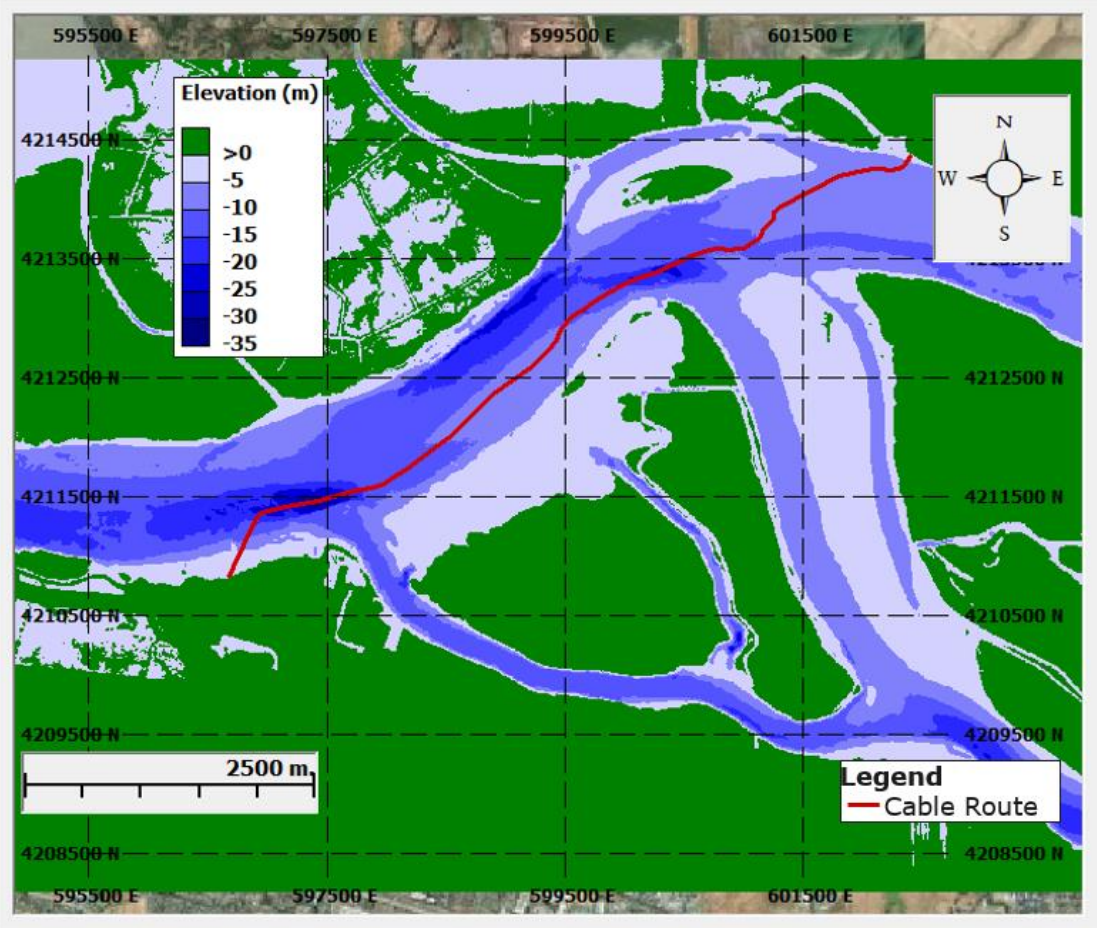

3.2.2.2 NORTHERN AND SOUTHERN SITE LOCATIONS

Elevations in the single raster grid described in Section 3.2.2.1 were referenced to the NAV88 vertical datum, and within the southern site location, trenching areas were above zero (i.e., on land), making sediment dispersion modeling infeasible. To fully submerge the southern open trenching area, the combined bathymetric data was uniformly adjusted downward by 2.62 m, matching the highest bathymetric contour line in the southern grid relative to NAVD88. Considering Mean Higher High Water (MHHW) level is 1.46 m relative to NAVD88, the dataset adjustment was 1.16m relative to MHHW. This modified bathymetric dataset ensured the entire southern site area was submerged and was applied to create both northern and southern site grids, taking a conservative approach that assumes sediment will disperse throughout the water column, and not on dry land. Figure 3-4, and Figure 3-5 zoom in at the final bathymetry used as input for the northern and southern site location model grids, respectively.

FIGURE 3-4: FINAL GENERATED BATHYMETRY FOR THE NORTHERN AREA, IN UTM 10N

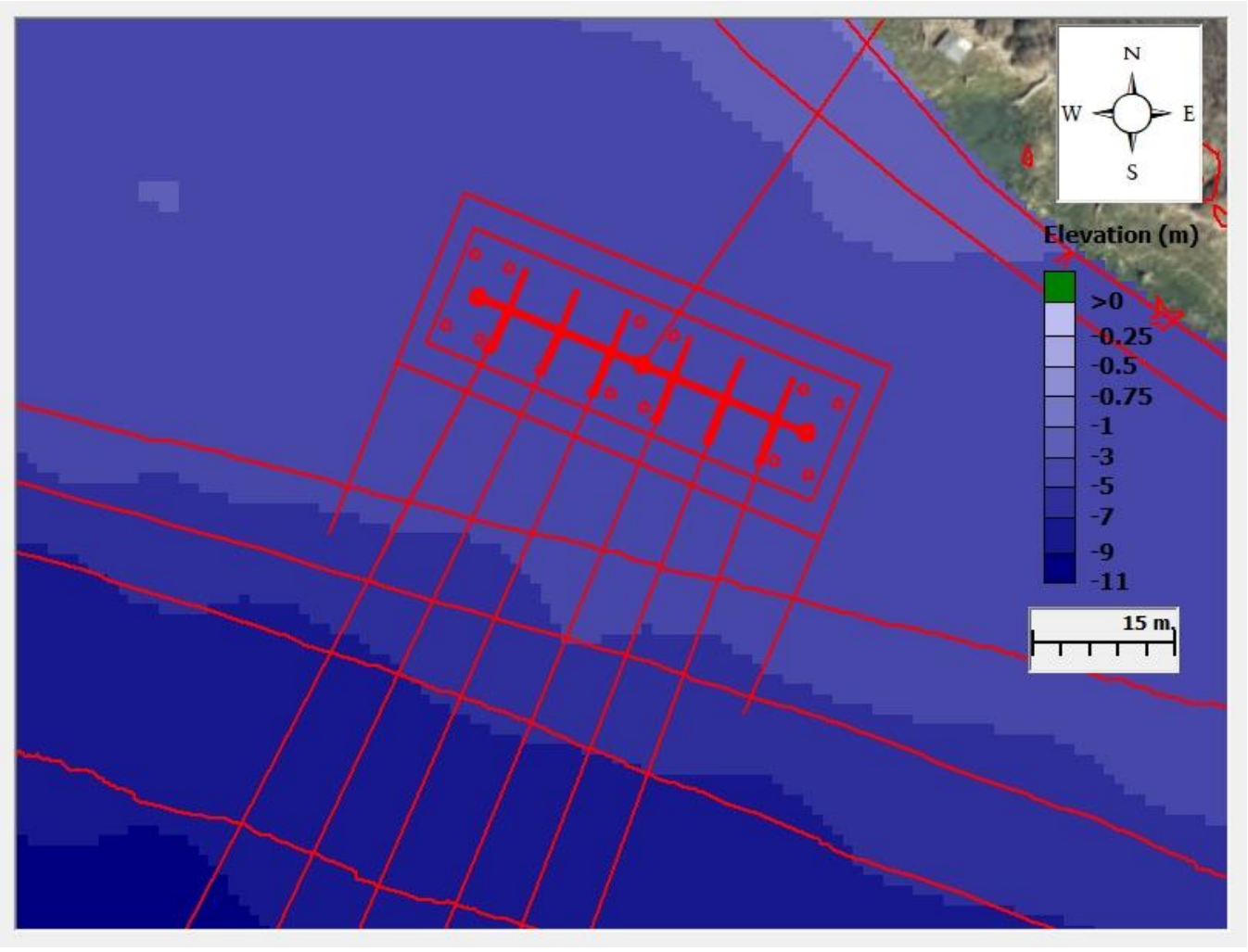

FIGURE 3-5: FINAL GENERATED BATHYMETRY FOR THE SOUTHERN AREA, IN UTM 10N

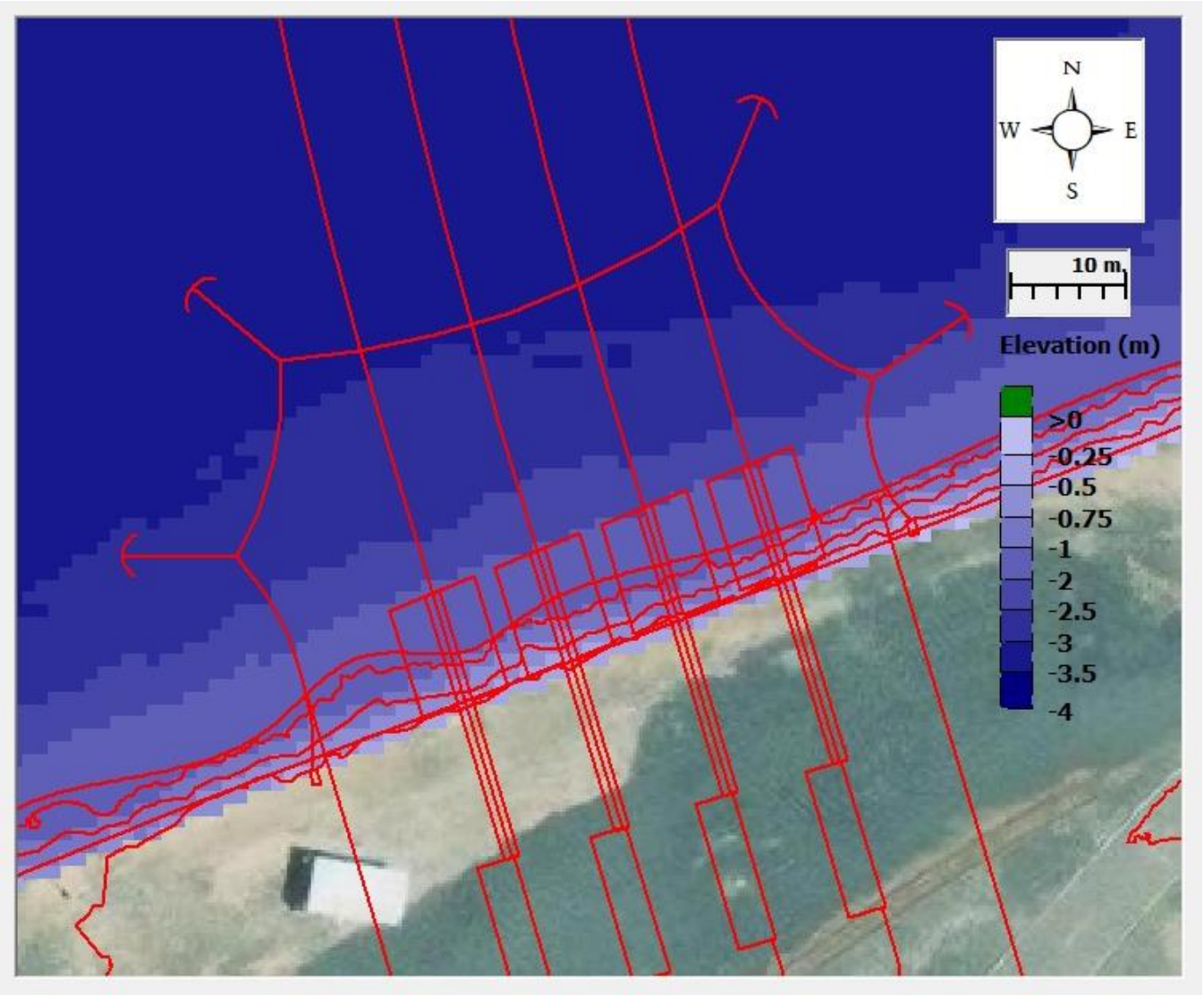

Using the vertically adjusted bathymetric dataset, additional bathymetry sets were developed for the backfilling operations at both the northern and southern locations. These datasets were deepened within the areas of excavation using the provided excavation depths (Table 2-1 and Table 2-2). In the northern section, the bathymetry data was deepened by 2.13 m in both R1 and R2 areas (Figure 3-6 and Figure 3-7, respectively). In the southern section, the bathymetry was deepened by 1.37 m within the areas of trenching (Figure 3-8). These bathymetry datasets were applied for the backfilling modeling scenarios.

FIGURE 3-6: FINAL GENERATED DREDGED BATHYMETRY FOR THE R1 NORTHERN AREA, IN UTM 10N

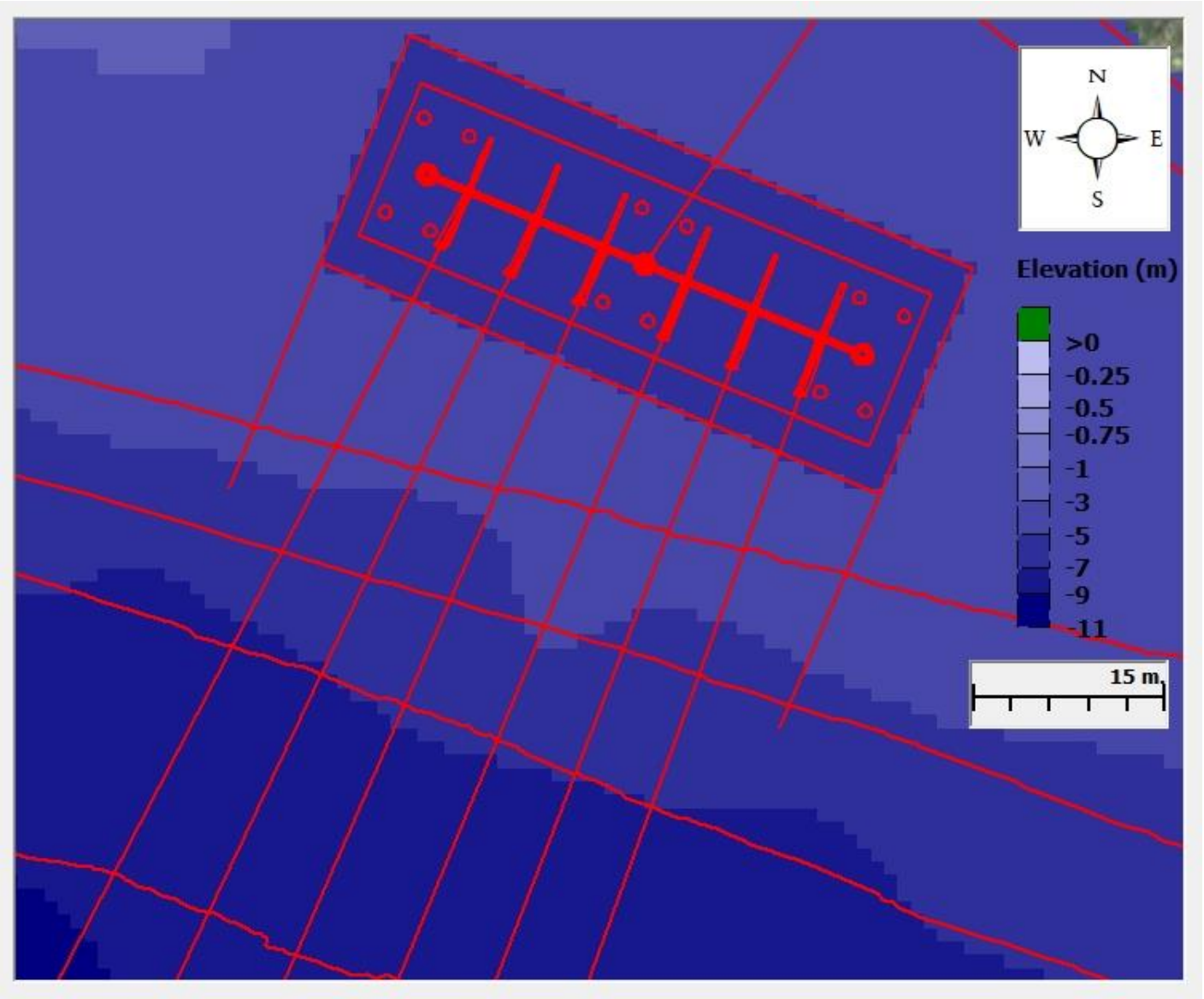

FIGURE 3-7: FINAL GENERATED BATHYMETRY FOR THE DREDGED R2 SCENARIOS NORTHERN AREA WITHIN SHEET PILES (ORANGE), IN UTM 10N

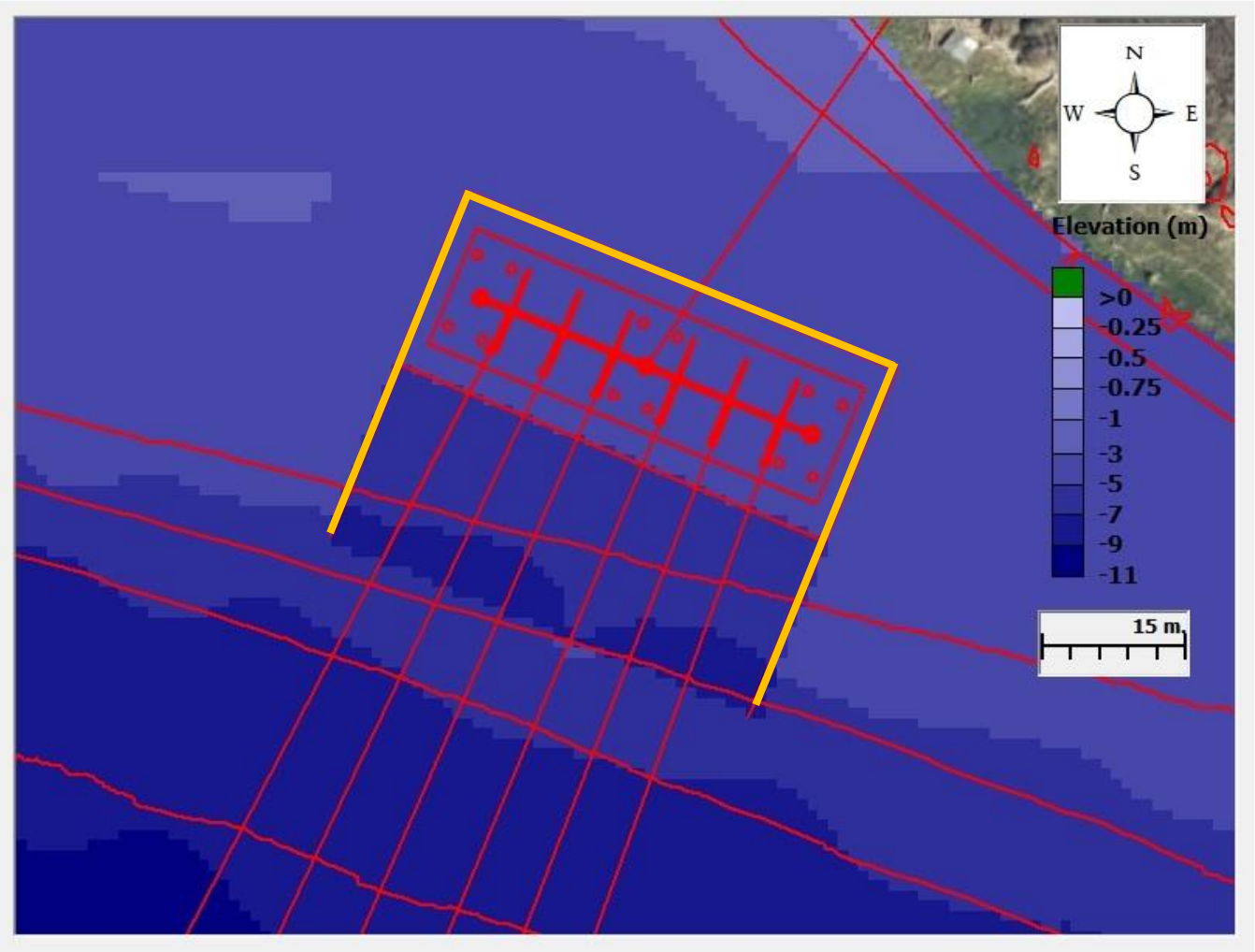

FIGURE 3-8 FINAL GENERATED DREDGED BATHYMETRY FOR THE SOUTHERN AREA, IN UTM 10N

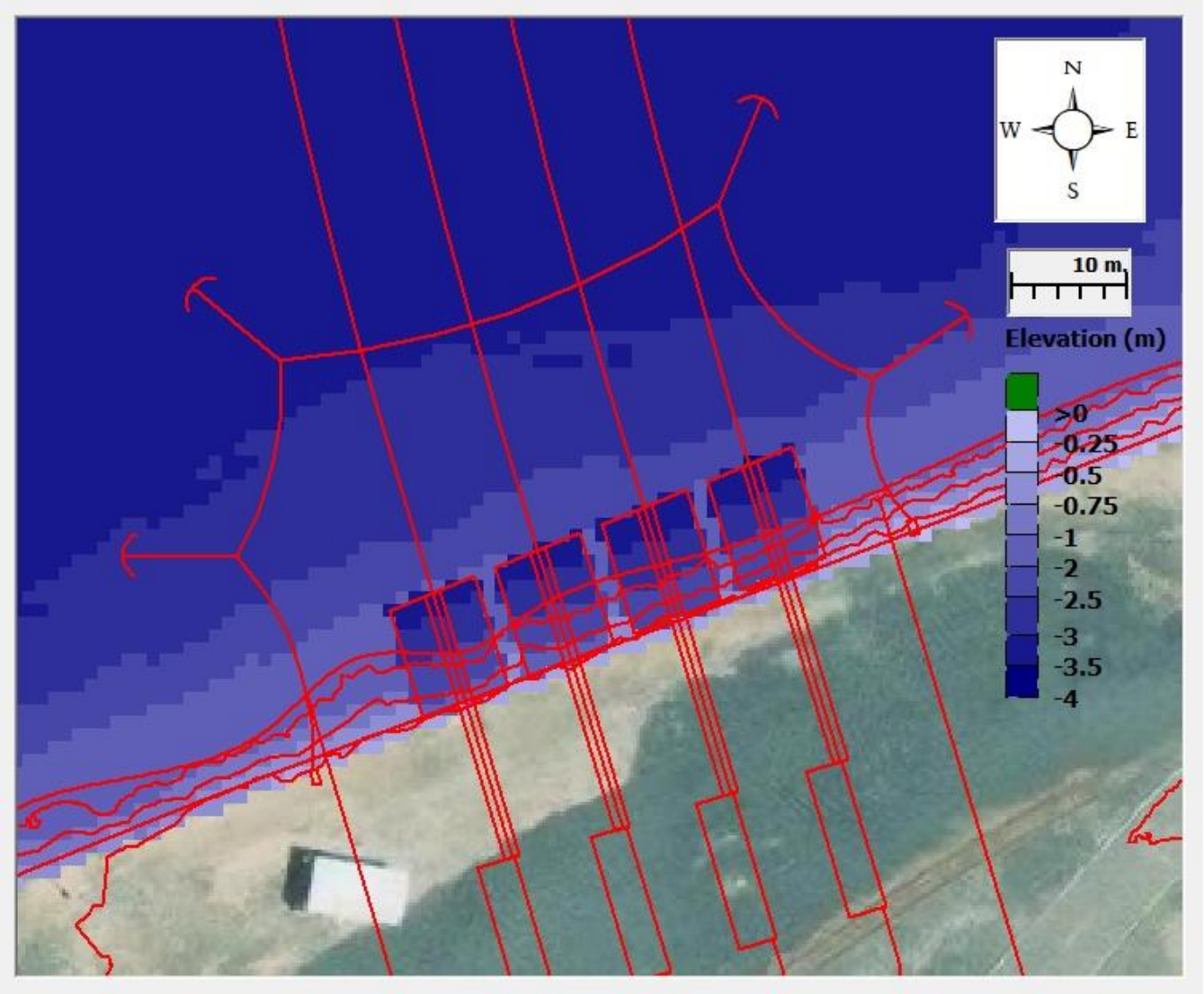

3.2.3 TIME VARYING HYDRODYNAMIC DATA

The time-varying data for the model include current speed and direction, water temperature, and salinity. For representation of the hydrodynamics of the study area, ERM relied on the National Oceanic and Atmospheric Administration (NOAA)'s San Francisco Bay Operational Forecast System (SFBOFS)[1]. It is a three-dimensional, high-resolution numerical model that uses the Finite Volume Coastal Ocean Model (FVCOM)[2] as its base. The resolution of this model ranges from 3.9 km in the open ocean to approximately 10 m in the navigational channels. This model provides both nowcasts and forecasts for the following parameters: water levels, currents, water temperature,

[1] https://tidesandcurrents.noaa.gov/ofs/sfbofs/sfbofs.html
[2] https://www.fvcom.org/

and salinity, on an hourly basis. For the determination of the modeling scenarios as discussed in section 3.3, current data from January 1, 2018, through December 31, 2022, was analyzed to determine the 5th and 95th percentile currents during the selected months for operations. A representative date within the scenarios' respective construction periods, which closely matched the percentile values, was chosen; the highest value at the 95th percentile value and the lowest value at the 5th percentile were used to determine the modeling timeframes. The 5th and 95th percentile bottom current speeds for Scenarios 1 and 2 (cable route, Table 1-1) were determined from the data from June to December (i.e., the construction period) for all years. The representative date selected for the 5th percentile was November 14, 2018, and the 95th percentile representative date was determined to be August 25, 2022. Table 3-2 summarizes the bottom current analysis. An example current time series for the two entire cable scenarios close to the site location is shown in Figure 3-9 and Figure 3-10. The hourly data of spatially varying salinity and temperature was also used for the modeling, where the average seabed water temperature for November 14, 2018, was around 14.5^{o} Celsius while on December 31, 2022, it was 9.23^{o} Celsius. The average seabed salinity on November 14, 2018, was 0.32 parts per thousand (ppt) and on December 31, 2022, it was 0.79 ppt for this freshwater environment.

FIGURE 3-9: EXAMPLE OF BOTTOM CURRENT MAGNITUDE TIME SERIES NEAR THE CABLE ROUTE ON NOVEMBER 14, 2018

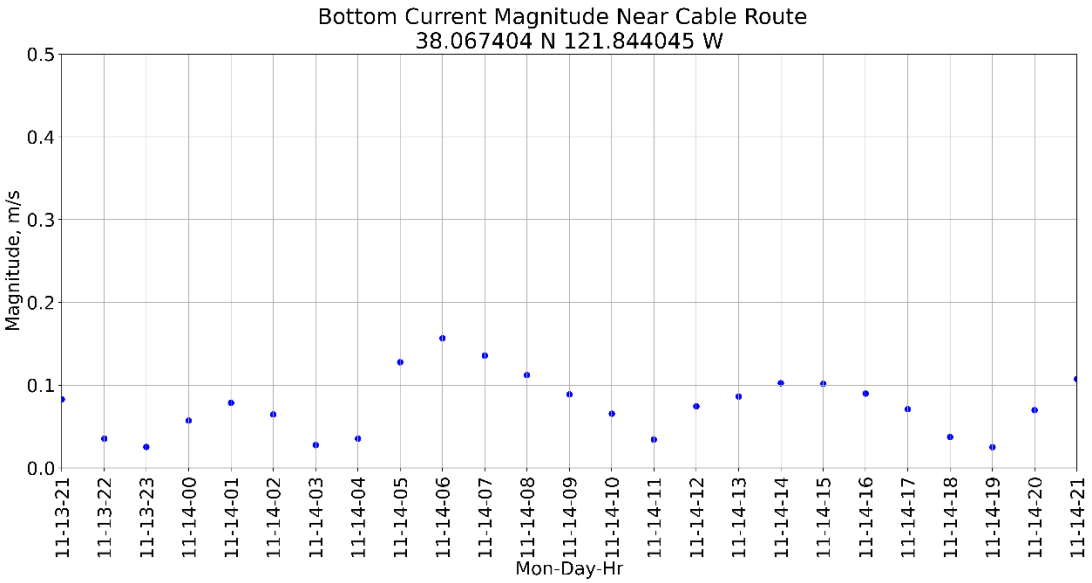

FIGURE 3-10: EXAMPLE OF BOTTOM CURRENT MAGNITUDE TIME SERIES NEAR THE CABLE ROUTE ON DECEMBER 31, 2022

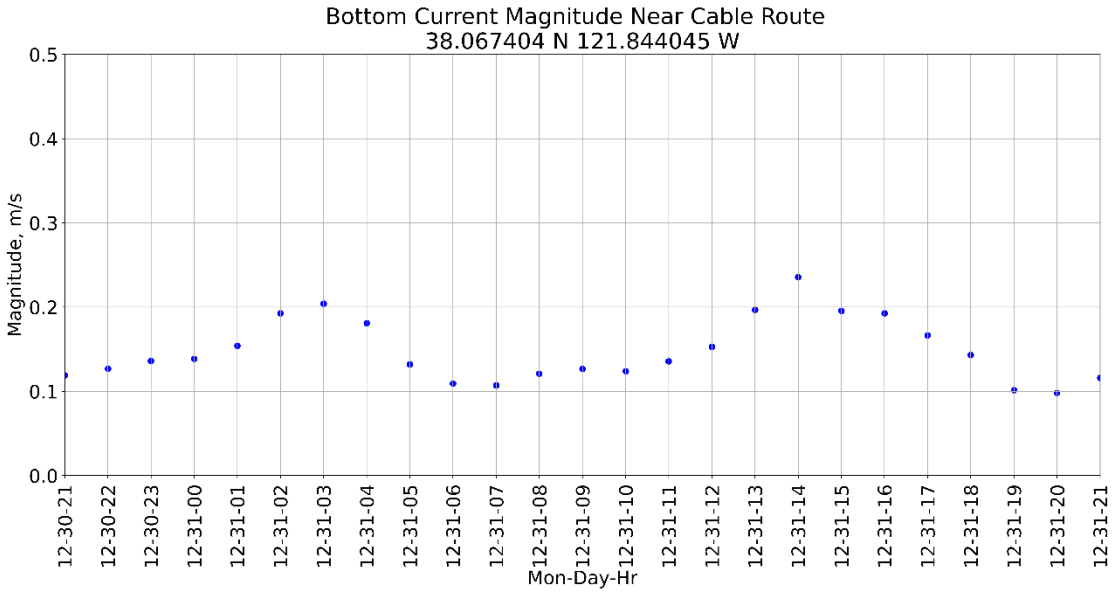

For modeling the northern and southern site scenarios six hourly data sets from the same data source described above were utilized[3]. These data sets were analyzed to determine the 5th and 95th percentile currents for the operational time period of July through November. The representative date selected for the 5th percentile was the same as the date for the entire cable installation, November 14, 2018. The 95th percentile representative date was determined to be August 25, 2022, for the northern and southern locations. For this date, the average riverbed temperature was 23.5° Celsius and the average salinity was 1.02 ppt.

TABLE 3-2: SUMMARY OF BOTTOM CURRENT ANALYSIS RESULTS FOR THE PERIOD OF 2018 TO 2022

Scenario	Percentile	Current Speed (m/s)	Representative Date of Current Speed
Cable installation across the river and Northern Site and Southern Site Locations, minimum currents	5th	0.029	14 November 2018
Cable installation across the river, maximum currents	95th	0.196	31 December 2022
Northern and Southern Site locations' maximum currents	95th	0.196	25 August 2022

Source: SFBOFS

Note: m/s = meter per second.

[3] NOAA SFBOFS Historical Archive at NCEI THREDDS data server was not accessible during the modeling of northern and southern areas, due to flooding events in NC from Hurricane Helene. Thus previously collected 6 hourly data was used.

3.3 SCENARIO SELECTION AND SIMULATION DESIGN

While the conditions with low ambient current speeds are highly desirable for cable installation activities, this modeling exercise selected both minimum (5th percentile) and maximum (95th percentile) current speed conditions to capture the full spectrum of potential impact. Sediment particles are expected to settle near the area of disturbance and will represent maximum depositional thickness during the minimum current conditions. Alternatively, sediment particles are expected to be advected and dispersed to a larger area during the maximum current conditions and represent the maximum area of TSS plumes. Accordingly, 14 scenarios were developed to simulate the disturbed and resuspended sediment behavior due to cable installation activities during extreme hydrodynamic conditions, as summarized in Table 1-1.

3.3.1 SCENARIOS 1 AND 2: CABLE INSTALLATION CROSSING THE RIVER

Table 3-3 through Table 3-5 present the volume, duration, and other characteristics of dispersed sediment due to cable installation activities. The following assumptions were made to design the simulations:

- Disturbed sediment was released 0.5 m above the seabed;
- Six sediment core properties were distributed along the cable route; and
- Wet sediment core densities used for mass release rate to be conservative.

There were six sediment cores taken along the cable route. For Scenarios 1 and 2, the sediment characteristics of the six cores were considered and distributed along the associated section of the cable route as shown in Figure 3-11. Six sediment releases were simulated along the submarine cable route, each corresponding to the start of each six sections along the cable route, where sediment core samples were taken from the seabed.

Table 3-3 summarizes the sediment release locations, amounts, and other characteristics for the installation of the entire cable route. The hourly release amount presented in Table 3-3 is derived from the density of each sediment core.

FIGURE 3-11: RELEASE REGION LOCATIONS, THE LIGHT GREEN LINES SHOW THE EXTENT OF EACH SEDIMENT TYPE SECTION ALONG THE CABLE ROUTE

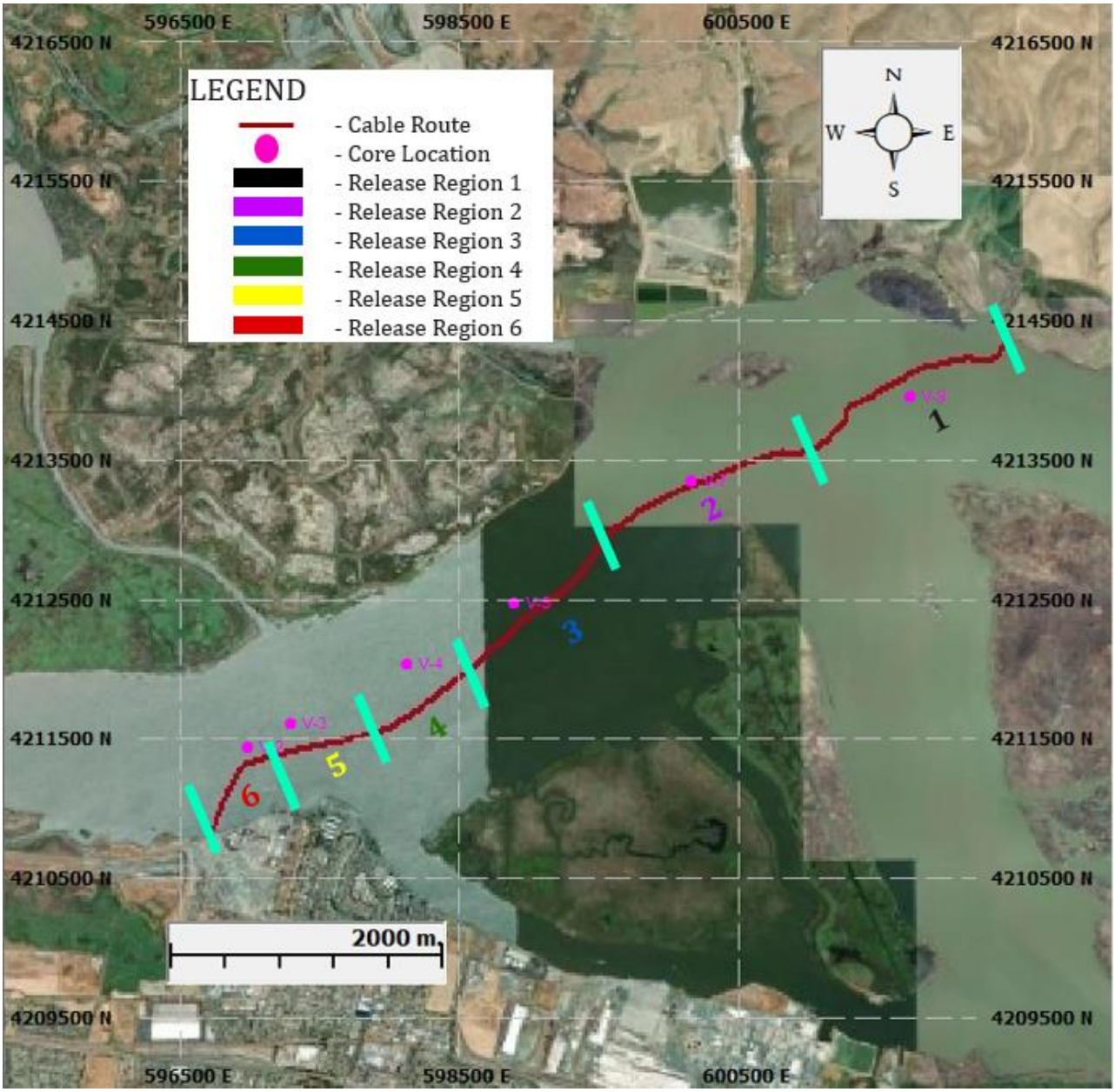

TABLE 3-3: VOLUME, DURATION, AND OTHER CHARACTERISTICS OF DISPERSED SEDIMENT DUE TO CABLE INSTALLATION IN EACH SECTION OF THE CABLE ROUTE (SCENARIOS 1 AND 2)

Release Region Number	Representative Core	Length of Cable Route in the section (m)	Release Amount per Hour (tons/hr)	Bulk Density (kg/m³)	Time Duration of Release (hours)
1	V9	1600	0.490	913.1	5.33
2	V7	1608	0.762	1709	5.37
3	V5	1281	0.791	1775	4.27
4	V4	820	0.721	1618	2.73
5	V3	715	0.823	1847	2.38
6	V2	687	0.863	1935	2.32

Note: m = meter; tons/hr = tons per hour; kg/m³ = kilogram per cubic meter.

3.3.2 SCENARIOS 3-10: NORTHERN SITE LOCATION

For Scenarios 3 through 10, the sediment characteristics of cores taken at location V-9 were considered, which corresponds to Release Region 1 in Figure 3-11. Sixty sediment releases were simulated within the excavation area, each corresponding to the start of excavation or backfilling activities. The releases were simulated to replicate the proposed schedule of operations. This entailed a 12-hour release period during the first day (assumed to be 8:00 A.M. to 8:00 P.M.), a 12-hour break, followed by a second release period beginning at 8:00 A.M. and releasing until all sediment was released (ending prior to 8:00 P.M.). The simulation was then continued for the remainder of the second day and an additional third day to analyze the propagation of the sediment after the operations had ceased. In these scenarios, it was assumed that:

- Disturbed sediment was released 0.1 m above the seabed;
- Clamshell bucket was 4 feet wide;
- Sediment loss of 4 percent; and
- Sheet pilings used for the in-river transition approach are impermeable.

The northern excavation and backfill are divided into different regions, R1 and R2, both with 1,783.6 cubic meters (2,333 cubic yards) of sediment removed in each (Figure 3-12). These areas are 18.3 meters by 45.7 meters (60 feet by 150 feet) and will be excavated 2.13 meters (7 feet) deep. These areas were divided into smaller sections, 3.05 meters by 4.57 meters (10 feet by 15 feet), in order to simulate the excavation/backfilling process. This resulted in a total of 60 sediment releases for each region. Table 3-4 details the excavation and backfilling rates, amounts, and timing for the northern scenarios. During dredging operations using a clamshell bucket, sediment loss from the bucket is assumed to occur during travel through the water column and as the bucket breaks the water surface (ERDC: DOER 2000). To be conservative, the loss percentage was assumed to be four percent of the total dredged volume. This volume of sediment loss was

assumed to be released during the excavation operation while for the backfilling operations, the entire excavated volume was released.

FIGURE 3-12: EXCAVATION AND BACKFILLING DETAILS FOR NORTHERN IN RIVER TRANSITION SITE

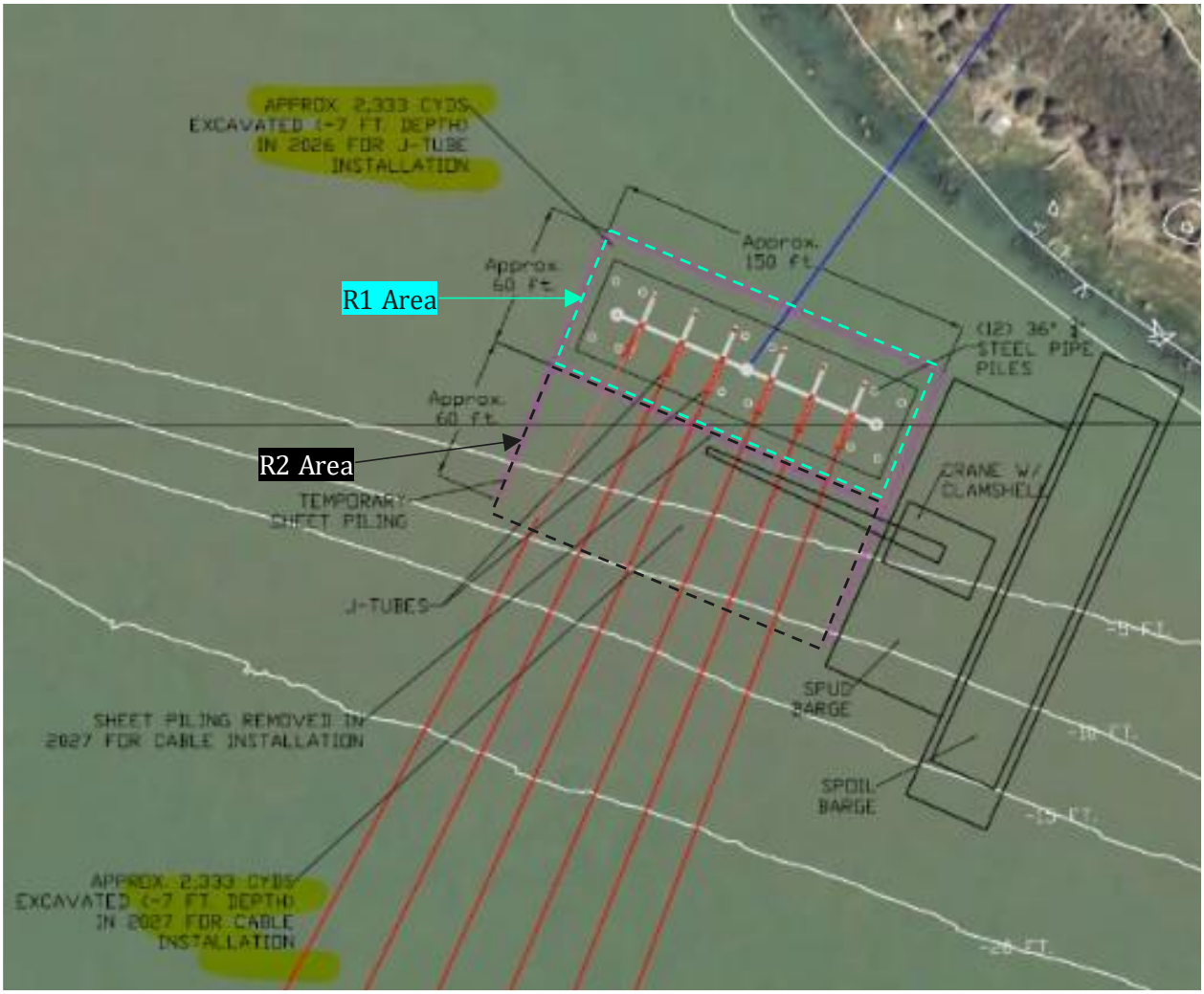

Source: LS Power, 2024

TABLE 3-4: VOLUME, DURATION, AND OTHER CHARACTERISTICS OF DISPERSED SEDIMENT DUE TO INSTALLATION ACTIVITIES IN THE NORTHERN SITE LOCATION

Type of Operation	Representative Core	Total Sediment Released (m^3)	Release Amount per Hour (tons/hr)	Total Duration of Release (hours)
Excavation	V9	71.3	3.36	23.3
Backfilling	V9	1783.6	84.1	23.3

Note: tons/hr = tons per hour; m^3 = cubic meter.

3.3.3 SCENARIOS 11-14: SOUTHERN SITE LOCATION

For Scenarios 11 through 14, the sediment characteristics of cores taken at location V-2 (Release Region 6 in Figure 3-11). Similar to the northern site location, the releases were simulated to replicate the proposed schedule of operations. This entailed a 12-hour release period during the first day (assumed to be 8:00 A.M. to 8:00 P.M.), a 12-hour break, followed by a second release period beginning at 8:00 A.M. and releasing until all sediment was released (ending prior to 8:00 P.M.). The simulation was then continued for the remainder of the second day and an additional third day to analyze the propagation of the sediment after the operations had ceased In these scenarios it was assumed that:

- Disturbed sediment was released 0.1 m above the seabed;
- Sediment loss of 4 percent;
- Silt curtains extend to the riverbed with no gap; and
- Silt curtains were semi-permeable and no sediment could pass through.

The southern excavation and backfill are divided into 4 different trench areas, with 91.7 cubic meters (120 cubic yards) of sediment removed in each (Figure 3-13), for a total amount of 366.9 cubic meters (480 cubic yards). These trenches are 9.14 meters by 5.48 meters (30 feet by 18 feet) and will be excavated 1.83 meters (6 feet) deep. These trenches were divided into smaller areas, 3.05 meters by 1.22 meters (10 feet by 4 feet), in order to simulate the excavation/ backfilling process. This resulted in 18 sediment releases for each trench and 72 releases in total. Table 3-5 details the excavation and backfilling rates, amounts, and timing for the southern scenarios. Similar to the clamshell bucket used in the northern operations, 4 percent of the total dredged volume was assumed as sediment loss and modeled as the sediment release during the excavation operation. For the backfilling operations, the entire excavated volume was released.

FIGURE 3-13: EXCAVATION AND BACKFILLING DETAILS FOR SOUTHERN OPEN TRENCHING SITE

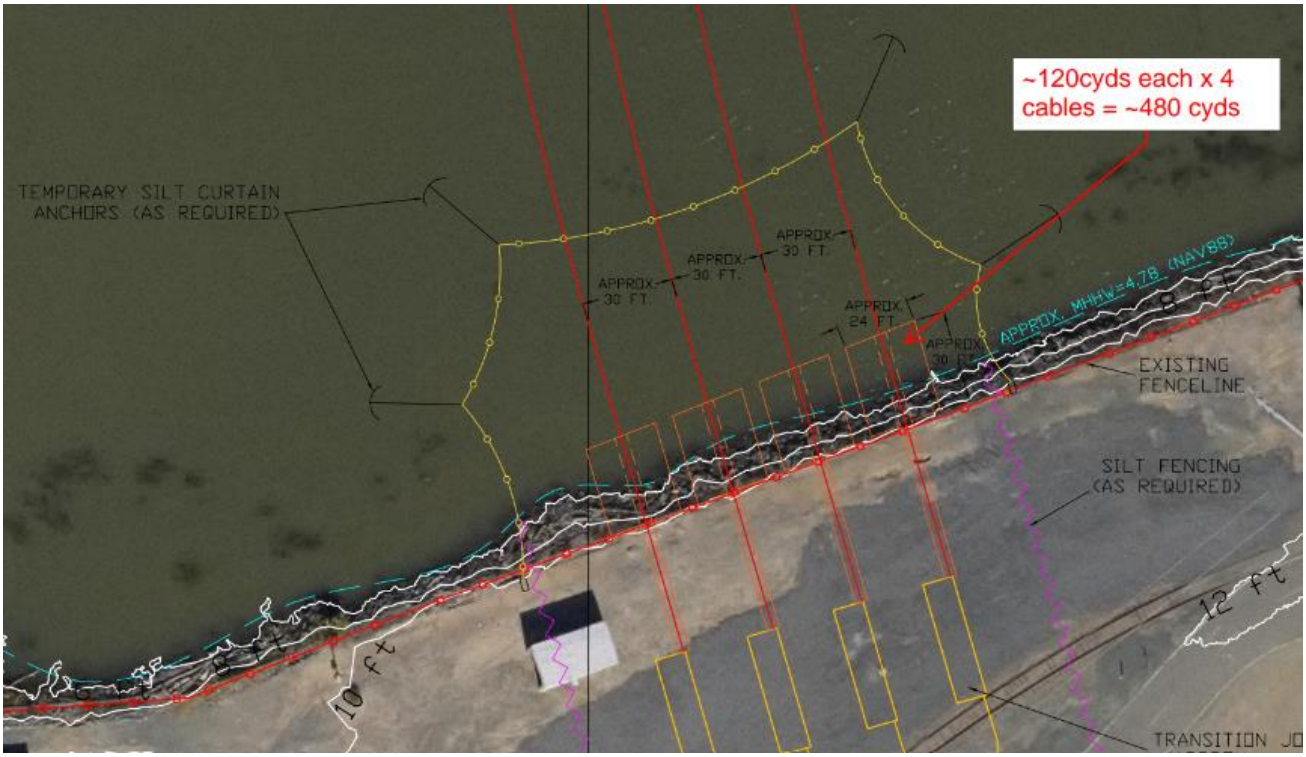

Source: LS Power, 2024

TABLE 3-5: VOLUME, DURATION, AND OTHER CHARACTERISTICS OF DISPERSED SEDIMENT DUE TO INSTALLATION ACTIVITIES IN THE SOUTHERN SITE LOCATION

Type of Operation	Representative Core	Total Sediment Released (m^3)	Release Amount per Hour (tons/hr)	Total Duration of Release (hours)
Excavation	V2	14.7	1.48	19.2
Backfilling	V2	366.9	36.9	19.2

Note: tons/hr = tons per hour; m^3 = cubic meter.

3.4 MODELING GRIDS

Three model grids, including a particle grid, a depositional grid, and a concentration grid were used in modeling. The movement of the displaced sediment particles using Lagrangian particles was computed within the particle grid. Each grid cell contains an interpolated depth value derived from the bathymetric dataset described in Section 3.2.2. Particles are free to move horizontally and vertically within this grid's domain, independently of the grid, except for movement past the grid boundaries representing the bed (as defined by the bathymetry), any shorelines, as well as

temporarily installed sheet piling and silt curtains. For the computation of the deposition on the bed, the model used a two-dimensional (2-D) depositional grid. The concentration grid is three-dimensional (3-D) and is used for the computation of TSS concentrations in the water column. Each type of grid used under the various modeling scenarios is described below.

3.4.1 CABLE ROUTE

The two-dimensional particle grid is a rectangle approximately covering a 10 kilometer by 7 kilometer domain, with each cell 10 meters by 7 meters. Figure 3-14 shows the extent of the particle grid.

FIGURE 3-14: PARTICLE GRID DOMAIN (BLACK BOX) AND CLOSE UP VIEW OF GRID (RED BOX) WITH CABLE ROUTE SHOWN IN MAROON

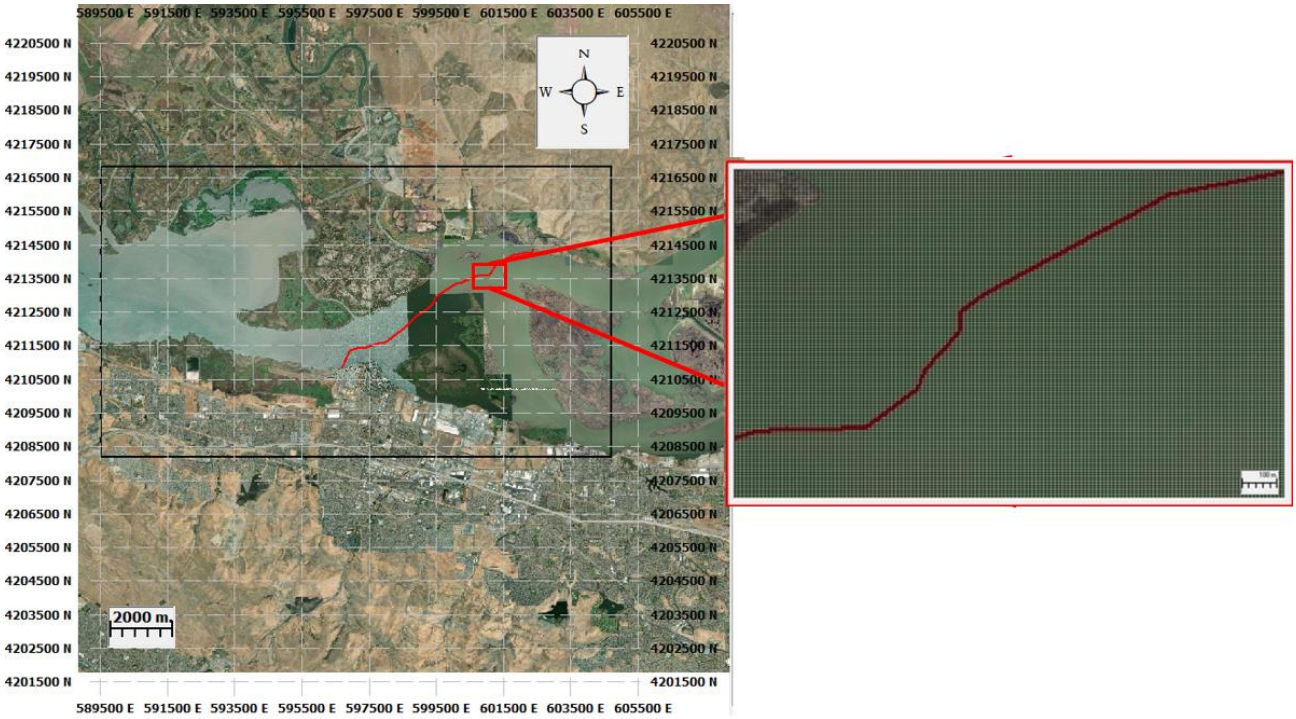

The depositional grid is a rectangle, approximately 6.6 kilometers by 3.9 kilometers with each cell 20 meters by 20 meters. Figure 3-15 shows a closer look at the depositional grid.

The concentration grid has the same horizontal dimensions as the depositional grid. Vertically, the cell thicknesses range from 10 meters at the surface to 1 meter at the bottom of the water column, where the maximum TSS concentrations are predicted to occur.

A summary of the dimensions of these grids is presented in Table 3-6.

FIGURE 3-15: DEPOSITIONAL AND CONCENTRATION GRID

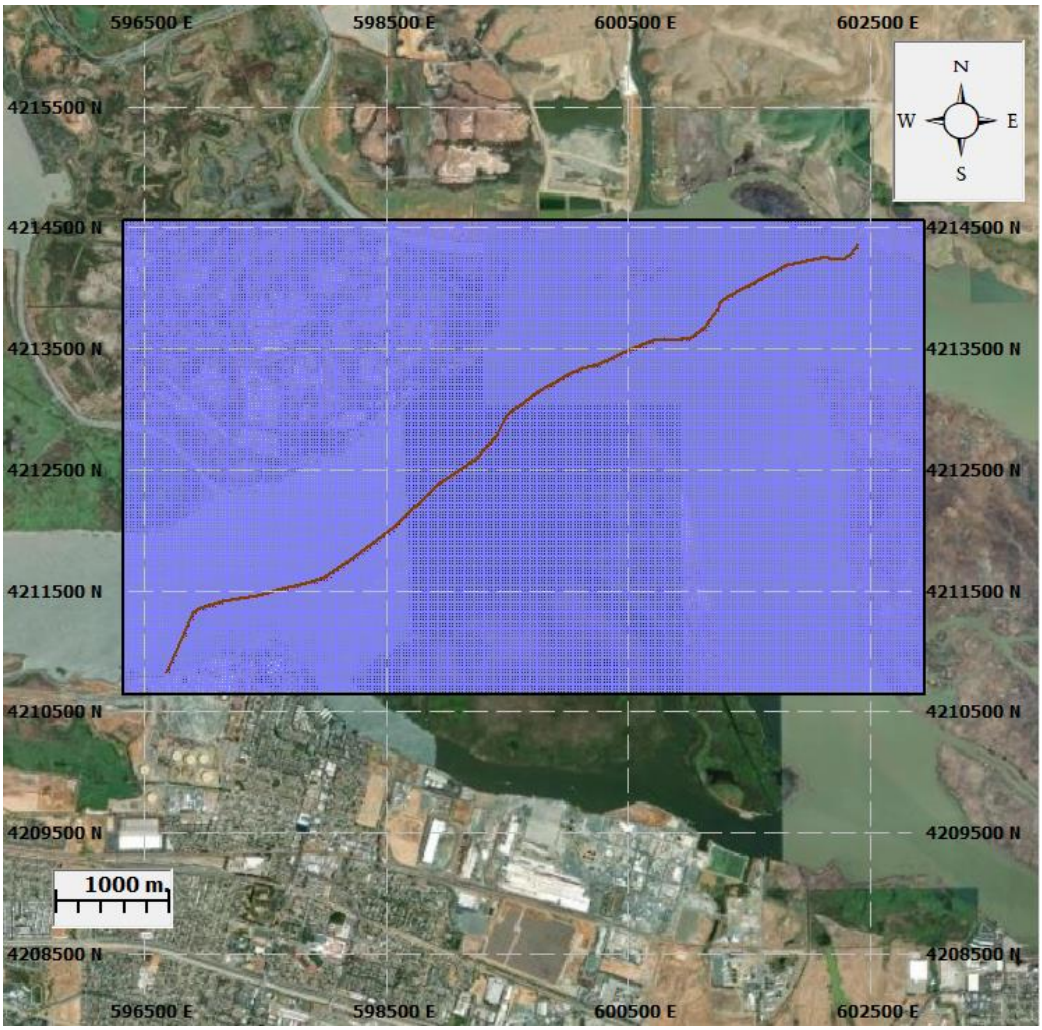

TABLE 3-6: GRID DIMENSIONS FOR ENTIRE CABLE ROUTE

Grid	Horizontal Grid Cell Dimensions (m)	Vertical Grid Cell Dimensions
Particle (2-D)	10 m x 7 m	N/A
Depositional (2-D)	20 m x 20 m	N/A
Concentration (3-D)	20 m x 20 m	Vertically variable: The smallest (1 m) near the bed between the depths of 34 m and 43 m to the largest (10 m) near the water surface

Note: m = meter; N/A = Not Applicable.

3.4.2 NORTHERN SITE LOCATION

The two-dimensional particle grid for the in-river transition approach in the northern area varied for each of the excavation regions considered (R1 and R2). The particle grid for the R1 scenarios is a rectangle approximately covering a 600 meter by 350 meter domain, with each cell 1 meter by 1 meter. Figure 3-16 shows the extent of the particle grid.

FIGURE 3-16: PARTICLE GRID DOMAIN (BLACK BOX) FOR R1 NORTHERN SCENARIOS AND CLOSE UP VIEW OF GRID

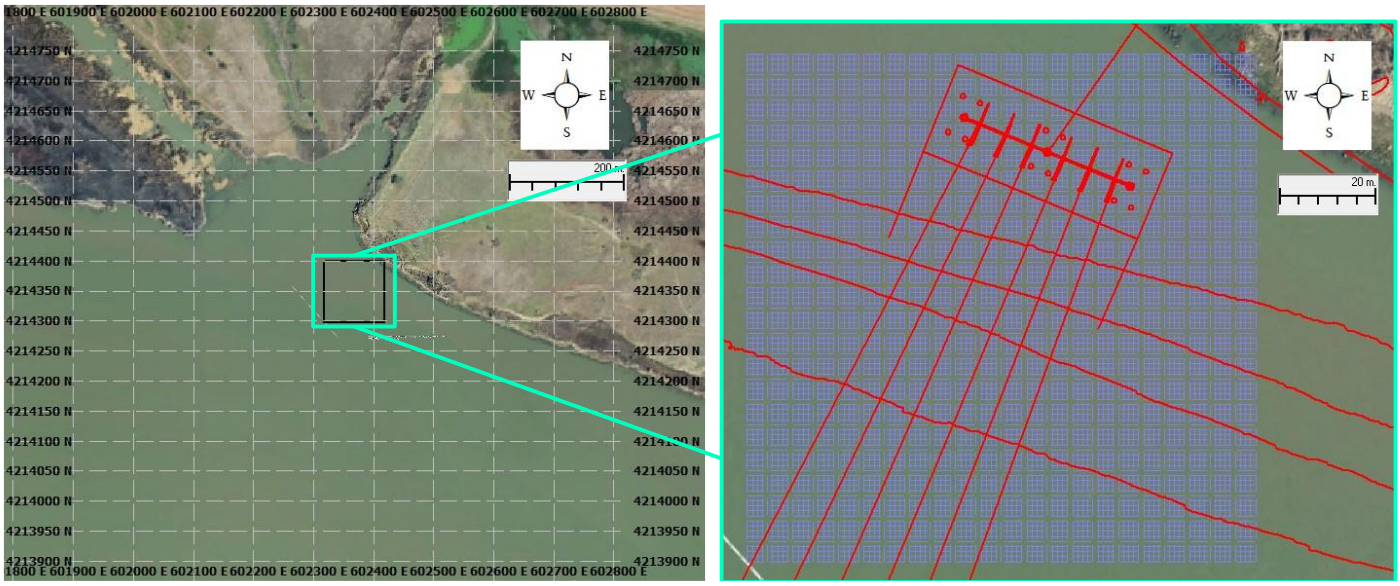

The depositional grid for the R1 scenarios is a square, approximately 100 meters by 100 meters, with 1 meter by 1 meter cells. Figure 3-17 shows a closer look at the depositional grid.

The concentration grid for R1 has the same horizontal dimensions as the depositional grid. Vertically, the cell thicknesses are constant throughout the water column at 1 meter.

A summary of the dimensions of these grids is presented in Table 3-7.

FIGURE 3-17: DEPOSITIONAL AND CONCENTRATION GRIDS FOR R1 NORTHERN SITE LOCATION

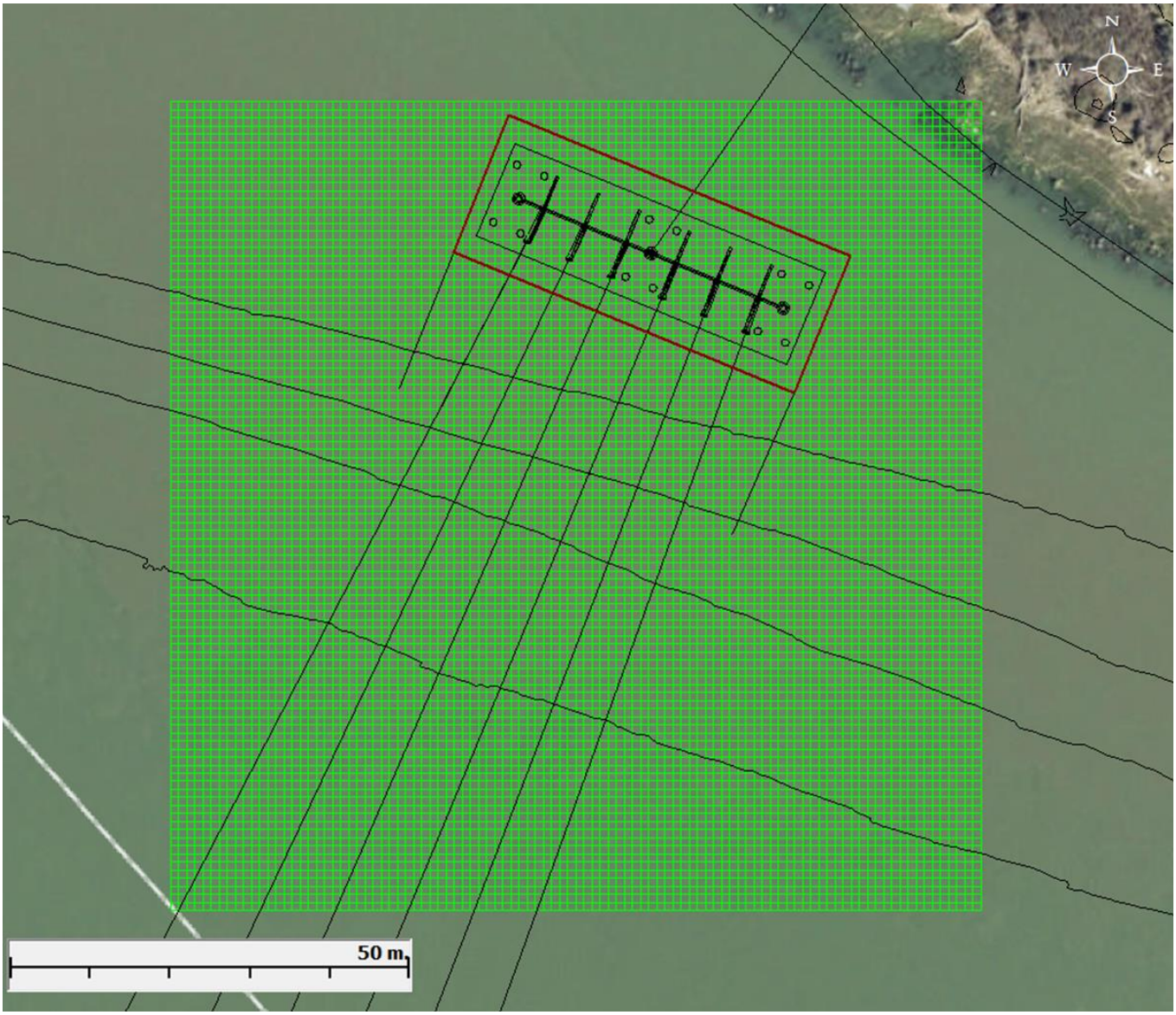

TABLE 3-7: GRID DIMENSIONS FOR R1 NORTHERN SITE LOCATION

Grid	Horizontal Grid Cell Dimensions (m)	Vertical Grid Cell Dimensions
Particle (2-D)	1 m x 1 m	N/A
Depositional (2-D)	1 m x 1 m	N/A
Concentration (3-D)	1 m x 1 m	1 m

Note: m = meter; N/A = Not Applicable.

There are two particle grids for the R2 scenarios: one for the minimum current simulations and one for maximum current simulations. This was needed as the current direction for the minimum current scenario was towards the north-west while the current direction for the maximum current scenario was toward the south-east. Due to the resolutions of the grids, it was determined to be more efficient to make timespan specific grids that were expanded in the direction of the currents. The particle grid for R2 minimum current simulations is a rectangle approximately covering a 500 meter by 350 meter domain, with each cell 1 meter by 1 meter (Figure 3-18). The particle grid for R2 maximum current simulations is a square approximately covering a 500 meter by 500 meter domain, with each cell 1 meter by 1 meter (Figure 3-19).

FIGURE 3-18: PARTICLE GRID DOMAIN (BLACK BOX) FOR R2 NORTHERN MINIMUM CURRENT SCENARIOS AND CLOSE UP VIEW OF GRID (GREEN BOX)

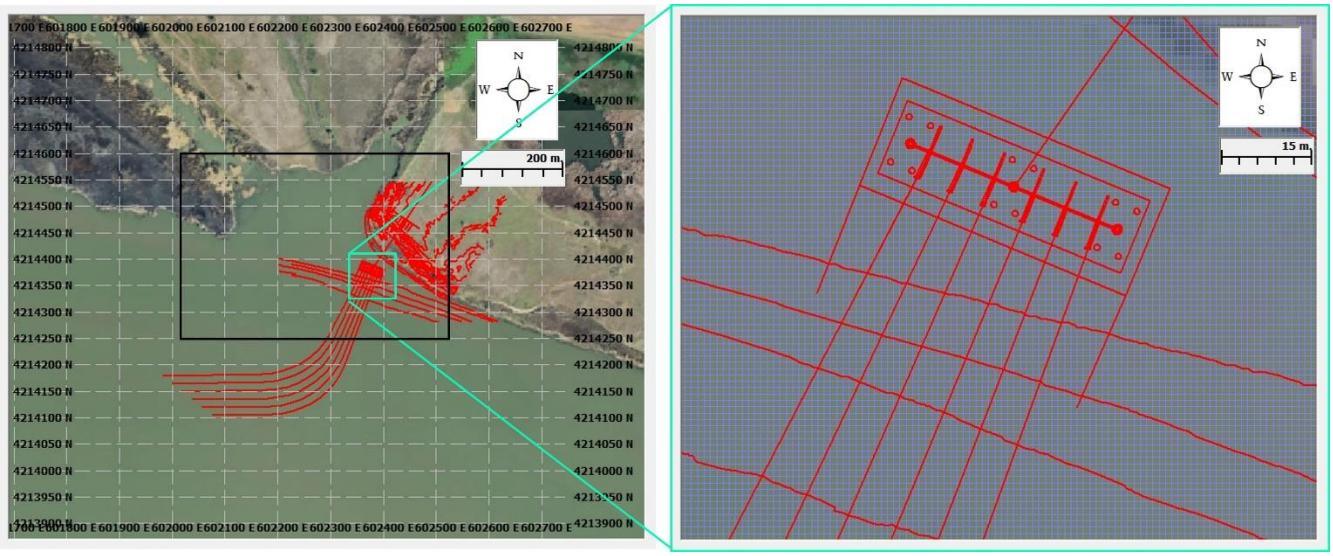

FIGURE 3-19: PARTICLE GRID DOMAIN (BLACK BOX) FOR R2 NORTHERN MAXIMUM CURRENT SCENARIOS AND CLOSE UP VIEW OF GRID (GREEN BOX)

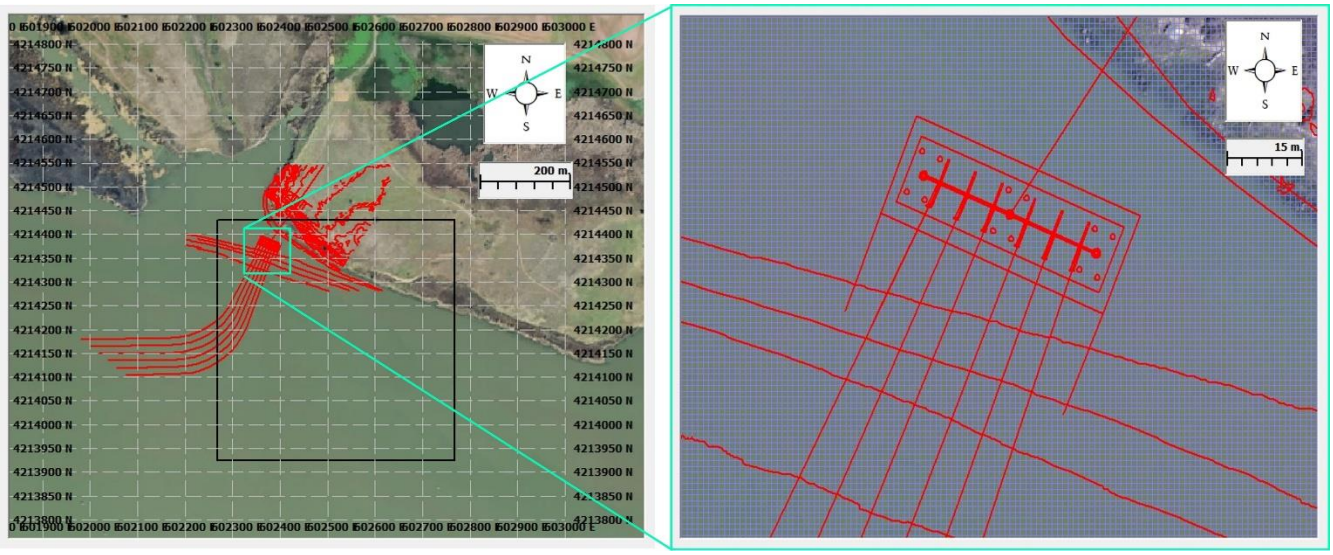

The depositional grid for the R2 scenarios (minimum and maximum currents) is a square, approximately 200 meters by 200 meters with each cell 1 meter by 1 meter. Figure 3-20 shows a closer look at the depositional grid.

The concentration grid for R2 has the same horizontal dimensions as the depositional grid. Vertically, the cell thicknesses are constant throughout the water column at 1 meter.

A summary of the dimensions of these grids is presented in Table 3-8.

FIGURE 3-20: DEPOSITIONAL AND CONCENTRATION GRID FOR R2 NORTHERN SITE LOCATIONS

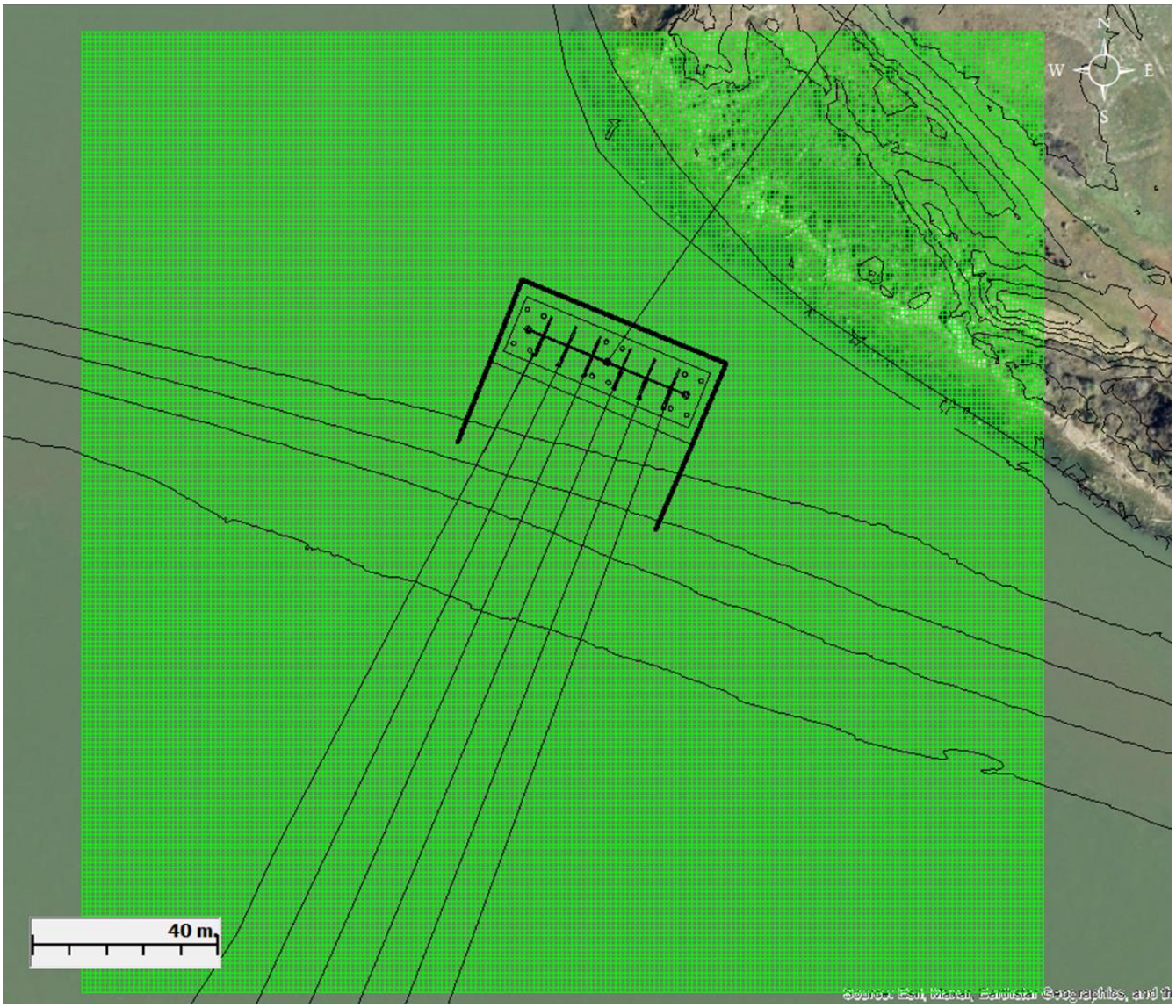

TABLE 3-8: GRID DIMENSIONS FOR R1 NORTHERN SITE LOCATION

Grid	Horizontal Grid Cell Dimensions (m)	Vertical Grid Cell Dimensions
Particle (2-D)	1 m x 1 m	N/A
Depositional (2-D)	1 m x 1 m	N/A
Concentration (3-D)	1 m x 1 m	1 m

Note: m = meter; N/A = Not Applicable.

3.4.3 SOUTHERN SITE LOCATION

The two-dimensional particle grid for the open trenching approach in the southern area is a rectangle approximately covering a 150 meter by 100 meter domain, with each cell 1 meter by 1 meter. Figure 3-21 shows the extent of the particle grid.

FIGURE 3-21: PARTICLE GRID DOMAIN (BLACK BOX) FOR SOUTHERN SCENARIOS AND CLOSE UP VIEW OF GRID (GREEN BOX)

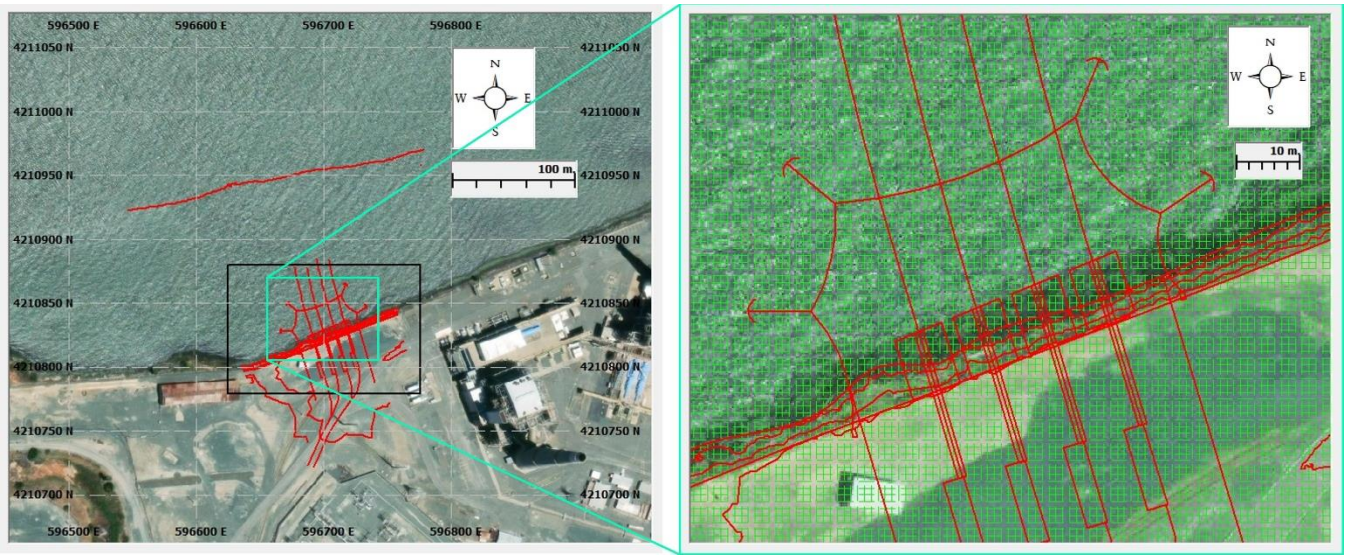

The depositional grid is a rectangle, approximately 150 meters by 100 meters with each cell 1 meter by 1 meter. Figure 3-22 shows a closer look at the depositional grid.

The concentration grid has the same horizontal dimensions as the depositional grid. Vertically, the cell thicknesses range from 0.1 meters at the surface to 1 meter at the bottom of the water column.

A summary of the dimensions of these grids is presented in Table 3-9.

FIGURE 3-22: DEPOSITIONAL AND CONCENTRATION GRID FOR SOUTHERN SITE LOCATION

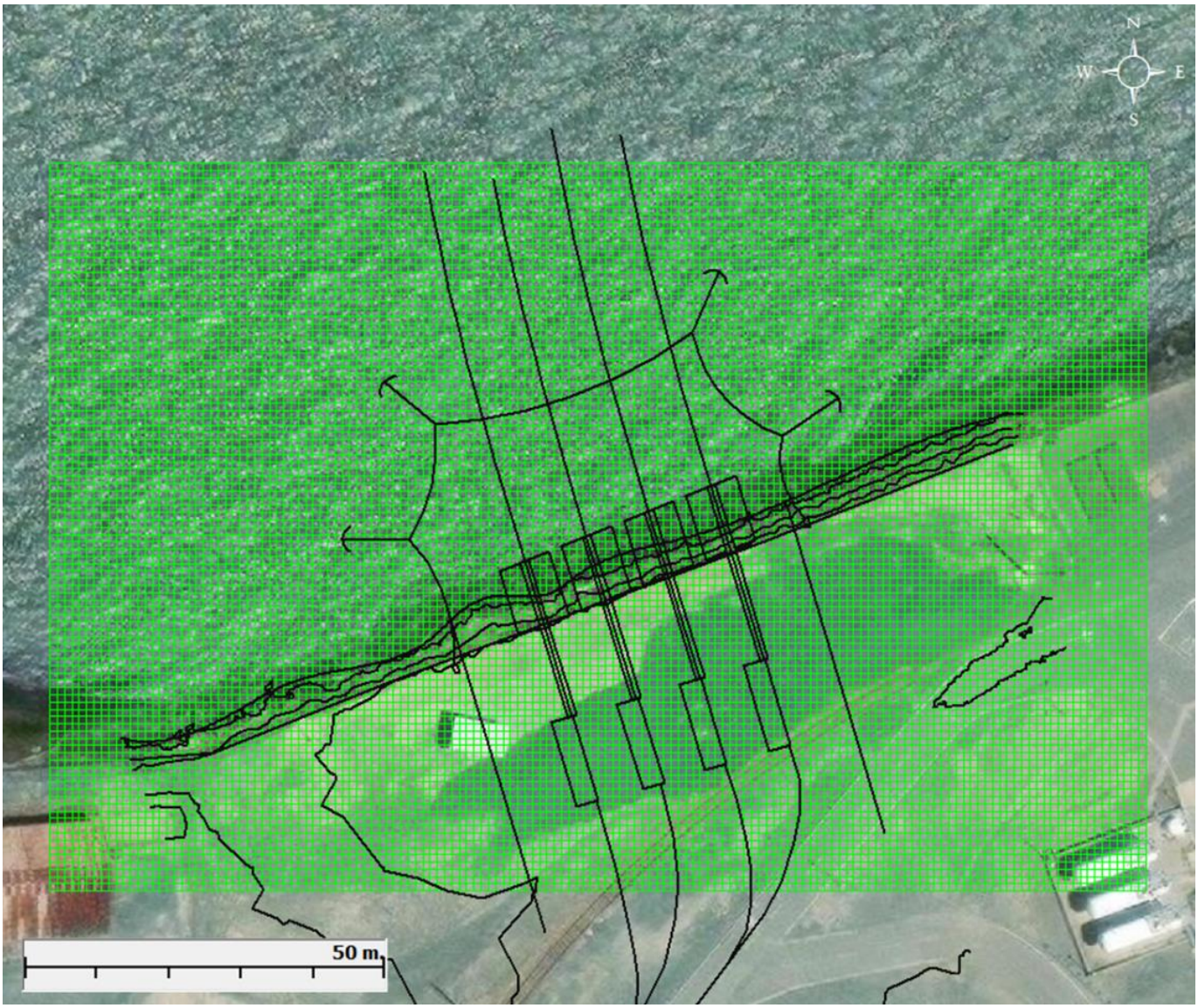

TABLE 3-9: GRID DIMENSIONS FOR SOUTHERN SITE LOCATION

Grid	Horizontal Grid Cell Dimensions (m)	Vertical Grid Cell Dimensions
Particle (2-D)	1 m x 1 m	N/A
Depositional (2-D)	1 m x 1 m	N/A
Concentration (3-D)	1 m x 1 m	Varies: 0.1 m near the water surface and 1 m near the riverbed

Note: m = meter; N/A = Not Applicable.

4. RESULTS

TSS and depositional thickness results of the simulations due to activities related to cable installation are presented in this section. The results are presented as contour plots and summary tables. The contour plots show the spatial spread of parameters of concern around the location of the proposed cable route. The results are presented for the following parameters:

- TSS is measured in milligrams per liter; and
- Depositional thickness in millimeters.

The seabed thickness values at the end of the simulations are discussed in Section 4.2, which represent the maximum accumulation of deposits to provide a conservative estimate of the potential environmental impact. This assumption of maximum accumulation of deposits is conservative because it does not account for natural processes such as erosion and slumping that would typically reduce the mound height over time. For the northern and southern scenarios (Scenarios 3 through 14), only the depositional footprint for the R2 northern scenarios was analyzed, as in the other scenarios dispersed sediments were contained in the enclosed environment by either silt curtains or sheet piles.

4.1 TOTAL SUSPENDED SOLIDS

4.1.1 ENTIRE CABLE ROUTE

For the 1-day simulation of sediment dispersion in both scenarios, TSS concentrations were examined. Figure 4-1 and Figure 4-2 show the maximum TSS concentrations that occur during Scenario 1 and Scenario 2, respectively. During Scenario 1 (minimum currents) and Scenario 2 (maximum currents), the maximum TSS concentrations within the plume are 15 mg/L and 20 mg/L, respectively. These maximum TSS concentrations do not have a long duration as, by the end of the 1-day simulations, the TSS has settled around the cable path.

FIGURE 4-1: SCENARIO 1 - MAXIMUM TSS CONCENTRATION, MINIMUM CURRENT SPEED

Note: TSS below 0.1 mg/L is not shown.

FIGURE 4-2: SCENARIO 2 - MAXIMUM TSS CONCENTRATION, MAXIMUM CURRENT SPEED

Note: TSS below 0.1 mg/L is not shown.

4.1.2 NORTHERN SITE IN-RIVER TRANSITION

For the 3-day simulation of sediment dispersion in Scenarios 3 through 10, TSS concentrations were examined. Table 4-1 summarizes the resulting maximum, average, and end of simulation TSS concentrations for all R1 region scenarios. Figure 4-3 and Figure 4-5 show the maximum TSS concentrations that occur during the excavation of the R1 region for Scenario 3 and Scenario 4, respectively. The maximum TSS concentrations are transient and occur very near the bed for a very short period of time during the initiation of each operation. That is depicted by the average

TSS concentrations which are much lower than the maximum TSS as shown in Table 4-1. In addition, TSS concentrations decrease to less than 1 mg/L within 28.5 hours after the end of the releases as shown in Table 4-1, Figure 4-4, and Figure 4-6. During Scenario 3 (minimum currents) and Scenario 4 (maximum currents), the maximum TSS concentrations within the plume are 9,995 mg/L and 10,035 mg/L, respectively. Note that given impermeability in the sheet piling assumption, there was no flow within the enclosed northern area; thus, results under minimum and maximum current speeds are nearly identical. Also due to excavation and backfilling of area R1 within the sheet piles, all TSS concentrations are contained only in the area within the sheet piles with no impact on the surroundings, as they form a completely enclosed area.

TABLE 4-1: SUMMARY OF TSS RESULTS FOR R1 REGION OF THE NORTHERN IN-RIVER TRANSITION SCENARIOS, WITHIN ENCLOSED AREA BY SHEET PILES

Scenario	Maximum TSS Concentration (mg/L)[A]	Average TSS Concentration (mg/L)	End of Simulation TSS Concentration (mg/L)
3 north-excavR1-min	9995	101	0.068
4 north-excavR1-max	10035	231	0.006
5 north-backR1-min	250030	2614	0.968
6 north-backR1-max	250238	2909	0.011

Note A: The maximum TSS concentrations are transient and occur very near the bed for a very short period of time at the start of each operation.

FIGURE 4-3: SCENARIO 3 - MAXIMUM TSS CONCENTRATION, R1 EXCAVATION, MINIMUM CURRENT SPEED

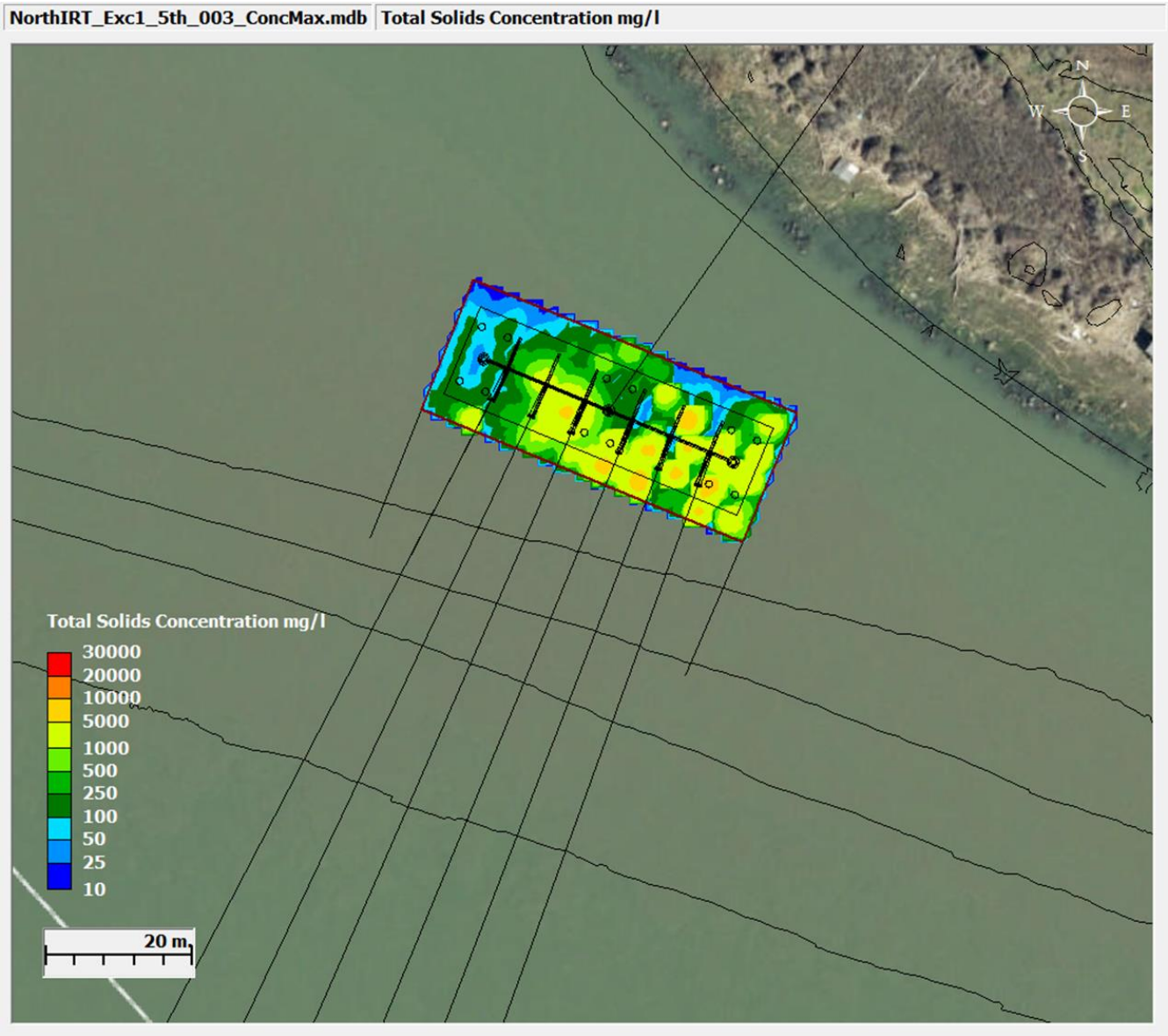

Note: TSS below 10 mg/L is not shown.

FIGURE 4-4: SCENARIO 3 – END OF SIMULATION TSS CONCENTRATION, R1 EXCAVATION, MINIMUM CURRENT SPEED

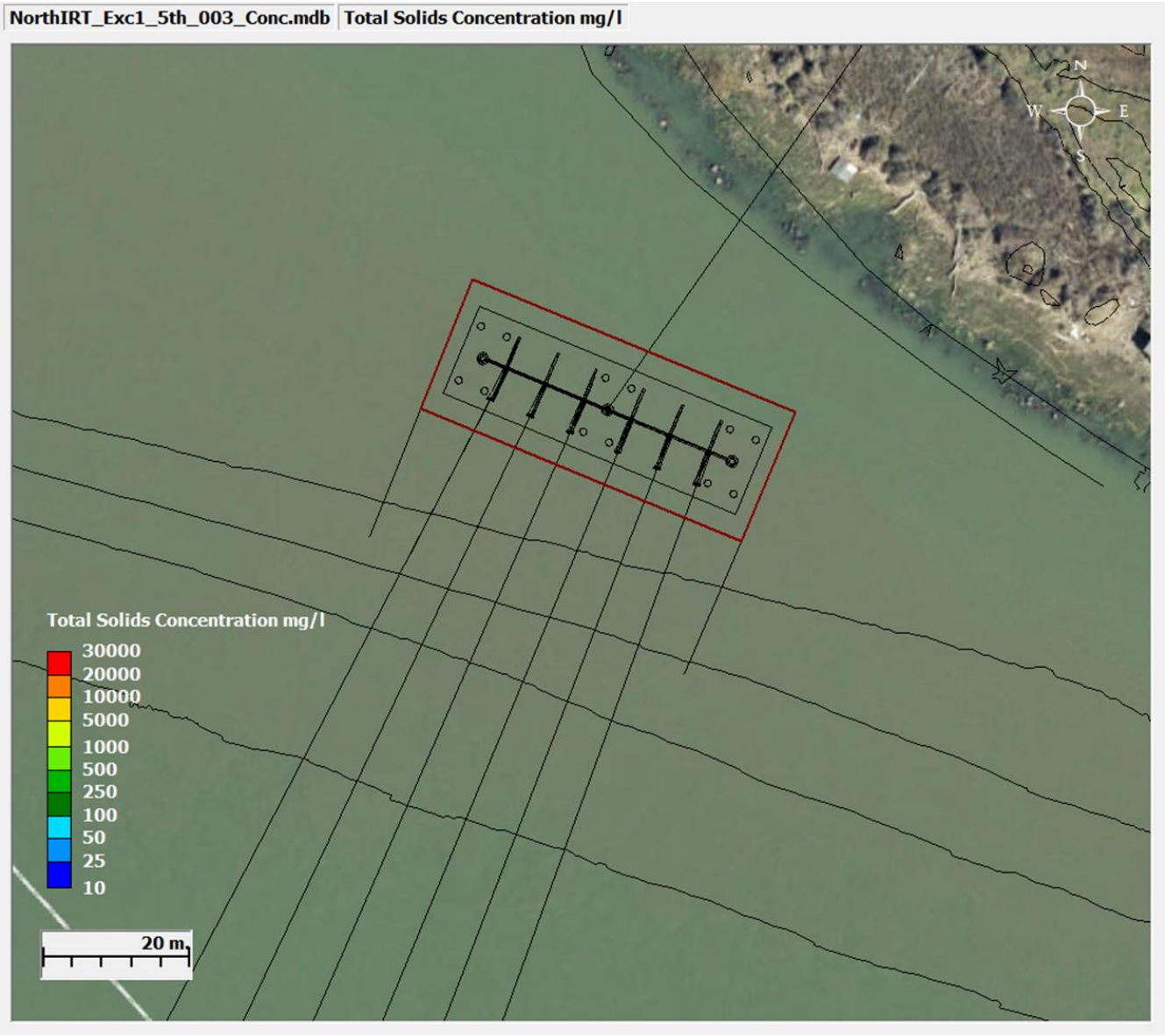

Note: TSS below 10 mg/L is not shown.

FIGURE 4-5: SCENARIO 4 - MAXIMUM TSS CONCENTRATION DURING R1 EXCAVATION, MAXIMUM CURRENT SPEED

Note: TSS below 10 mg/L is not shown.

FIGURE 4-6: SCENARIO 4 – END OF SIMULATION TSS CONCENTRATION, R1 EXCAVATION, MAXIMUM CURRENT SPEED

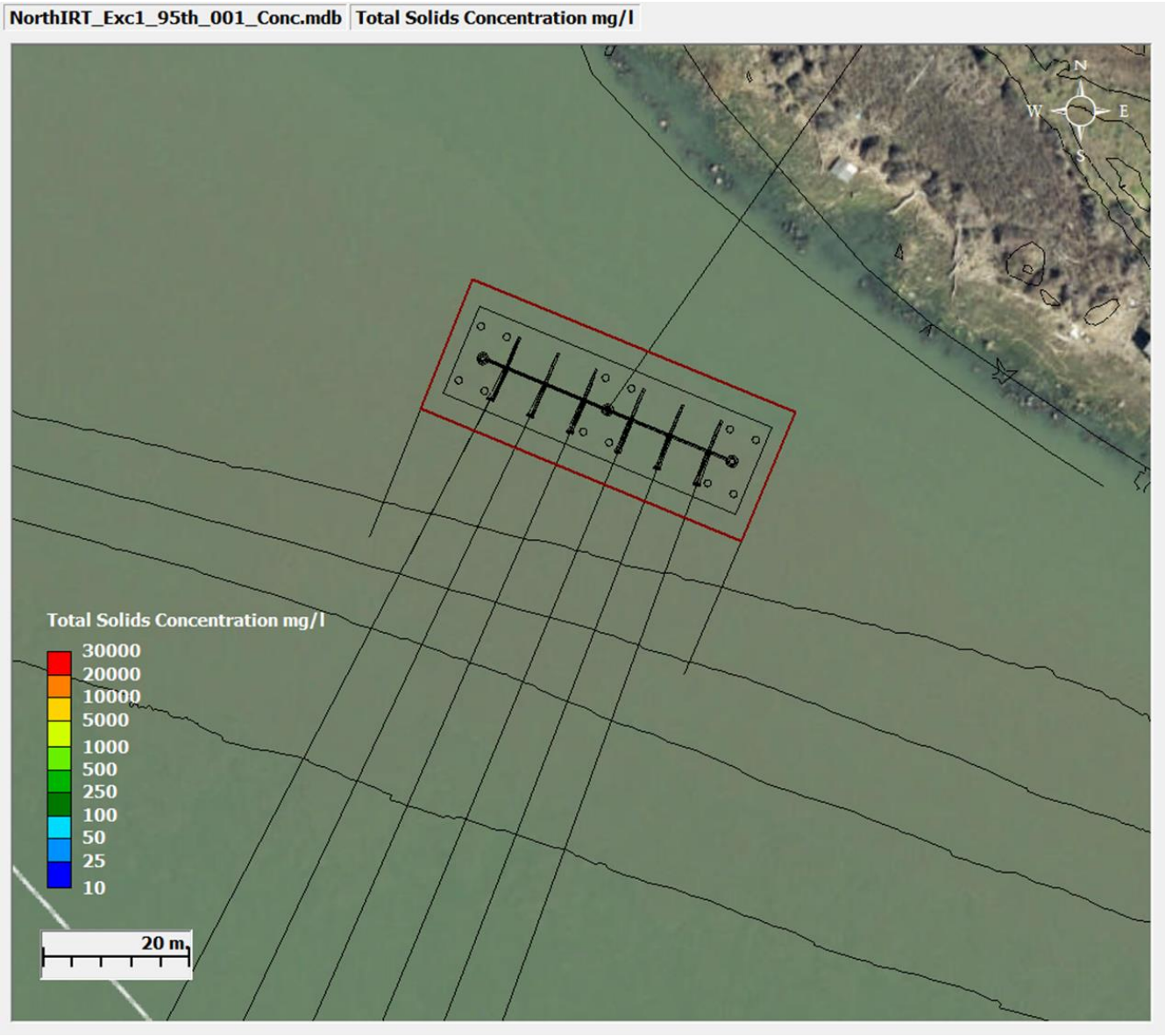

Note: TSS below 10 mg/L is not shown.

During backfilling scenarios (Scenarios 5 and 6), the TSS values were larger than those seen during the excavation, as the release amount was large. Figure 4-7 and Figure 4-9 show the maximum TSS concentrations that occur during Scenario 5 and Scenario 6, respectively. During Scenario 5 (minimum currents) and Scenario 6 (maximum currents), the maximum TSS concentrations within the plume are 250,030 mg/L and 250,238 mg/L, respectively. The maximum TSS concentrations are transient and occur very near the bed for a very short period of time during the initiation of each operation. That is depicted by the average TSS concentrations which are much lower than the maximum TSS as shown in Table 4-1. In addition, TSS concentrations decrease to less than 1 mg/L within 28.5 hours after the end of the releases as shown in Figure

4-8 and Figure 4-10. As with the excavation operations for the R1 region, the TSS concentrations during backfilling are contained only in the area within the sheet piles with no impact on the surroundings, as they form a completely enclosed area.

FIGURE 4-7: SCENARIO 5 - MAXIMUM TSS CONCENTRATION DURING R1 BACKFILLING, MINIMUM CURRENT SPEED

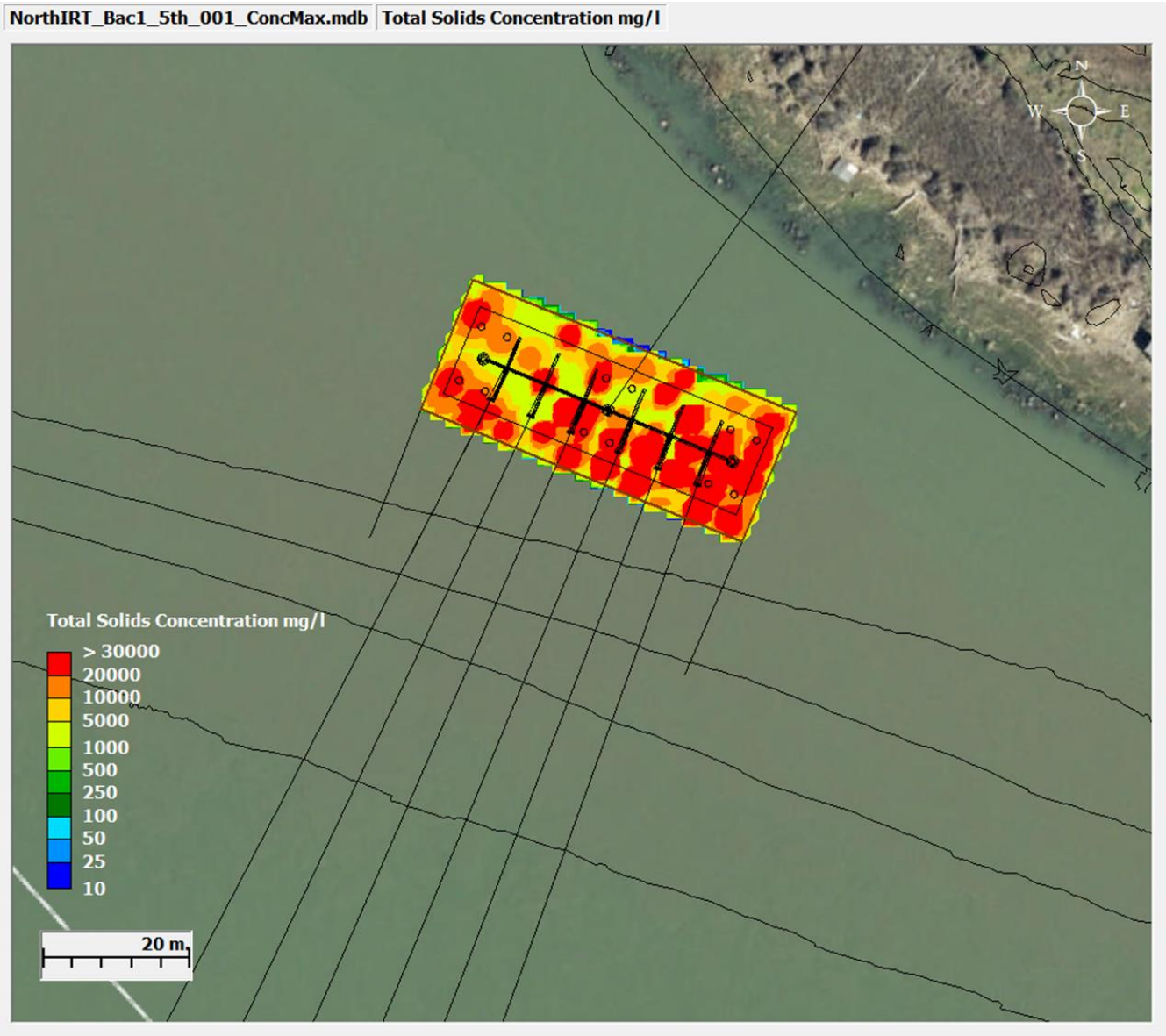

Note: TSS below 10 mg/L is not shown.

FIGURE 4-8: SCENARIO 5 – END OF SIMULATION TSS CONCENTRATION R1 BACKFILLING, MINIMUM CURRENT SPEED

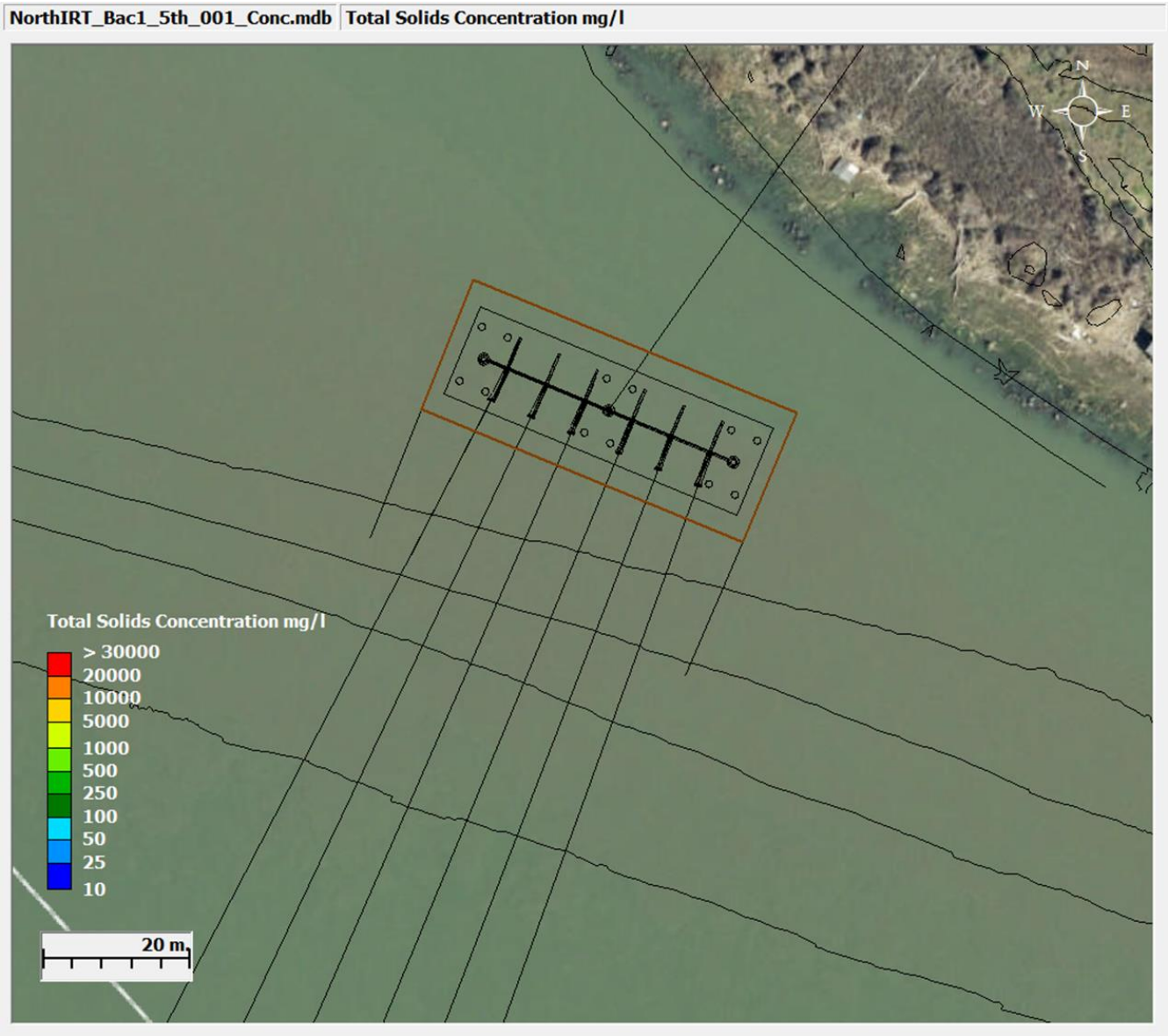

Note: TSS below 10 mg/L is not shown.

FIGURE 4-9: SCENARIO 6 - MAXIMUM TSS CONCENTRATION DURING R1 BACKFILLING, MAXIMUM CURRENT SPEED

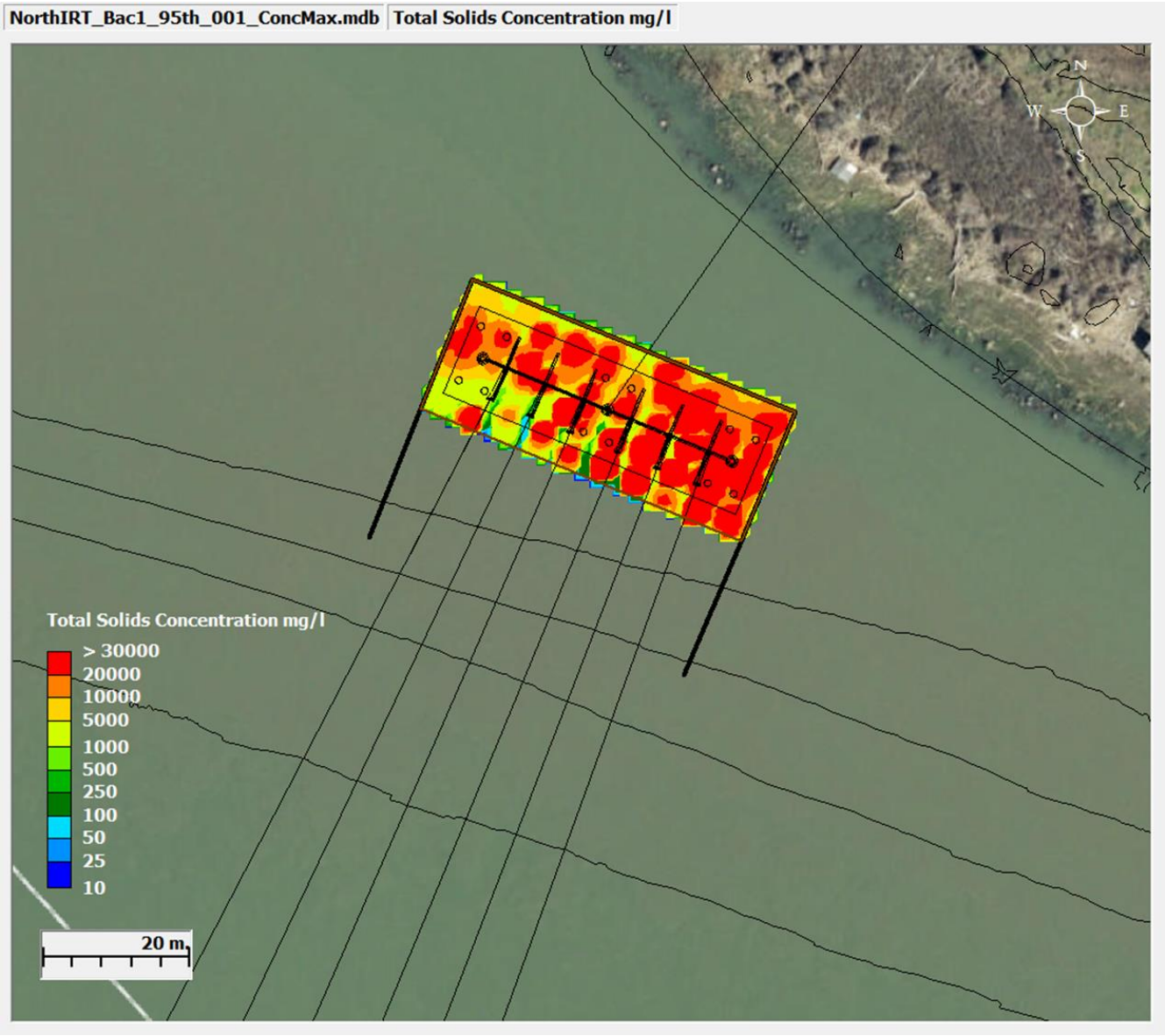

Note: TSS below 10 mg/L is not shown.

FIGURE 4-10: SCENARIO 6 – END OF SIMULATION TSS CONCENTRATION, R1 BACKFILLING, MAXIMUM CURRENT SPEED

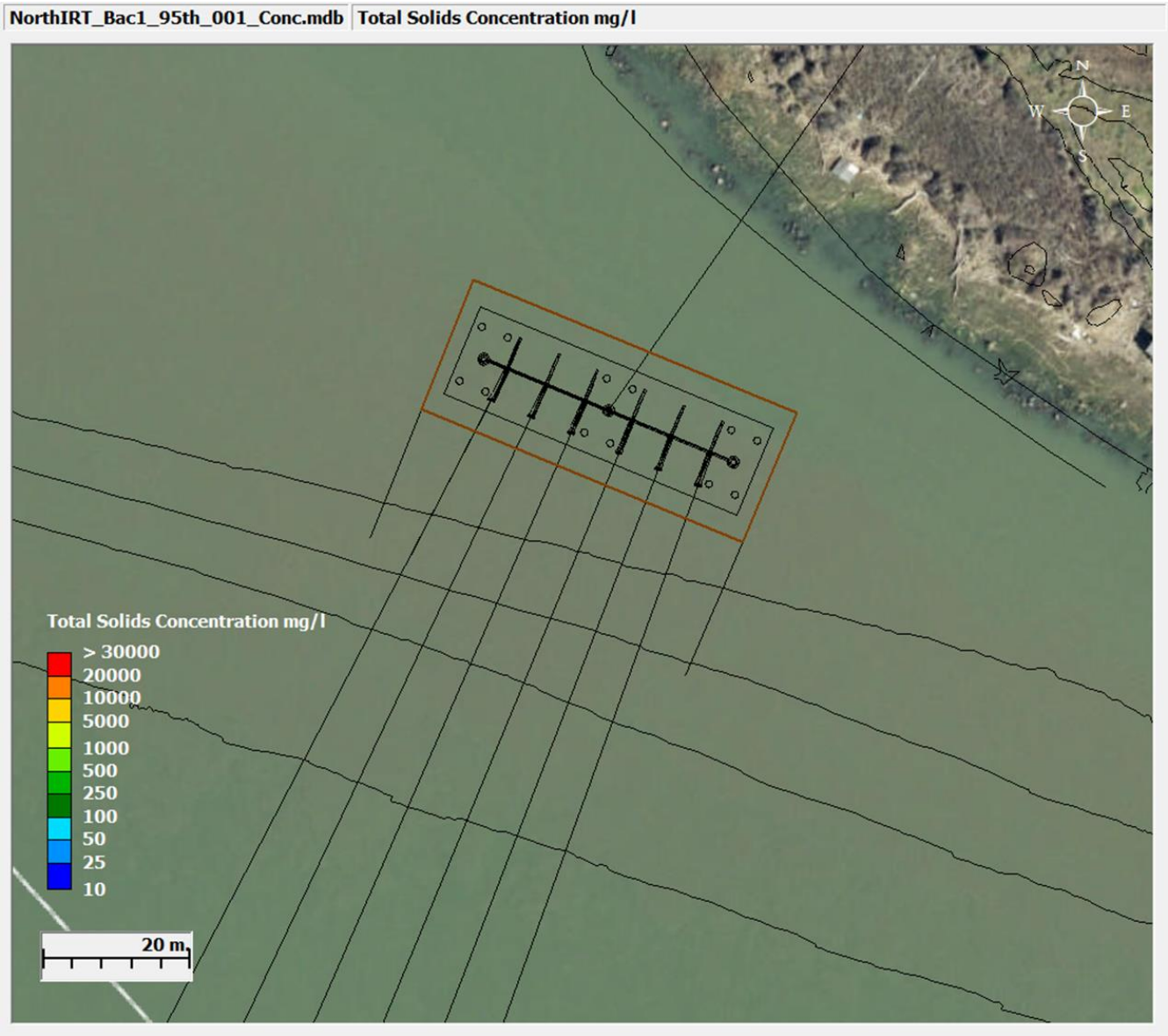

Note: TSS below 10 mg/L is not shown.

During the excavation of the R2 region, TSS levels were examined. Table 4-2 summarizes the resulting maximum, average, and end of simulation TSS concentrations for all R2 region scenarios. Figure 4-11 and Figure 4-13 show the maximum TSS concentrations that occur during Scenario 7 and Scenario 8, respectively. During Scenario 7 (minimum currents) and Scenario 8 (maximum currents), the maximum TSS concentrations within the plume are 10,380 mg/L and 10,381 mg/L, respectively. The maximum TSS concentrations are transient and occur very near the bed for a very short period of time during the initiation of each operation. That is depicted by the average TSS concentrations which are much lower than the maximum TSS as shown in Table

4-2. In addition, TSS concentrations decrease to less than 1 mg/L within 28.5 hours after the end of the releases as shown in Figure 4-12 and Figure 4-14.

TABLE 4-2: SUMMARY OF TSS RESULTS FOR R2 REGION OF THE NORTHERN IN-RIVER TRANSITION SCENARIOS

Scenario	Maximum TSS Concentration (mg/L)[A]	Average TSS Concentration (mg/L)	End of Simulation TSS Concentration (mg/L)
7 north-excavR2-min	10380	104	0.00
8 north-excavR2-max	10381	78	0.00
9 north-backR2-min	259493	2557	0.00
10 north-backR2-max	261919	2106	0.72

Note A: The maximum TSS concentrations are transient and occur very near the bed for a very short period of time at the start of each operation.

FIGURE 4-11: SCENARIO 7 - MAXIMUM TSS CONCENTRATION DURING R2 EXCAVATION, MINIMUM CURRENT SPEED

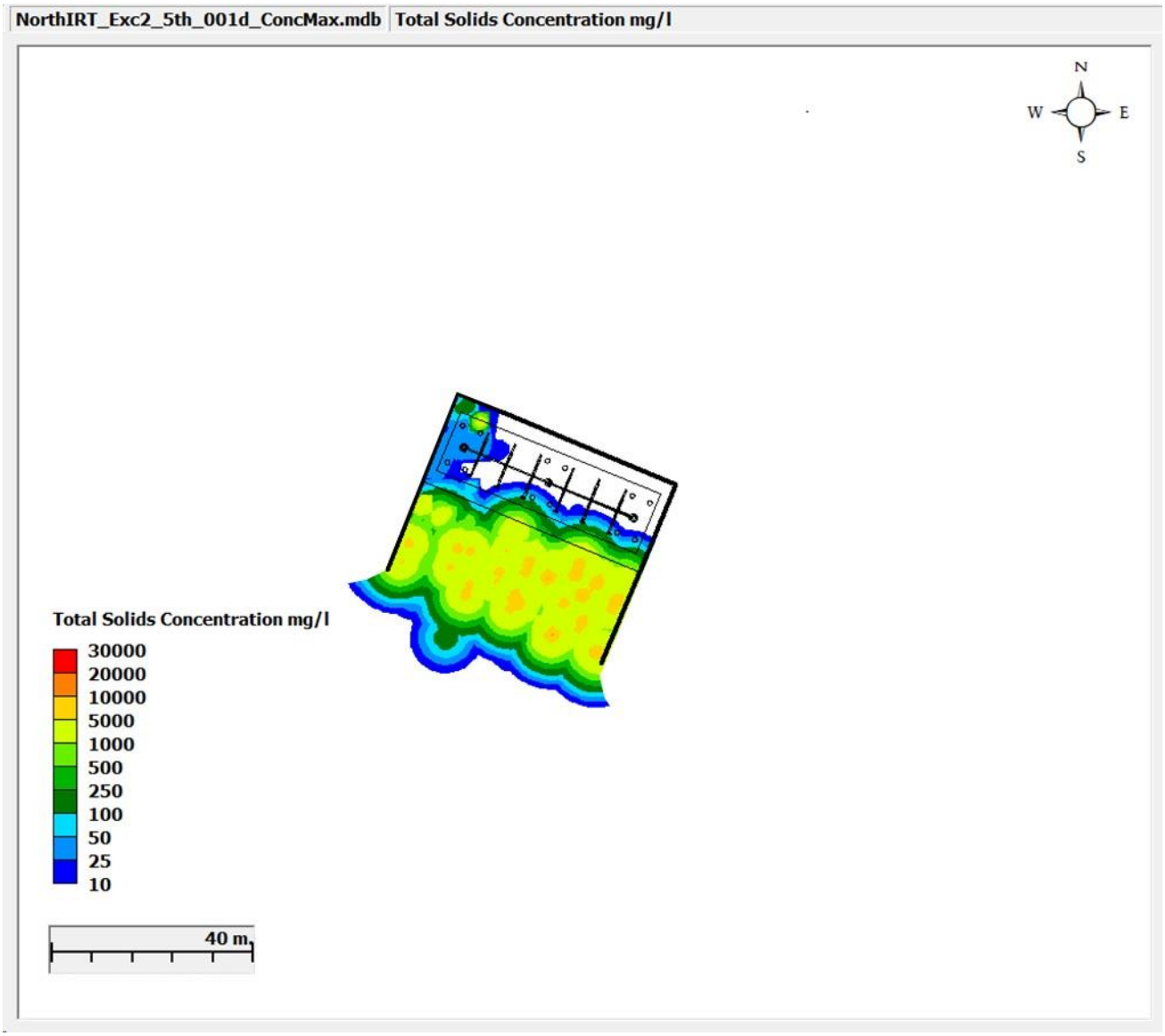

Note: TSS below 10 mg/L is not shown.

FIGURE 4-12: SCENARIO 7 – END OF SIMULATION TSS CONCENTRATION DURING R2 EXCAVATION, MINIMUM CURRENT SPEED

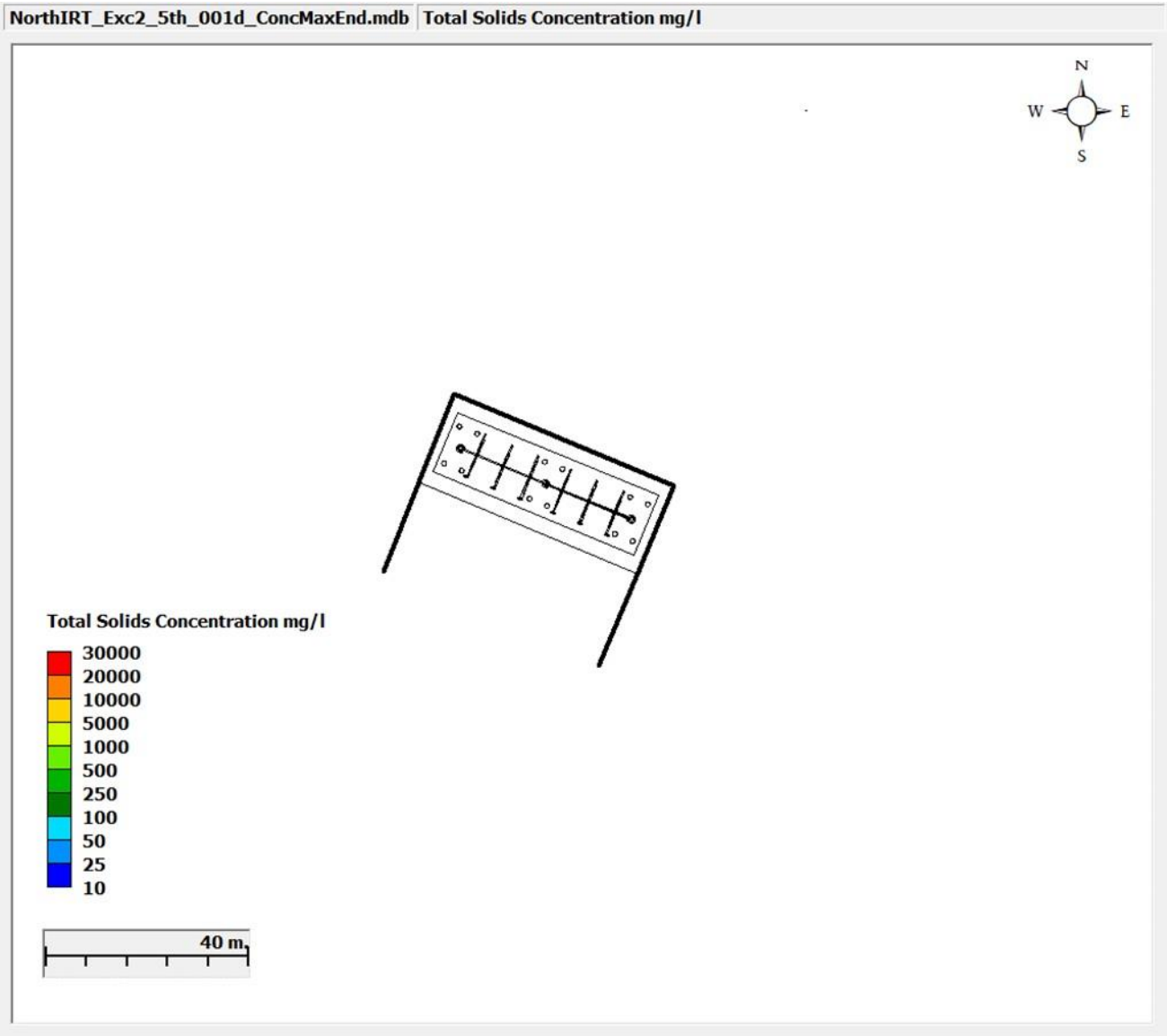

Note: TSS below 10 mg/L is not shown.

FIGURE 4-13: SCENARIO 8 - MAXIMUM TSS CONCENTRATION DURING R2 EXCAVATION, MAXIMUM CURRENT SPEED

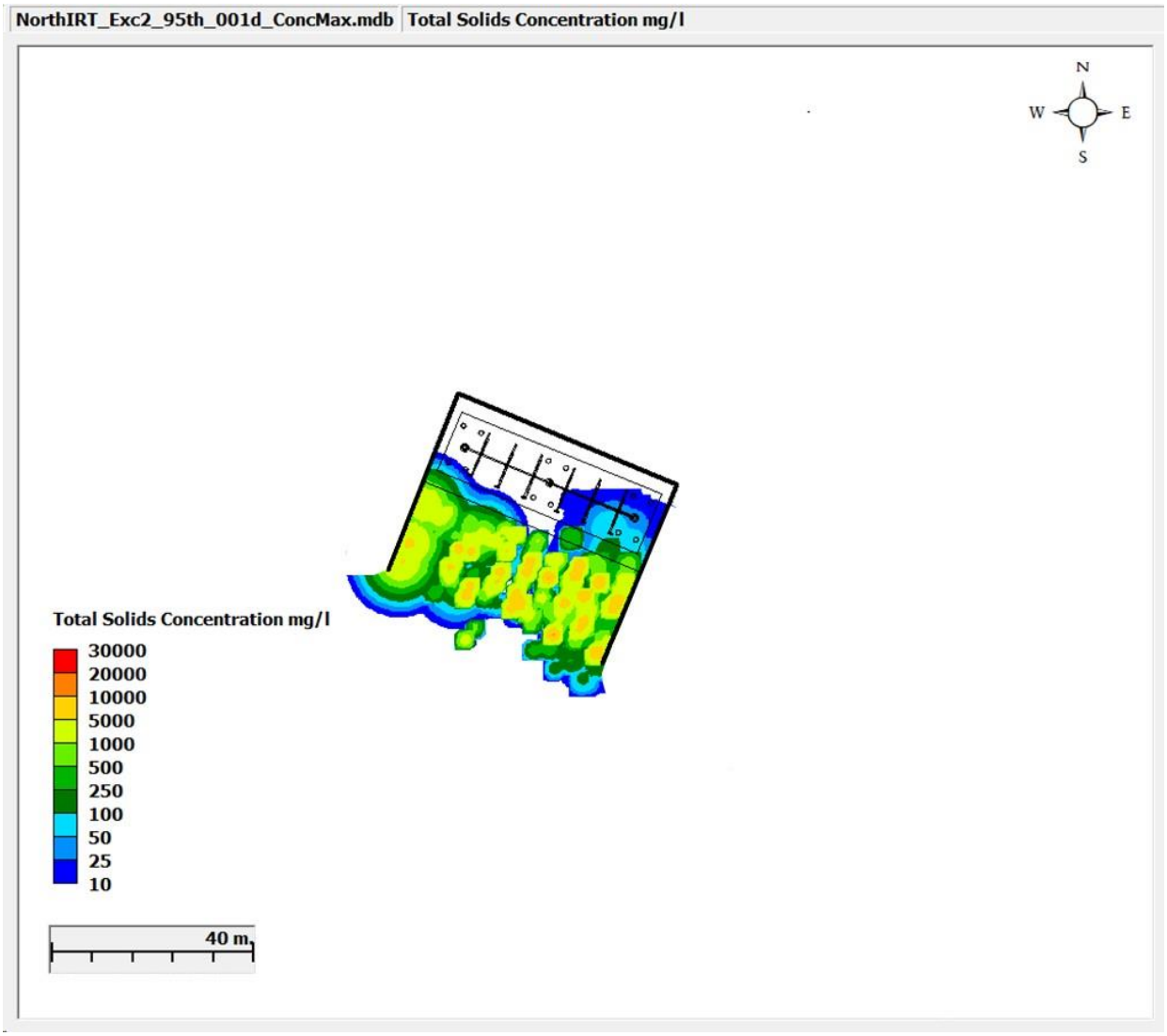

Note: TSS below 10 mg/L is not shown.

FIGURE 4-14: SCENARIO 8 – END OF SIMULATION TSS CONCENTRATION, R2 EXCAVATION, MAXIMUM CURRENT SPEED

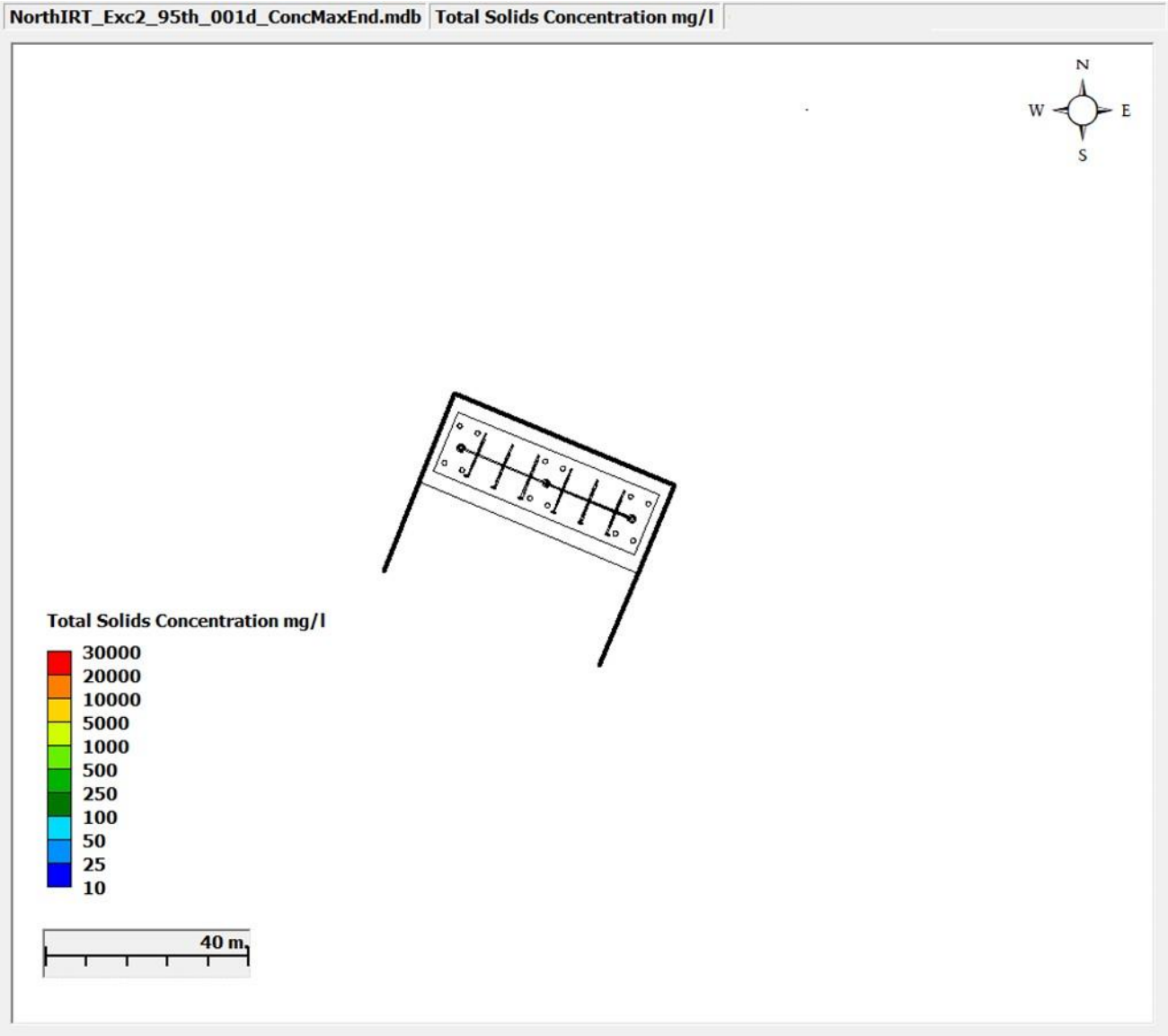

Note: TSS below 10 mg/L is not shown.

During backfilling scenarios (Scenarios 9 and 10) of R2, the TSS values were larger than those seen during the excavation operations as the released sediment amount was larger (Table 4-2). Figure 4-15 and Figure 4-17 show the maximum TSS concentrations that occur during Scenario 9 and Scenario 10, respectively. During Scenario 9 (minimum currents) and Scenario 10 (maximum currents), the maximum TSS concentrations within the plume are 259,493 mg/L and 261,919 mg/L, respectively. The maximum TSS concentrations are transient and occur very near the bed for a very short period of time during the initiation of each operation. That is depicted by the average TSS concentrations which are much lower than the maximum TSS as shown in Table 4-2.

In addition, TSS concentrations decrease to less than 1 mg/L within 28.5 hours after the end of the releases as shown in Figure 4-16 and Figure 4-18.

FIGURE 4-15: SCENARIO 9 - MAXIMUM TSS CONCENTRATION, R2 BACKFILLING, MINIMUM CURRENT SPEED

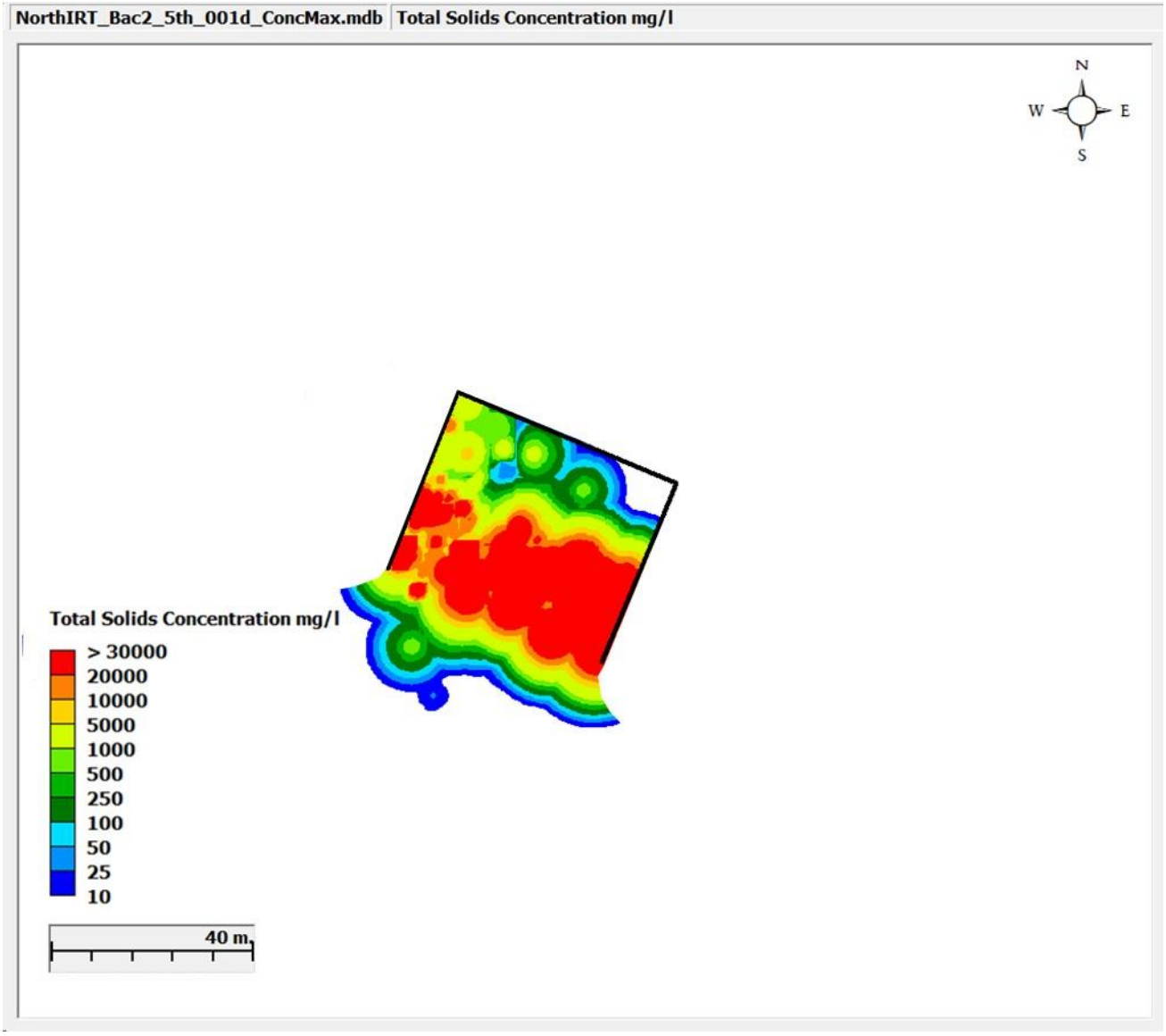

Note: TSS below 10 mg/L is not shown.

FIGURE 4-16: SCENARIO 9 – END OF SIMULATION TSS CONCENTRATION, R2 BACKFILLING, MINIMUM CURRENT SPEED

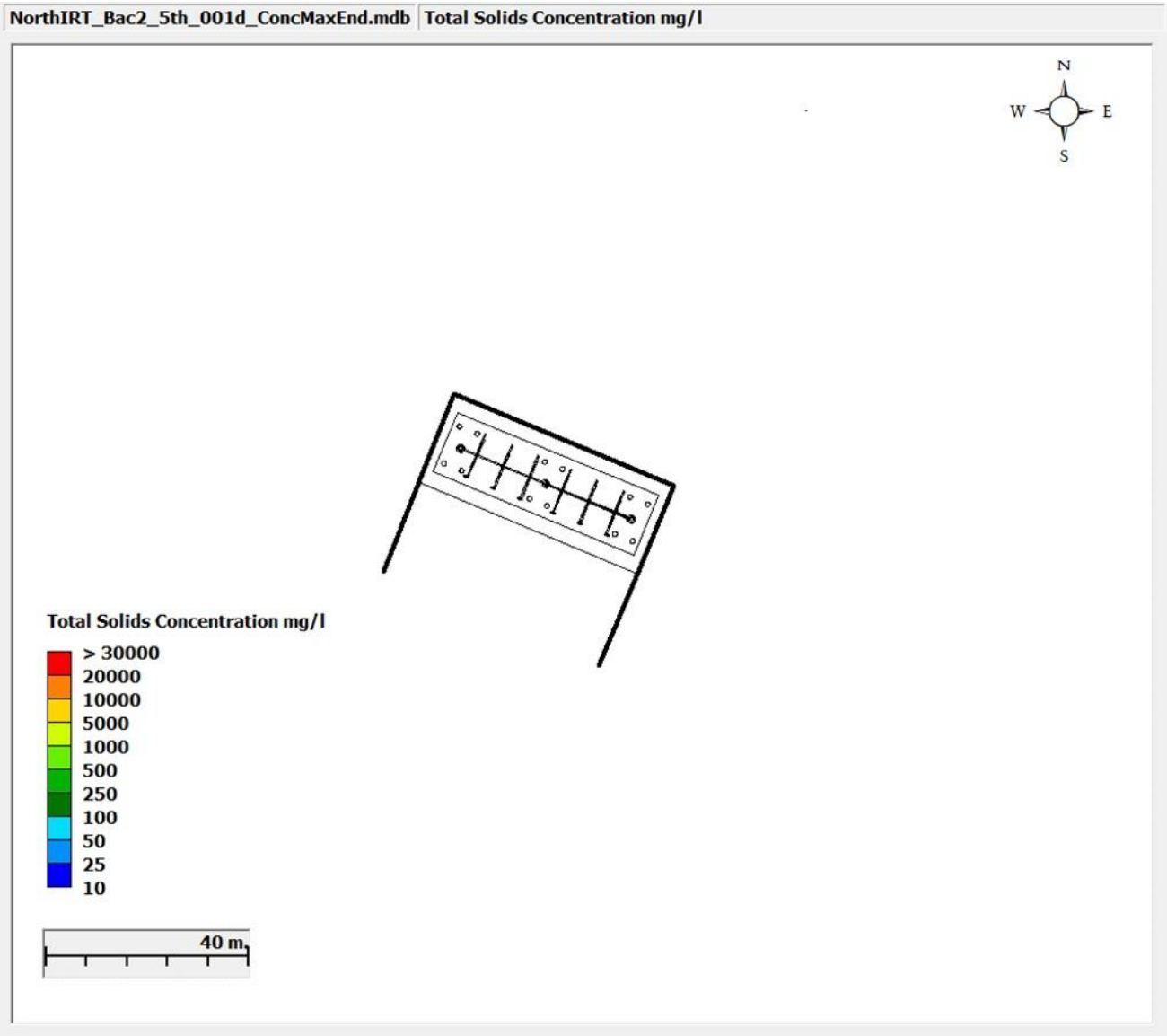

Note: TSS below 10 mg/L is not shown.

FIGURE 4-17: SCENARIO 10 - MAXIMUM TSS CONCENTRATION DURING R2 BACKFILLING, MAXIMUM CURRENT SPEED

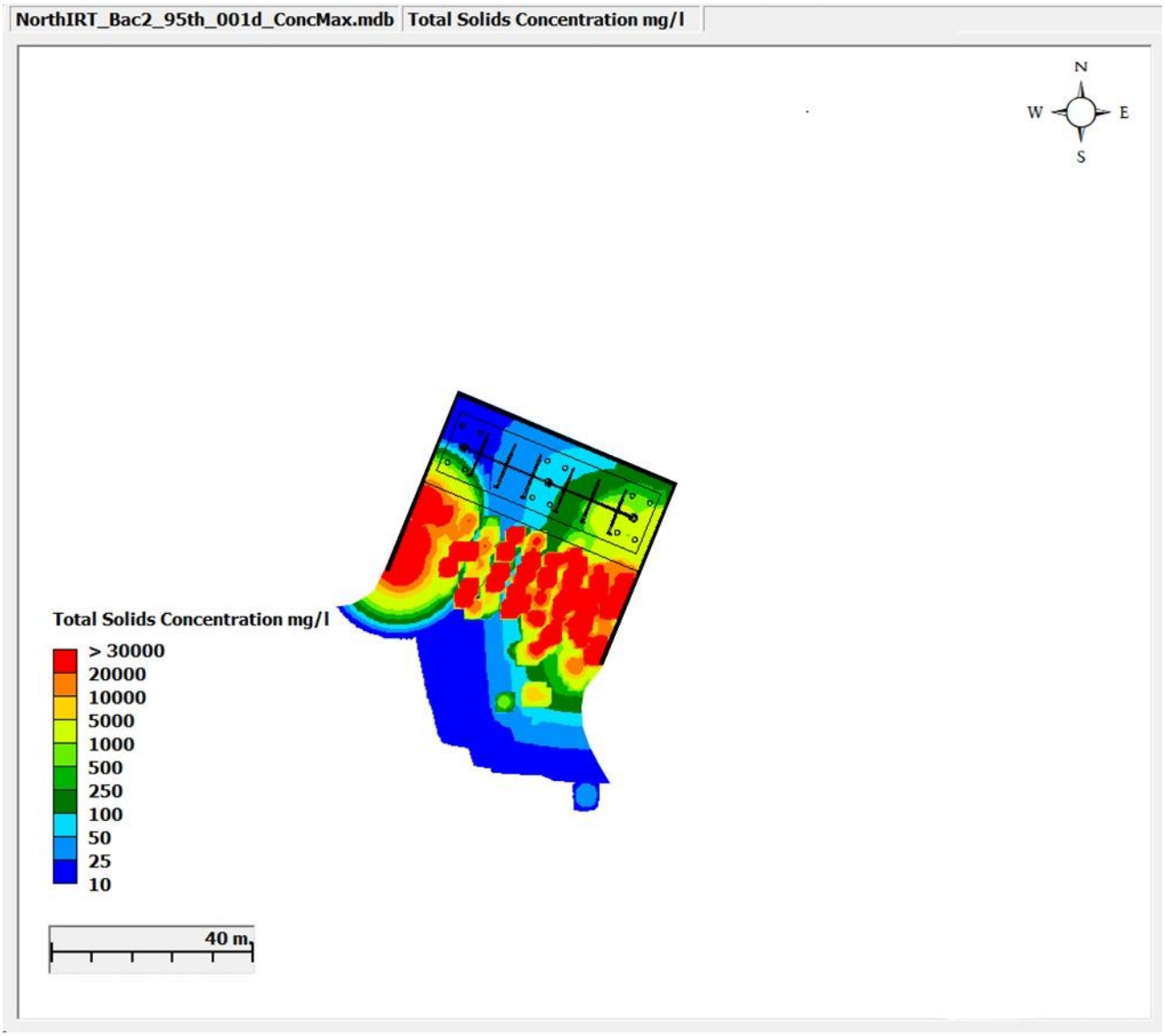

Note: TSS below 10 mg/L is not shown.

FIGURE 4-18: SCENARIO 10 – END OF SIMULATION TSS CONCENTRATION R2 BACKFILLING, MAXIMUM CURRENT SPEED

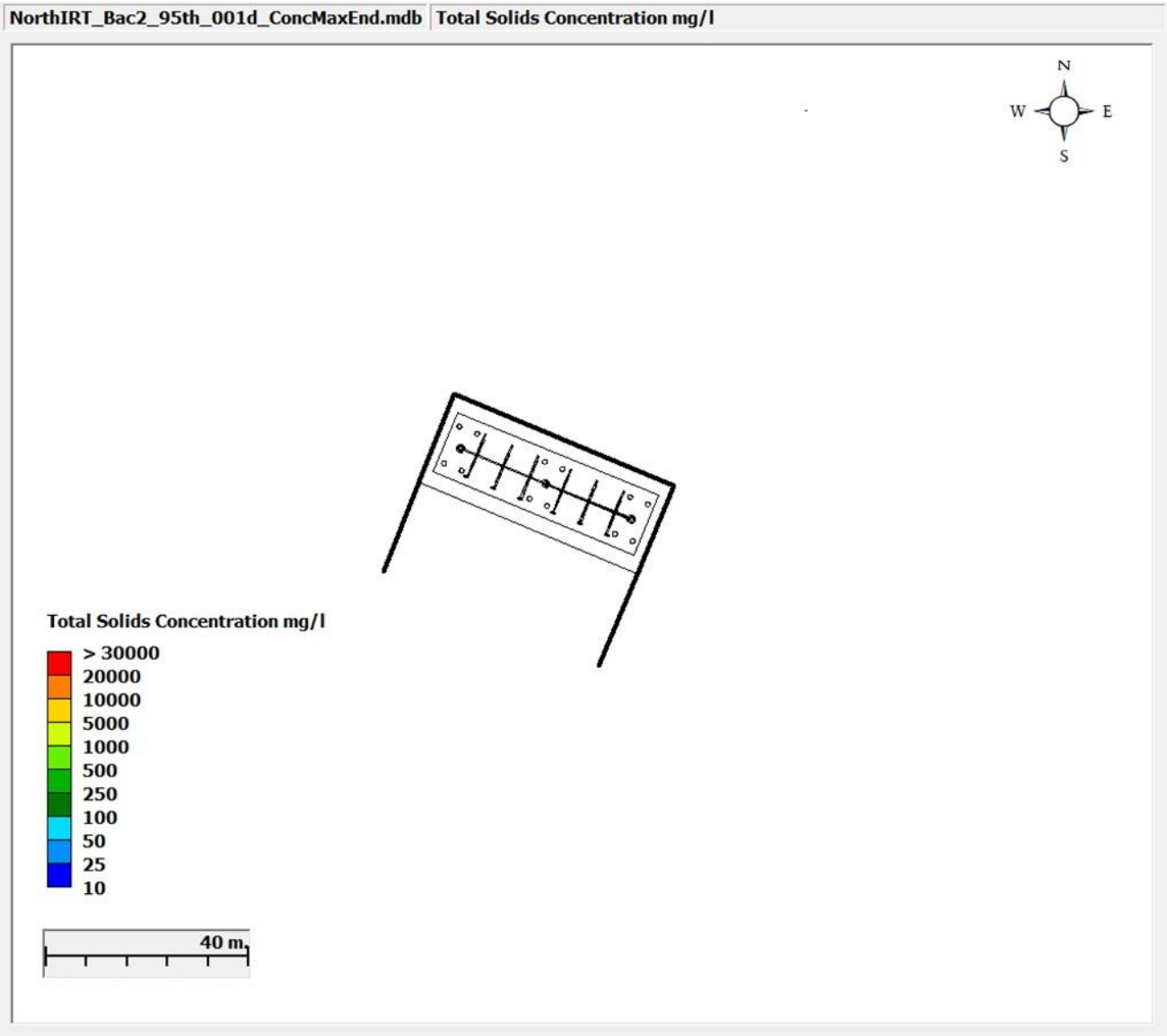

Note: TSS below 10 mg/L is not shown.

4.1.3 SOUTHERN SITE OPEN TRENCHING

For the 3-day simulation of particle deposition in Scenarios 11 through 14, TSS concentrations were examined. Given the assumption of semi-permeable silt curtains at the southern site location, there was current flow into the enclosed area, but the sediment was contained within the area. This resulted in TSS concentrations contained only in the area within the silt curtains with no impact on the surroundings, due to the completely enclosed area. Table 4-3 summarizes the resulting maximum, average, and end of simulation TSS concentrations for all southern site scenarios. Figure 4-19 and Figure 4-21 show the maximum TSS concentrations that occur during excavation Scenario 11 (minimum current) and Scenario 12 (maximum current), respectively.

During Scenario 11 (minimum currents) and Scenario 12 (maximum currents), the maximum TSS concentrations within the plume are 1,153 mg/L and 2,599 mg/L, respectively. The maximum TSS concentrations are transient and occur very near the bed for a very short period of time during the initiation of each operation. That is depicted by the average TSS concentrations which are much lower than the maximum TSS as shown in Table 4-3. In addition, TSS concentrations decrease to less than 1 mg/L within 32.7 hours after the end of the releases as shown in Figure 4-20, Figure 4-22, and Table 4-3.

TABLE 4-3: SUMMARY OF TSS RESULTS FOR SOUTHERN OPEN TRENCHING SCENARIOS

Scenario	Maximum TSS Concentration (mg/L)[A]	Average TSS Concentration (mg/L)	End of Simulation TSS Concentration (mg/L)
11 south-excav-min	1153	23	0.000
12 south-excav-max	2599	278	0.000
13 south-back-min	27469	359	0.000
14 south-back-max	31411	4299	0.068

Note A: The maximum TSS concentrations are transient and occur very near the bed for a very short period of time at the start of each operation.

FIGURE 4-19: SCENARIO 11 - MAXIMUM TSS CONCENTRATION DURING EXCAVATION, MINIMUM CURRENT SPEED

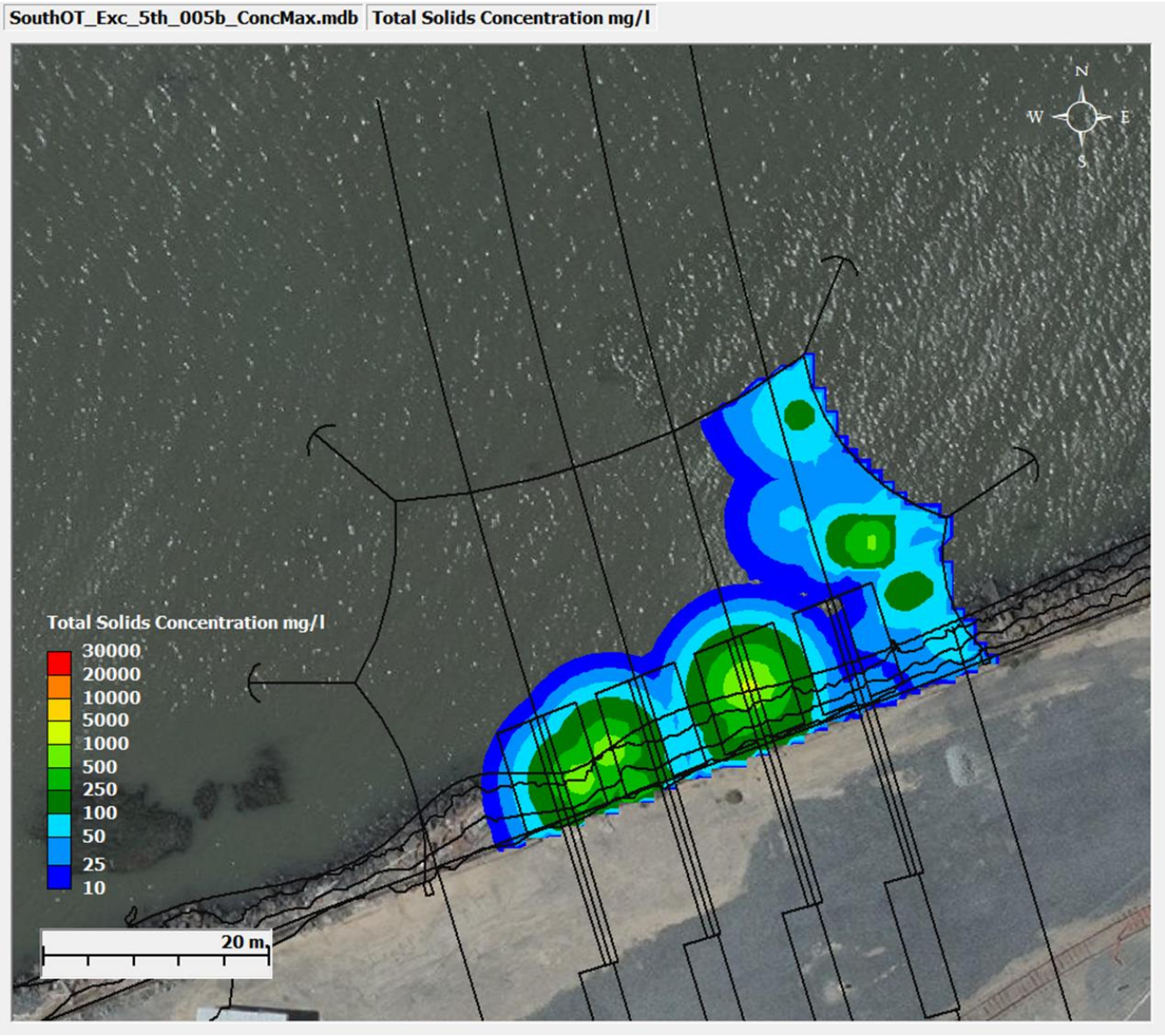

Note: TSS below 10 mg/L is not shown.

FIGURE 4-20: SCENARIO 11 – END OF SIMULATION TSS CONCENTRATION , EXCAVATION, MINIMUM CURRENT SPEED

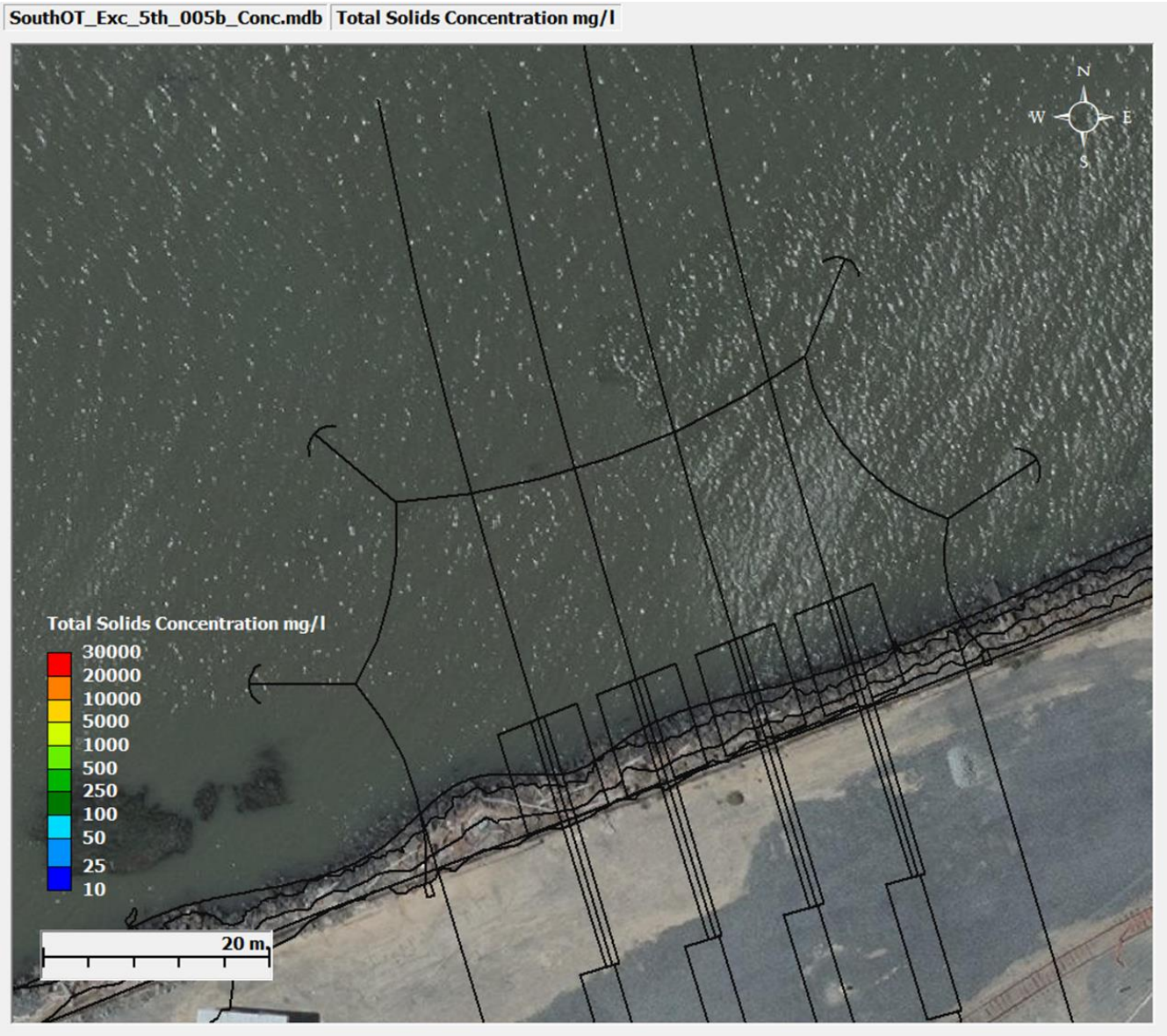

Note: TSS below 10 mg/L is not shown.

FIGURE 4-21: SCENARIO 12 - MAXIMUM TSS CONCENTRATION DURING EXCAVATION, MAXIMUM CURRENT SPEED

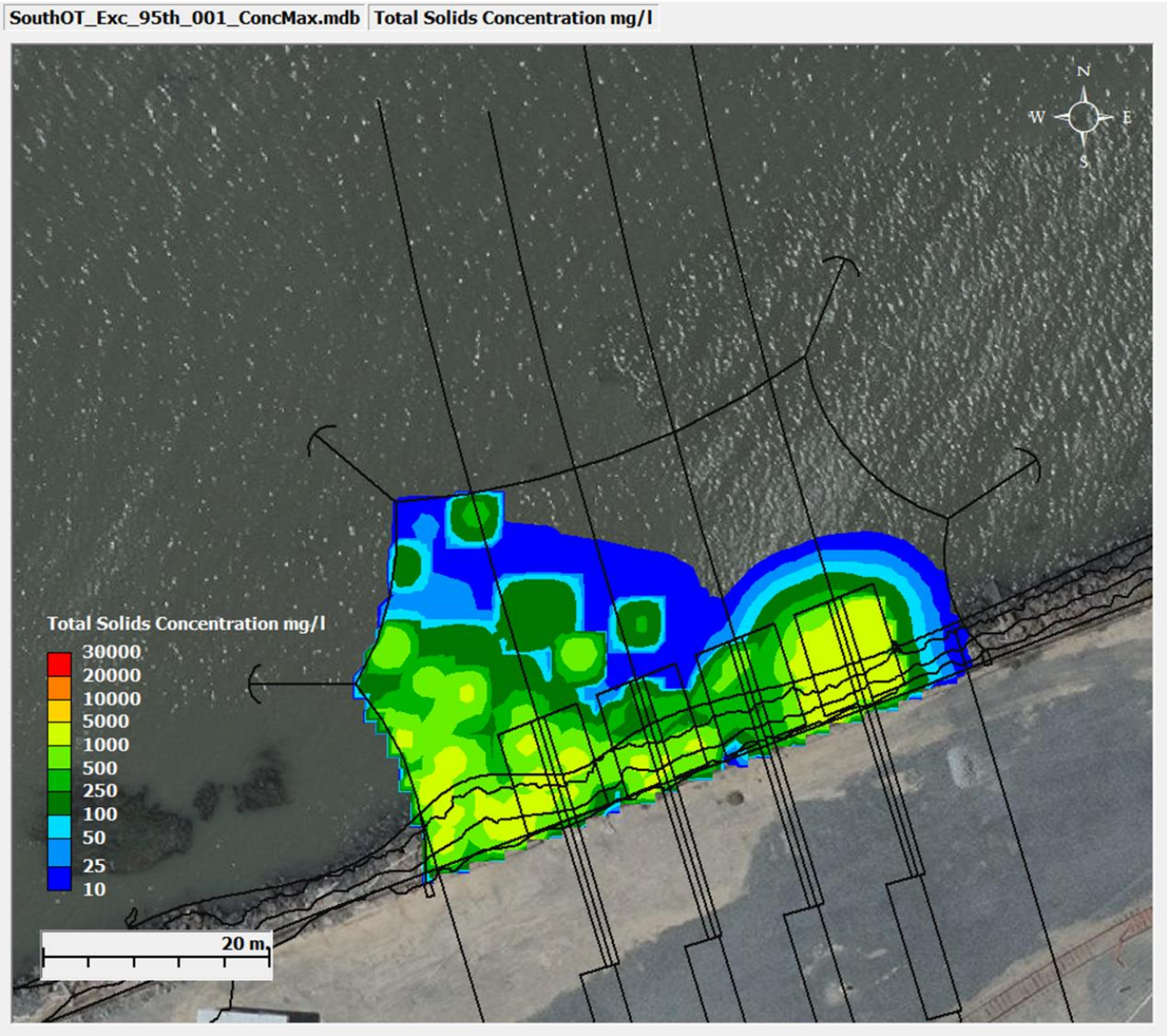

Note: TSS below 10 mg/L is not shown.

FIGURE 4-22: SCENARIO 11 – END OF SIMULATION TSS CONCENTRATION, EXCAVATION, MAXIMUM CURRENT SPEED

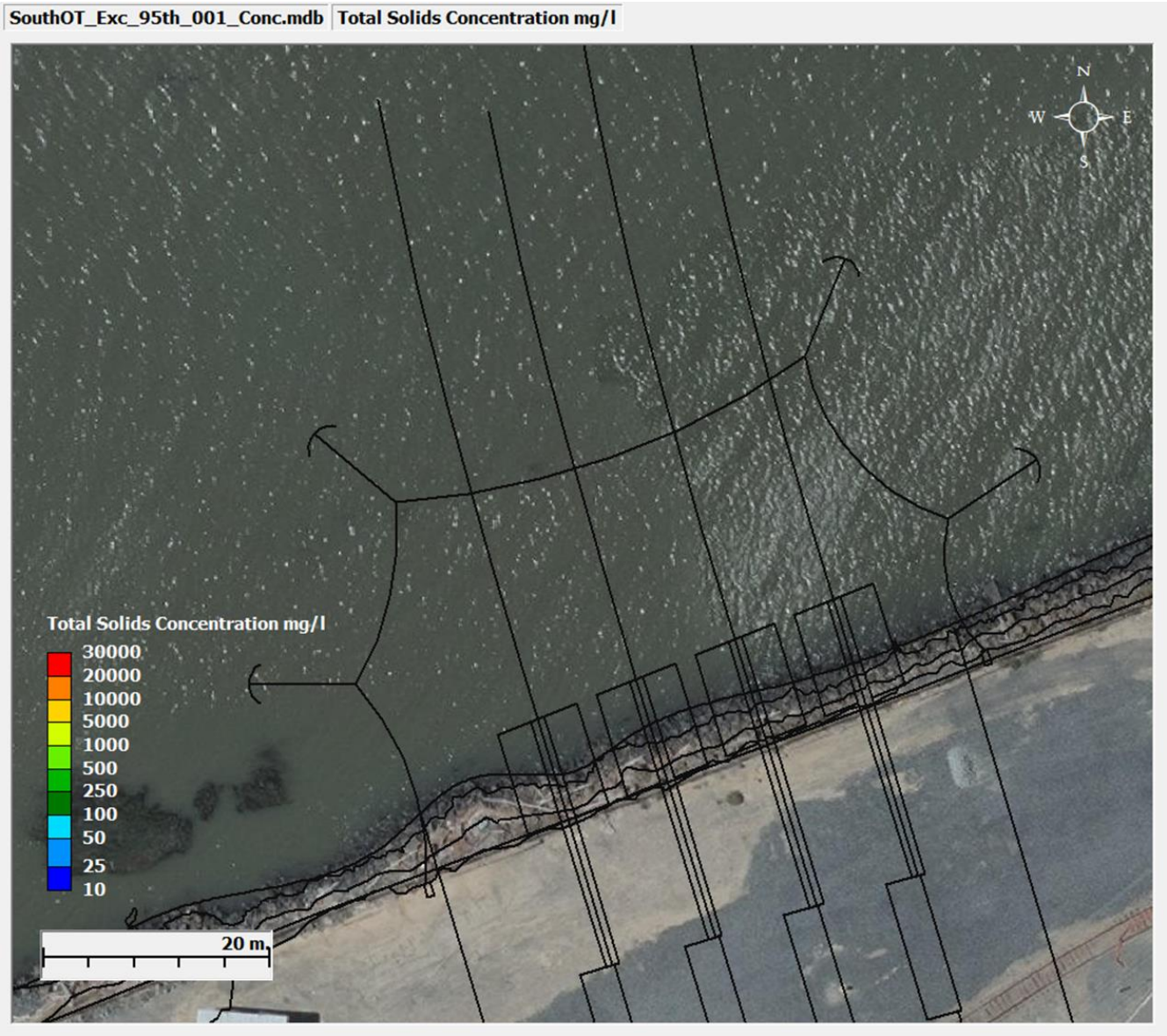

Note: TSS below 10 mg/L is not shown.

During backfilling scenarios (Scenarios 13 and 14), the TSS values were larger than those seen during the excavation operations, as the release amount was larger (Table 4-3). Figure 4-23 and Figure 4-25 show the maximum TSS concentrations that occur during Scenario 13 (minimum current) and Scenario 14 (maximum current), respectively. During Scenario 13 (minimum currents) and Scenario 14 (maximum currents), the maximum TSS concentrations within the plume are 27,469 mg/L and 31,411 mg/L, respectively. The maximum TSS concentrations are transient and occur very near the bed for a very short period of time during the initiation of each operation. That is depicted by the average TSS concentrations which are much lower than the maximum TSS as shown in Table 4-3. In addition, TSS concentrations decrease to less than 1

mg/L within 32.7 hours after the end of the releases as shown in Figure 4-24, Figure 4-26, and Table 4-3. Similar to the excavation operations, the TSS concentrations during backfilling are contained only in the area within the silt curtains with no impact on the surroundings, as they form a completely enclosed area.

FIGURE 4-23: SCENARIO 13 - MAXIMUM TSS CONCENTRATION DURING BACKG FILLING, MINIMUM CURRENT SPEED

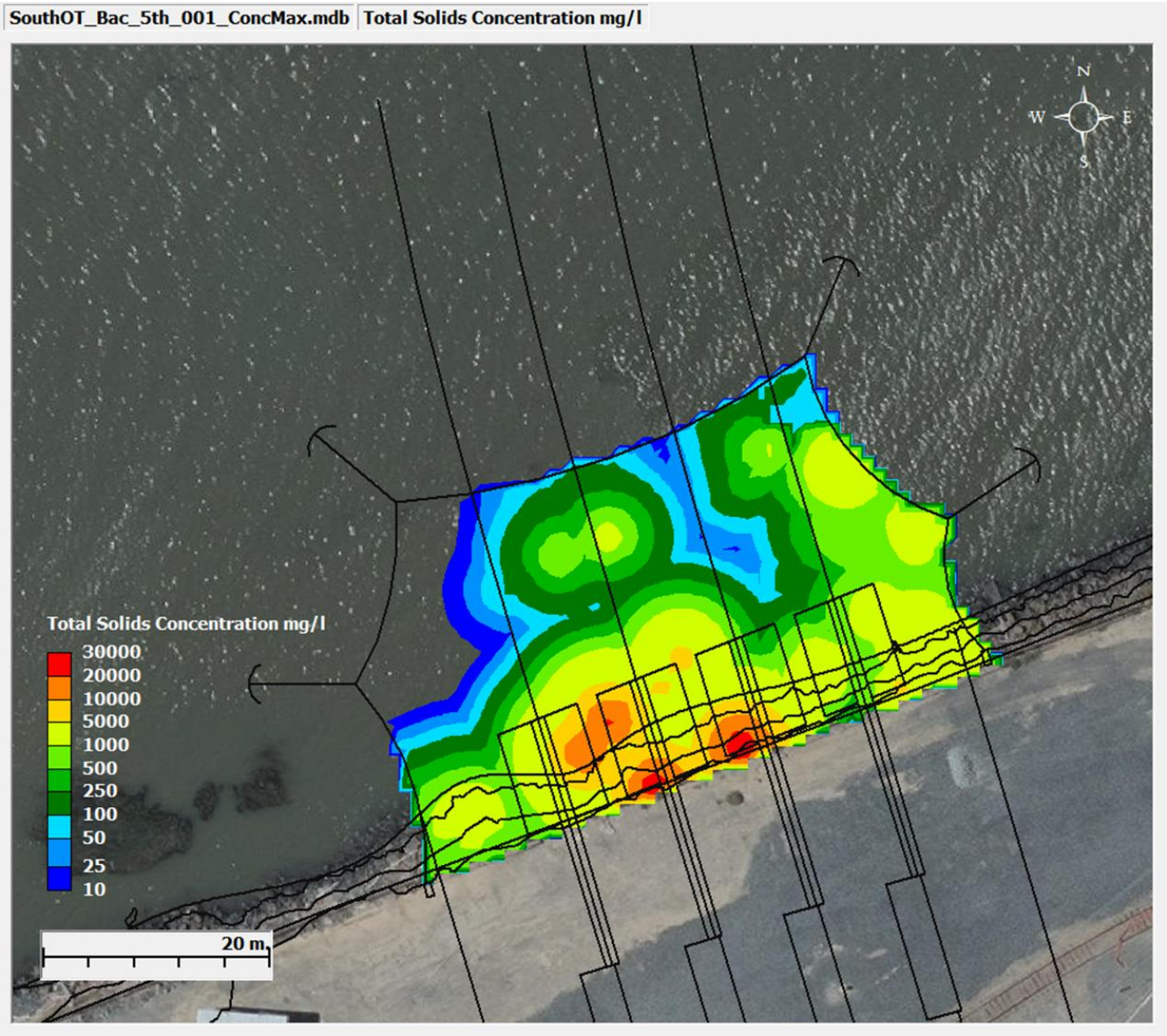

Note: TSS below 10 mg/L is not shown.

FIGURE 4-24: SCENARIO 13 – END OF SIMULATION TSS CONCENTRATION, BACKFILLING, MINIMUM CURRENT SPEED

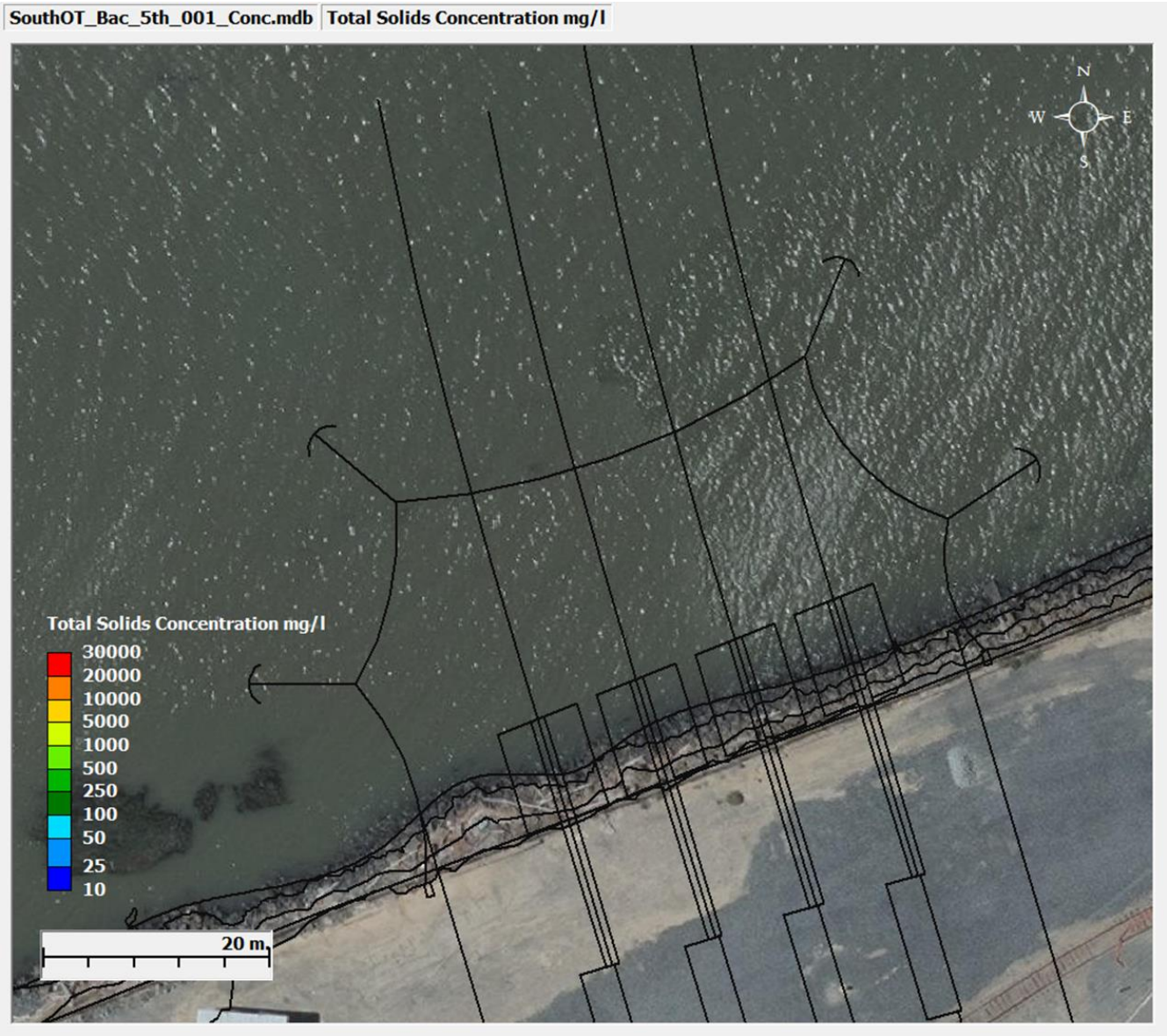

Note: TSS below 10 mg/L is not shown.

FIGURE 4-25: SCENARIO 14 - MAXIMUM TSS CONCENTRATION DURING BACKFILLING, MAXIMUM CURRENT SPEED

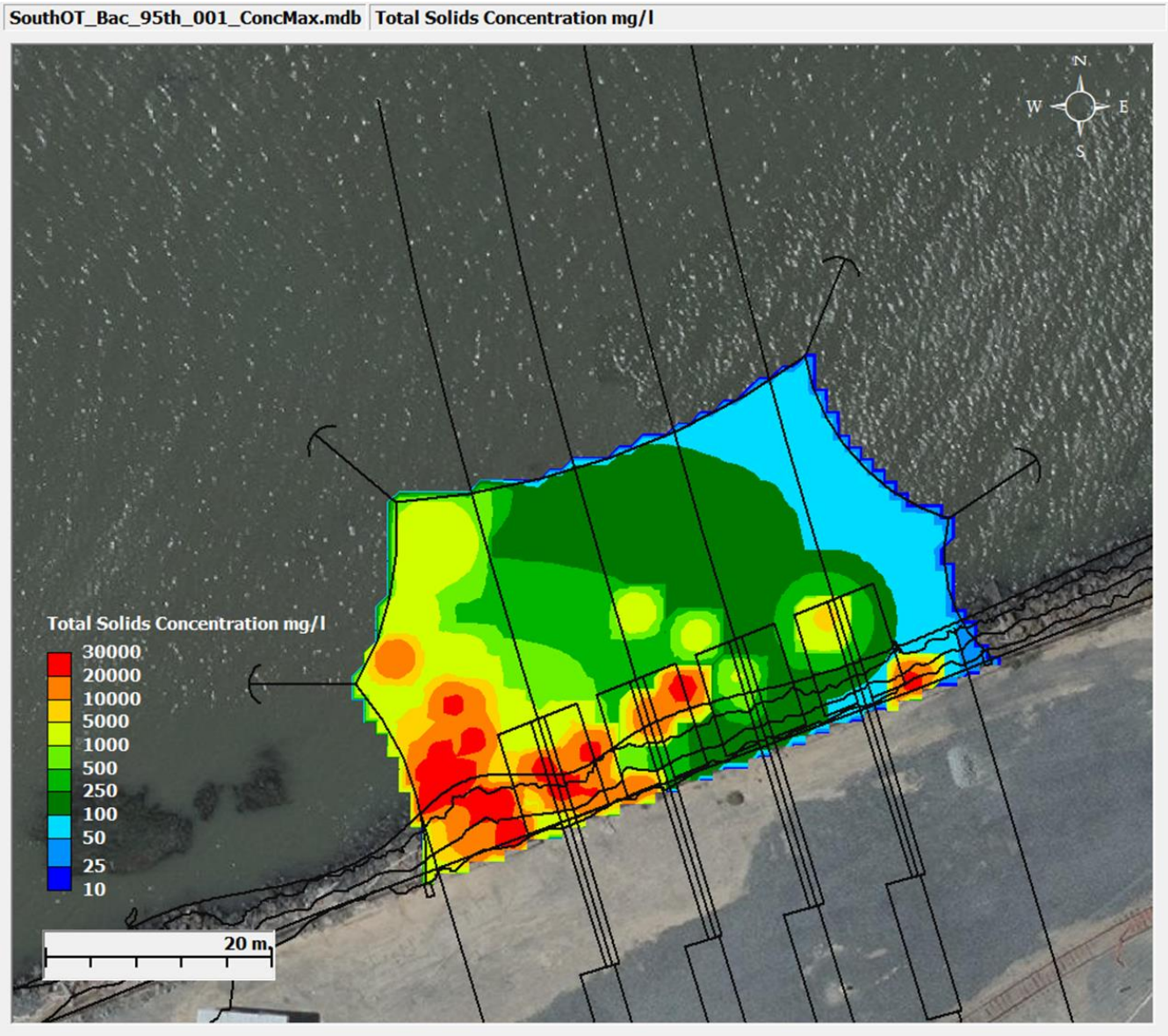

Note: TSS below 10 mg/L is not shown.

FIGURE 4-26: SCENARIO 14 – END OF SIMULATION TSS CONCENTRATION, BACKFILLING, MAXIMUM CURRENT SPEED

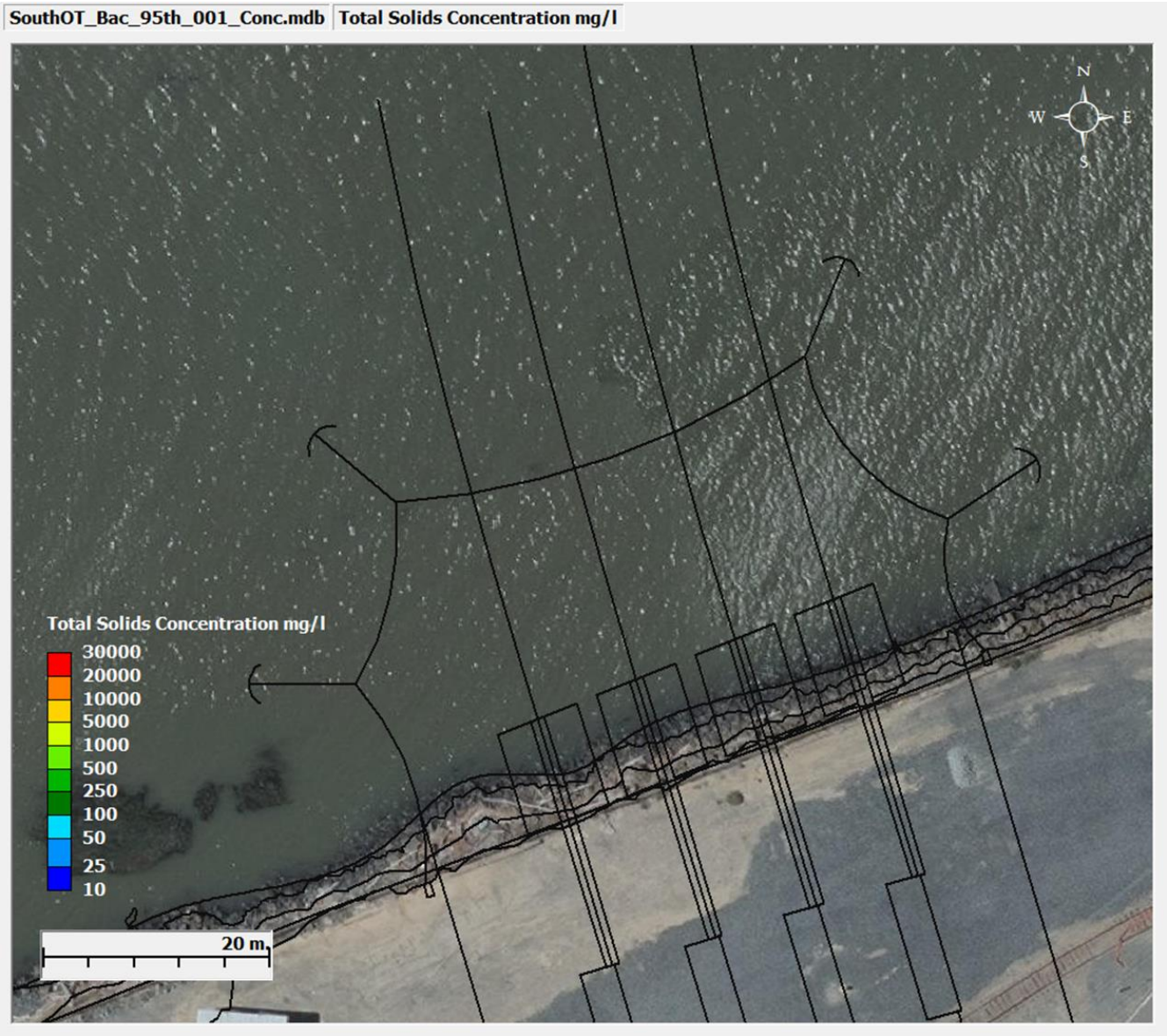

Note: TSS below 10 mg/L is not shown.

4.2 BOTTOM DEPOSITION

This section summarizes the depositional thickness for cable trenching and the R2 northern scenarios. As discussed earlier, since other scenarios contained sediments within an enclosed environment, either by silt curtains or sheet piles, there was no need to assess the settlement of dispersed sediments, as all sediment would settle within these confined areas.

4.2.1 ENTIRE CABLE ROUTE

For the 1-day deterministic simulation of particle deposition for both scenarios, the thickness of bed deposits was examined. Figure 4-27 and Figure 4-28 show the expected thickness of resuspended sediments on the bed to occur during Scenario 1 and Scenario 2, respectively. In each of these scenarios, the thickness of the resuspended sediments was less than 0.1 mm.

FIGURE 4-27: SCENARIO 1 – MAXIMUM DEPOSITIONAL THICKNESS DURING MINIMUM CURRENT SPEED

Note: Thickness below 0.001 mm is not shown.

FIGURE 4-28: SCENARIO 2 – MAXIMUM DEPOSITIONAL THICKNESS DURING MAXIMUM CURRENT SPEED

Note: Thickness below 0.001 mm is not shown.

4.2.2 NORTHERN R2 REGION LOCATION

For the 3-day deterministic simulation of particle deposition at the northern and southern sites, the thickness of bed deposits was examined only for the scenarios relevant to the R2 region (Scenarios 7 through 10). For the other scenarios, both in the northern and southern operations, the deposition would be limited within the defined barriers, and thus TSS was the main concern.

During the excavation of the R2 region, based on the 4 percent loss rate described in Section 3.3, the expected thickness during Scenarios 7 (minimum current) and 8 (maximum current) is around 85.3 mm. Figure 4-27 to Figure 4-30 show the expected thickness of resuspended sediments on the bed to occur during Scenario 7 and Scenario 8, respectively. Note that due to the assumption that the northern site location's sheet piling is impermeable, restricted flow occurred within the enclosed area as the southern side of the area was open to flow. This resulted in a varying depositional thickness spread outside of the sheet pile for each of the scenarios.

FIGURE 4-29: SCENARIO 7 - MAXIMUM DEPOSITIONAL THICKNESS, R2 EXCAVATION, MINIMUM CURRENT SPEED

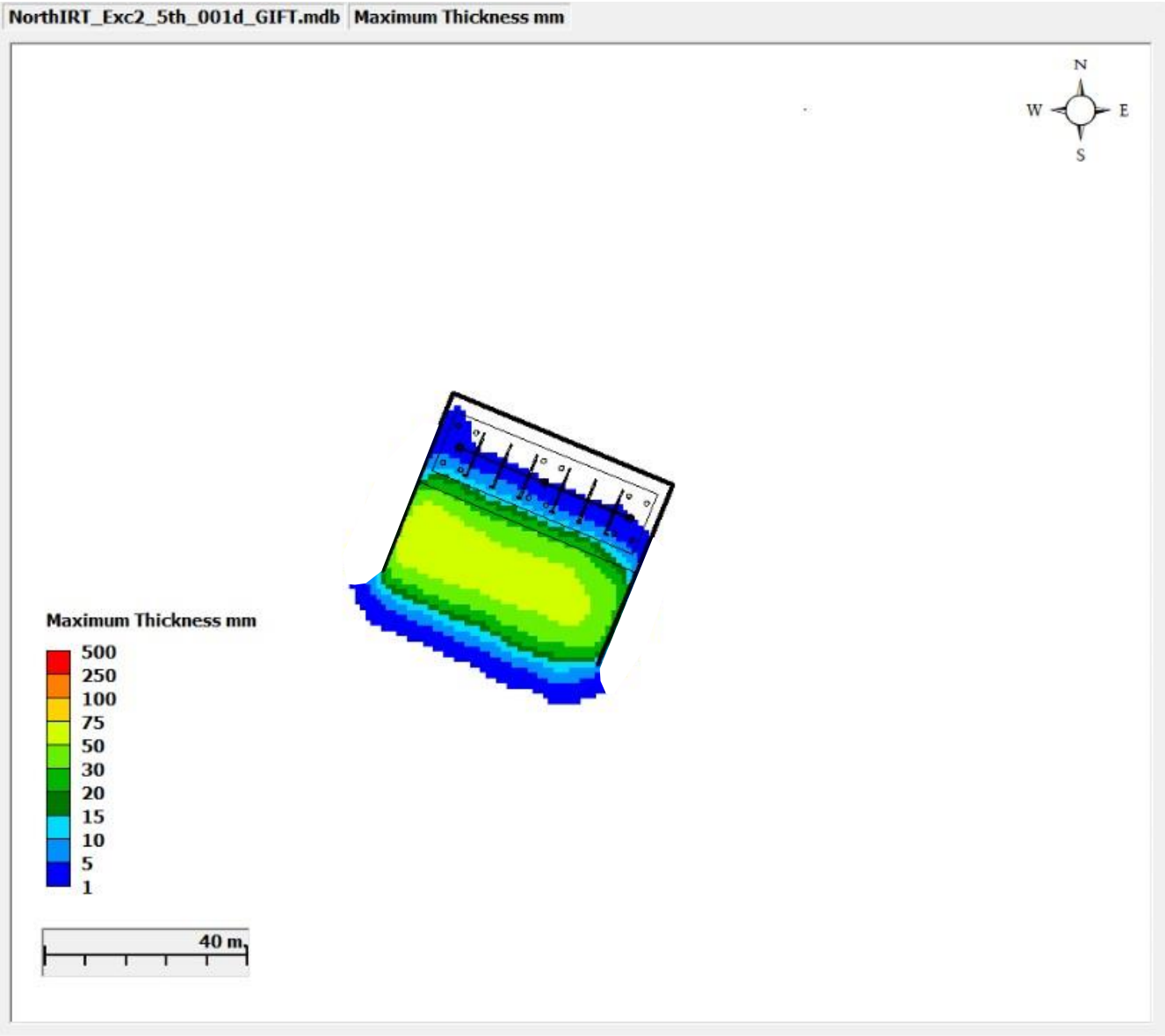

Note: Thickness below 1 mm is not shown.

FIGURE 4-30: SCENARIO 8 - MAXIMUM DEPOSITIONAL THICKNESS, R2 EXCAVATION, MAXIMUM CURRENT SPEED

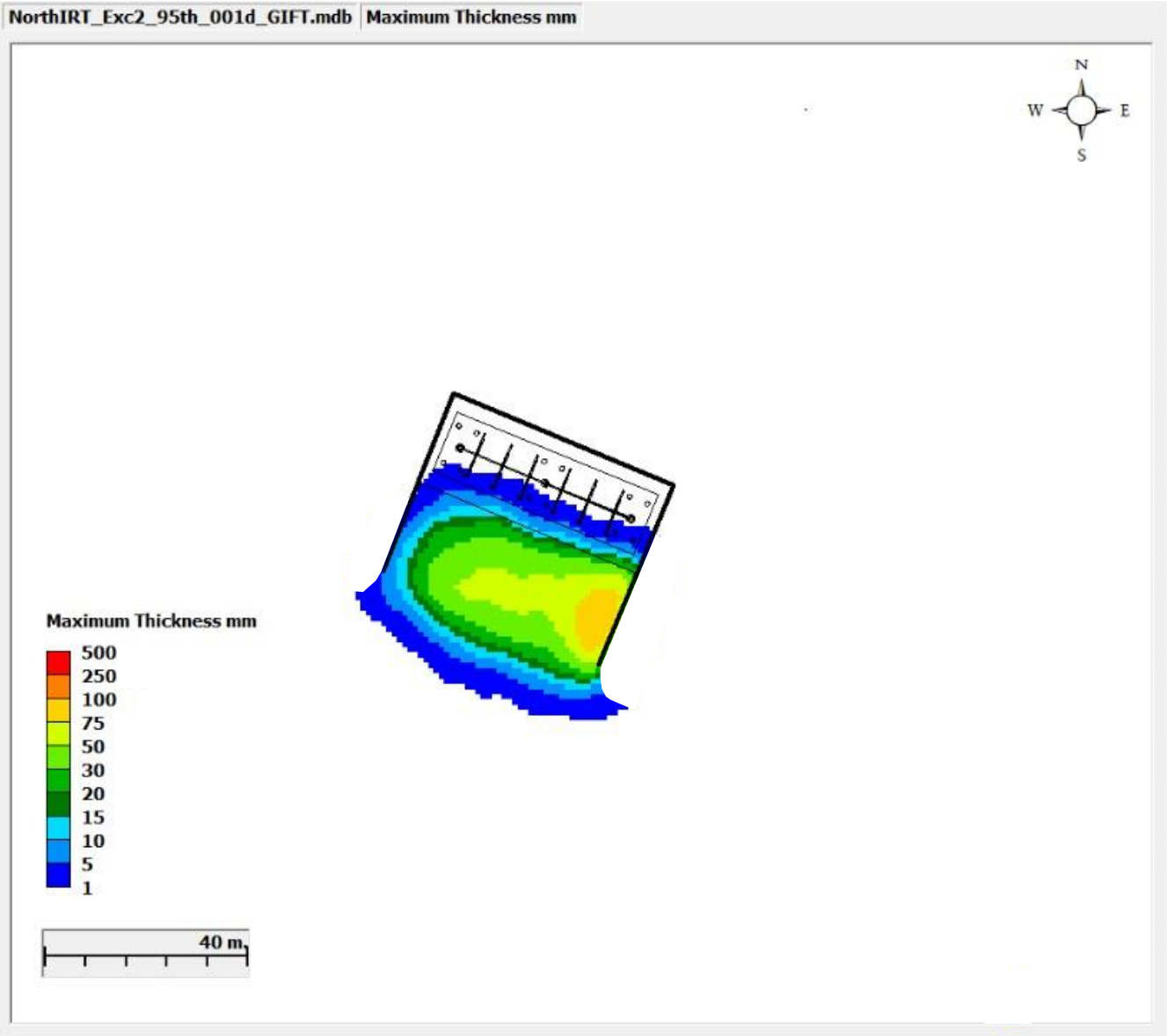

Note: Thickness below 1 mm is not shown.

The expected thickness during backfilling operations for the R2 area, Scenarios 9 (minimum currents), and Scenario 10 (maximum currents) is based on the excavation depth of 2.13 meters (7 feet) and was around 2133.6 mm. Note that the purpose of backfilling operations is to replace the sediment that was removed during excavation; thus, the depositional thickness for these scenarios is expected to be high -close to the depth of excavation- to replace the dredged sediment. Figure 4-31 and Figure 4-32 show the expected thickness of resuspended sediments on the bed to occur during Scenario 9 and Scenario 10, respectively. While the majority of the sediment deposition occurred within the sheet piles for both scenarios, there was a spread of the

thickness outside due to the currents. This was due to the restricted flow that occurred within the enclosed area as the southern side of the area was open to flow.

FIGURE 4-31: SCENARIO 9 - MAXIMUM DEPOSITIONAL THICKNESS, R2 BACKFILLING, MINIMUM CURRENT SPEED

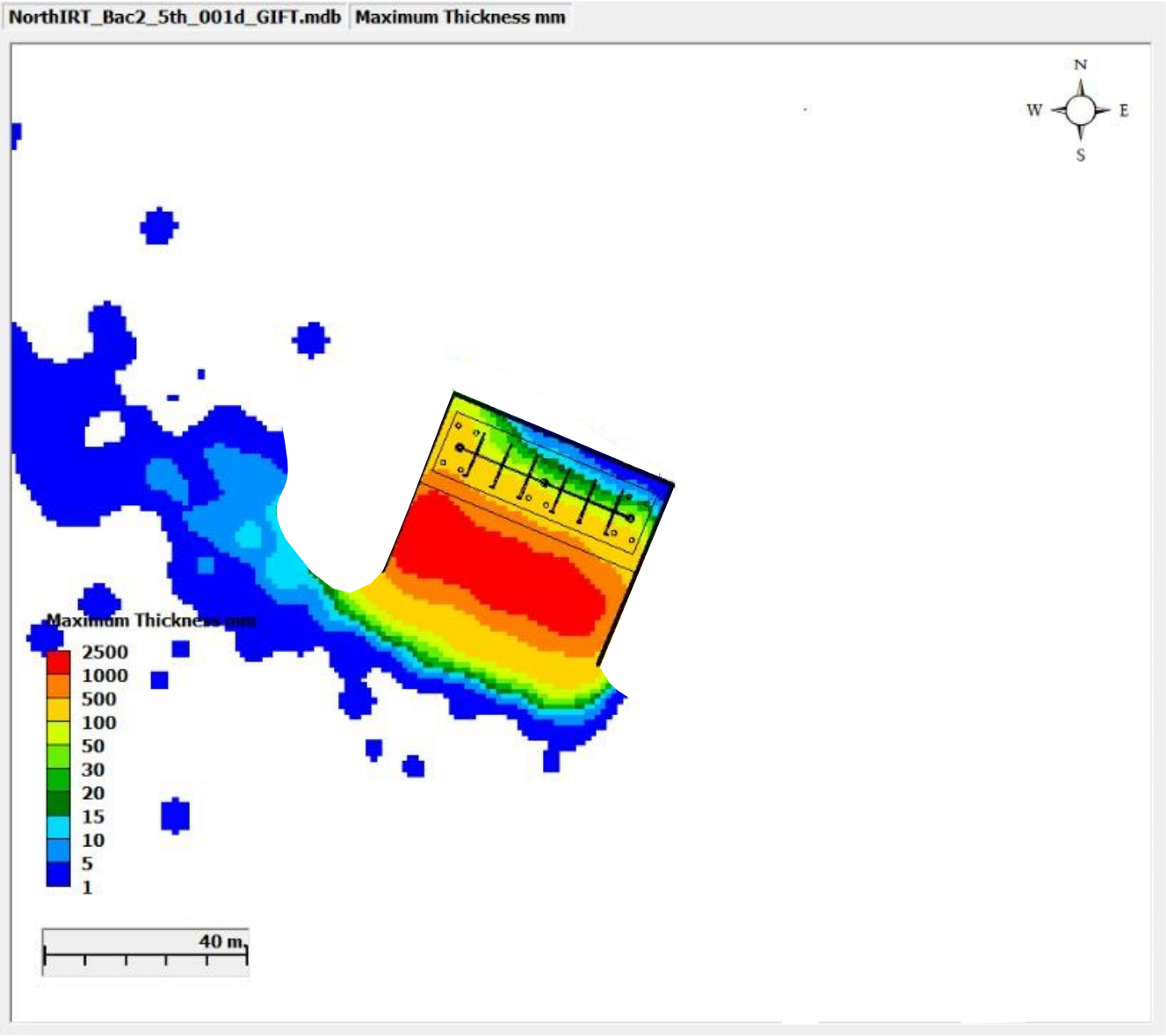

Note: Thickness below 1 mm is not shown.

FIGURE 4-32 SCENARIO 10 - MAXIMUM DEPOSITIONAL THICKNESS, R2 BACKFILLING, MAXIMUM CURRENT SPEED

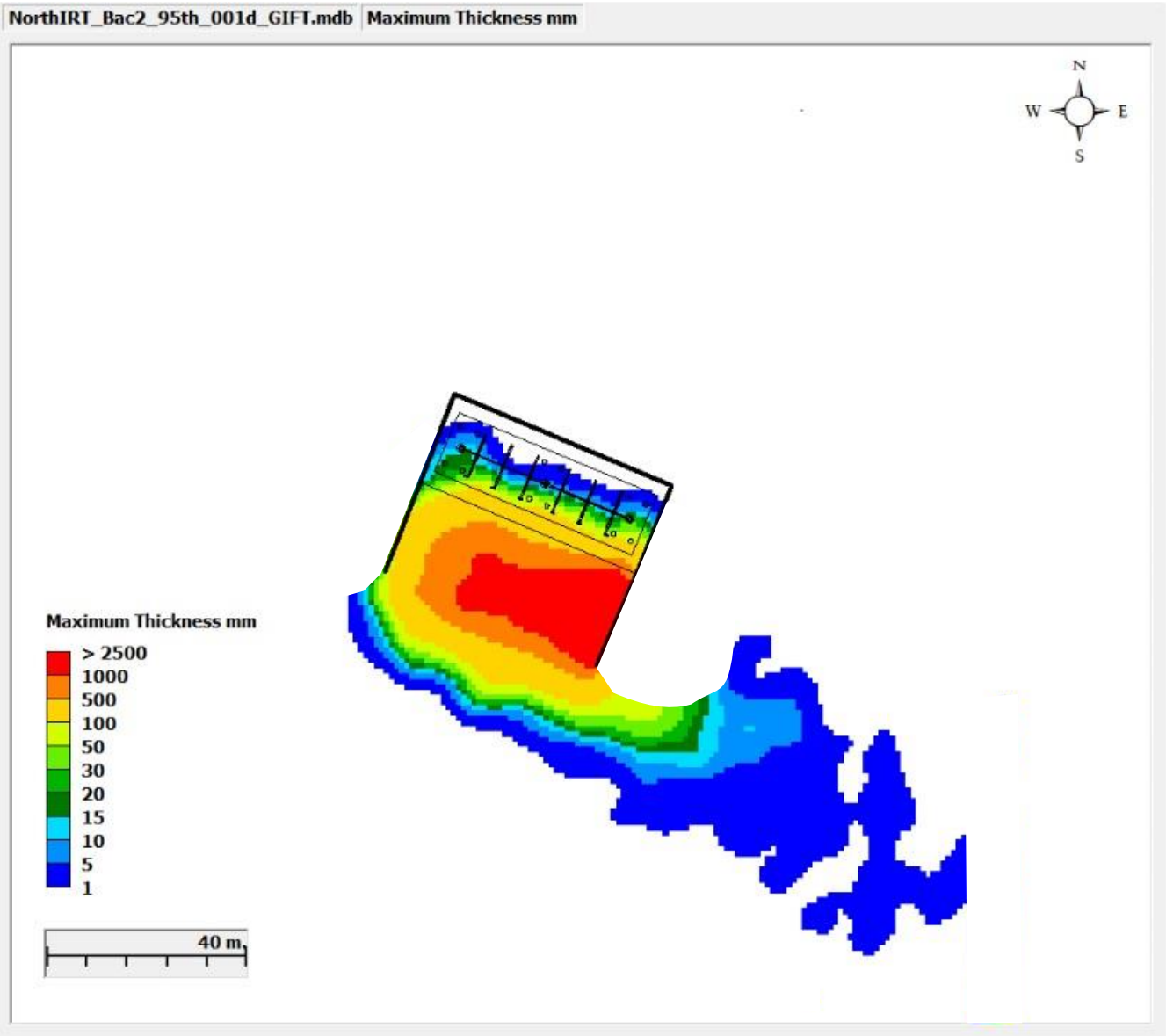

Note: Thickness below 1 mm is not shown.

5. CONCLUSIONS

Modeling was conducted to predict the TSS concentrations in the water column and bed accumulation (depositional thickness) from disturbed and resuspended sediments during excavation, backfilling, and trenching activities for cable installation. Fourteen scenarios were simulated to evaluate sediment under two extreme hydrodynamic conditions:

- Minimum ambient current conditions at the bed
- Maximum ambient current conditions at the bed

The modeled depositional thickness represents a conservative impact estimate, as it does not account for natural erosion and slumping processes that would reduce mound height over time.

Key findings from the modeling of TSS and depositional thickness are as follows:

For cable trenching:

- Maximum TSS levels remained at or below 20 mg/L in both Scenario 1(minimum currents) and Scenario 2 (maximum currents).
- The maximum depositional thickness remains below 0.1 mm in both minimum (Scenario 1) and maximum (Scenario 2) current scenarios.

For excavation and backfilling in the northern site location:

- In R1 scenarios, TSS peaked at 250,238 mg/L with an average of 2,909 mg/L during backfilling in maximum current conditions (Scenario 6).
- In R2 scenarios, TSS reached 261,919 mg/L with an average of 2,106 mg/L during backfilling in maximum currents (Scenario 10).

For excavation and backfilling modeling in the southern site location:

- TSS levels peaked at 31,411 mg/L, with an average of 4,299 mg/L during backfilling under maximum current conditions (Scenario 14).

Across all scenarios, TSS concentrations peaked near the bed during the initial stages of each operation, and returned to zero or below 1 mg/L within 28 to 33 hours post-operation. This rapid decline demonstrates the effectiveness of LS Power's sediment management strategy, which successfully minimizes TSS levels around the project footprint in Suisun Bay, ensuring minimal impact on surrounding water quality.

Depositional thickness is not a concern in most scenarios, as the majority of sediment remains effectively contained within the sediment control measures. However, in the R2 scenarios (i.e., excavation and backfilling at the in-river transition structure), some sediment has dispersed through the southern open boundary, resulting in a minor deposition outside the designated semi-enclosed sheet pile containment area.

6. REFERENCES

Ellis, D., and C. Heim. 1985. Submersible surveys of benthos near a turbidity cloud. Marine Pollution Bulletin, 16(5), 197-203.

eTrac. September 2023. Provided by LS Power Grid California, LLC. LS POWER BATHYMETRY DELIVERABLES

Fichera, M. J., and V. S. Kolluru. 2007. GEMSS-GIFT: A comprehensive sediment discharge and transport modeling system. SETAC North America 28th Annual Meeting, 11-15 November 2007.

Francingues, Norman R. and M. R. Palmero. 2005. "Silt curtains as a dredging project management practice." ERDC TN-DOER-E21, September 2005, 18 pp.

Fregoso, T. A., B. E. Jaffe, and A. C. Foxgrover, 20210708, Digital elevation model (DEM) of central San Francisco Bay, California, created using bathymetry data collected between 2009 and 2020 (NAVD88): data release DOI:10.5066/P9TJTS8M, U.S. Geological Survey, Pacific Coastal and Marine Science Center, Santa Cruz, CA.

Kolluru, V.S. and M.L. Spaulding, 1993. SEASHELL - Software for the Simulation of Fate and Transport of pollutants in Coastal Waters. In Proceedings of the 3rd International Conference of Estuarine and Coastal Modeling, Oakbrook, September 8-10, Illinois.

Kolluru, V. S., E. M. Buchak and J. E. Edinger, 1998. Integrated Model to Simulate the Transport and Fate of Mine Tailings in Deep Waters to be published in the Proceedings of the Tailings and Mine Waste '98 Conference, Fort Collins, Colorado, USA, January 26-29.

LS Power Grid California, LLC (LS Power). 2022. Provided by LS Power Grid California, LLC. Collinsville 500/230 kV Substation Project; Section 10: T-Line Design and Eng; Question T-2; Attachment T-2 Submarine Geotechnical Report

LS Power. 2024. Provided by LS Power Grid California, LLC. Coffer Dam Plan. 24-9-30_Riser Cofferdam.pdf

LS Power. 2024. Provided by LS Power Grid California, LLC. South Shore Approach Open Trenching Plan. 24-9-30_Southern Shore Approach.pdf

Prakash, S. and. V. S. Kolluru, 2014. Implementation of Integrated Modeling Approach to Impact Assessment Applications for LNG Operations Using 3-D Comprehensive Modeling Framework. International Environmental Modelling and Software Society (iEMSs), 7th Intl. Congress on Env. Modelling and Software, San Diego, CA, USA, Daniel P. Ames, Nigel W.T. Quinn and Andrea E. Rizzoli (Eds.), http://www.iemss.org/society/index.php/iemss-2014-proceedings.

Steel Piling Group, 2018. Retaining Walls. https://www.steelpilinggroup.org/steel-piling-overview/common-uses-for-steel-piling-products/retaining-walls/

United States Army Engineer Research and Development Center (ERDC): Dredging Operations and Environmental Research (DOER). 2000. Demonstration of the SSFATE Modeling System. ERDC TN-DOER-E12. July 2000.

APPENDIX A GEMSS MODEL SUITE

The Generalized Environmental Modelling System for Surfacewaters (GEMSS) is an integrated system of three-dimensional hydrodynamic and transport modules embedded in a geographic information and environmental data system. GEMSS is in the public domain and has been used for hydrodynamic and water quality studies in the United States and worldwide. ERM staff contribute to the source code and have completed many applications with the model. Organizations in Korea (Ewha Womans University, National Institute of Environmental Research), Canada (Golder Associates Ltd., Stantec Inc., Matrix Solutions Inc.), Norway (Norwegian Institute for Water Research and Akvaplan-niva AS), Poland (Maritime Institute in Gdańsk) and Sweden (Royal Institute of Technology), among others, routinely use GEMSS. GEMSS has been identified as an appropriate 3-D model for hydrodynamics, water quality, and eutrophication studies of various surface waterbodies for the assessment of total maximum daily loads of industrial discharges (HGL and Aqua Terra. 1999).

GEMSS was developed in the mid-1980s as a hydrodynamic platform for the transport and fate modeling of many types of constituents introduced into water bodies. The hydrodynamic platform ("kernel") provides three-dimensional flow fields from which the distribution of various constituents can be computed. The constituent transport and fate computations are grouped into modules. GEMSS modules include those used for thermal analysis, water quality, sediment transport, particle tracking, oil and chemical spills, entrainment, and toxics.

The theoretical basis of the hydrodynamic kernel of GEMSS is the three-dimensional Generalized, Longitudinal-Lateral-Vertical Hydrodynamic and Transport (GLLVHT) model, which was first presented in Edinger and Buchak (1980) and subsequently in Edinger and Buchak (1985). The GLLVHT computation has been peer-reviewed and published (Edinger and Buchak, 1995; Edinger, et al., 1994 and 1997; Edinger and Kolluru 1999). The kernel is an extension of the well-known longitudinal-vertical transport model written by Buchak and Edinger (1984) that forms the hydrodynamic and transport basis of the U.S. Army Corps of Engineers water quality model CE-QUAL-W2 (U. S. Army Engineer Waterways Experiment Station 1986). Improvements to the transport scheme, construction of the constituent modules, incorporation of supporting software tools, geographic information system interoperability, visualization tools, graphical user interface, and post-processors have been developed by Kolluru et al. (1998, 1999, 2003), Kolluru and Fichera (2003), and Prakash and Kolluru (2006).

GEMSS development continues as additional applications are completed. A second hydrodynamic kernel, the Princeton Ocean Model, has been added as an alternative to GLLVHT for deep ocean systems. In addition, new constituent modules have been developed and tested, including source water protection (Kolluru and Prakash 2012), watershed nutrient load allocation (Kolluru et al. 2009), chlorine and chlorine byproducts fate and transport (Kolluru et al. 2012); mine pit lake analysis (Vandenberg et al. 2011; Prakash et al. 2012); debris fouling at cooling water intakes (Prakash et al. 2012); coliform fate and transport (Tryland, et al., 2012); thermal avoidance calculations (Buchak et al. 2012); impact assessment (Fichera et al. 2013); and contaminated sediment transport (Kolluru et al. 2006.)

GEMSS applications to estuarine and coastal waterbodies have been validated by comparisons to extensive, field-collected datasets. These include currents, temperature, and chlorine and chlorine byproducts offshore Qatar (Kolluru et al. 2005; Adenekan et al. 2009; Febbo et al. 2012; Kolluru et al. 2003; Kolluru et al., 2012); currents, temperatures, and nutrient water quality in Puget Sound (Albertson et al. 2009); nutrients in coastal Delaware (Kolluru and Fichera 2003), and the Vistula River in Poland (Kruk et al. 2011); currents, temperature and salinity and complex hydrodynamic circulation in the Baltic Sea (Dargahi et. al., 2014); currents and temperatures in the New York Harbor area (Edinger et al. 1997); larval populations in coastal Alaska (Edinger et al.1994); and mine tailings ponds (Prakash et al. 2011).

For inland waterbodies, GEMSS has been validated for temperatures in cooling lakes (Buchak et al. 2012; Long et al. 2011); temperatures and nutrients in the Han River and Lake Paldang, Korea (Kim and Park, 2012a and 2012b; Na and Park, 2005 and 2006, respectively); and temperature and fecal coliforms in Norwegian water supply reservoirs (Tryland, et al., 2012). Many other inland, estuarine, and coastal waterbody validations have been completed and published as client reports.

Customization of the suite of hydrodynamic, transport, and water quality models to reflect the needs of each application is easily done because of the modular design of GEMSS. A list of modules available within GEMSS is shown in Figure A-1 and Figure A-2.

FIGURE A-1 GEMSS MODULES: FIRST SET

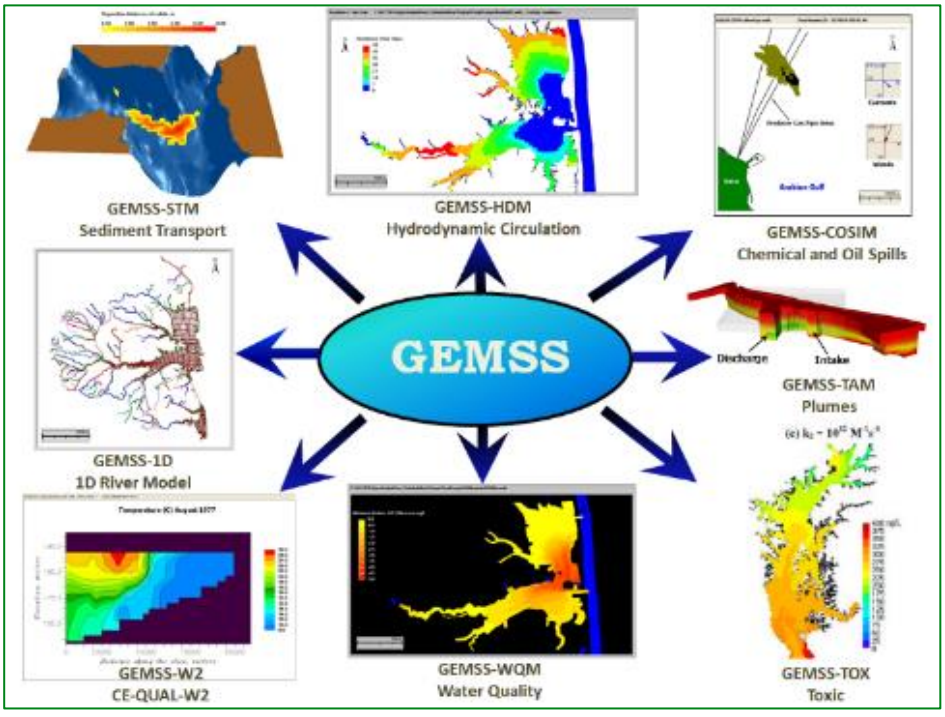

Source: ERM

FIGURE A-2 GEMSS GEMSS MODULES: SECOND SET

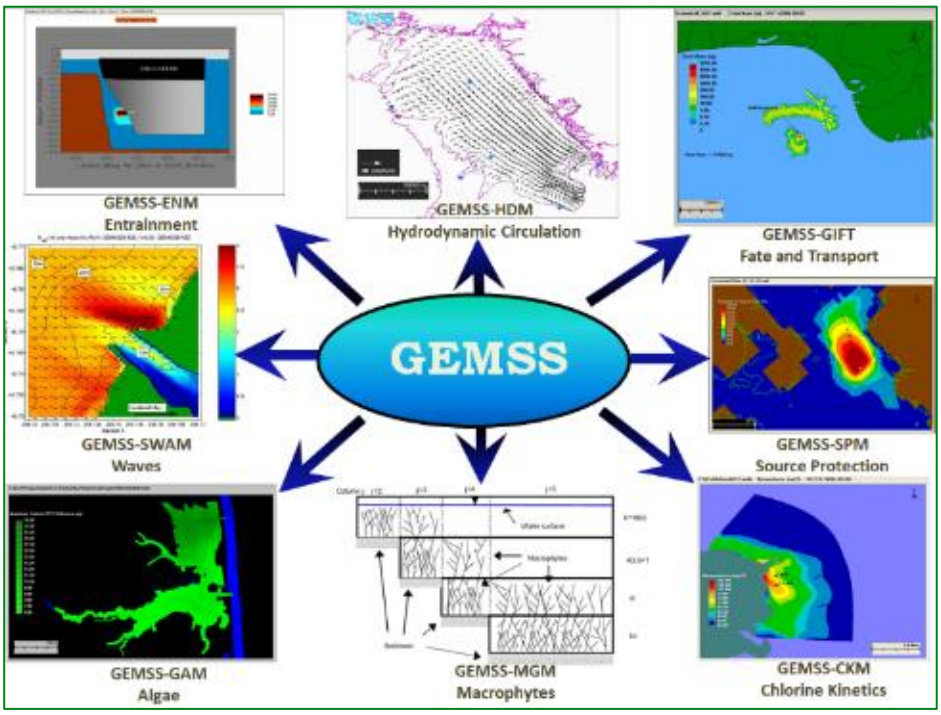

Source: ERM

REFERENCES

Adenekan, A.E., V.S. Kolluru, and J.P. Smith. 2009. Transport and Fate of Chlorination By-Products Associated with Cooling Water Discharges. Proceedings of the 1st Annual Gas Processing Symposium pp. 1-13.

Albertson, S., A. Ahmed, M. Roberts, G. Pelletier, and V. Kolluru. 2009. "Model-Derived Hydrodynamics of Inlets in South Puget Sound." Proceedings of the Eleventh Annual Conference on Estuarine and Coastal Modelling. American Society of Civil Engineers. pp. 128-136, 2009.

Buchak, E. M. and J. E. Edinger. 1984. Generalized, Longitudinal-Vertical Hydrodynamics and Transport: Development, Programming and Applications. Prepared for U.S. Army Corps of Engineers Waterways Experiment Station, Vicksburg, Miss. Contract No. DACW39-84-M-1636. Prepared by J. E. Edinger Associates, Wayne, PA. Document No. 84-18-R. June.

Buchak, E.M., S. Prakash, D. Mathur, S.E. Sklenar. 2012. "Comparison of Modelled and Observed Avoidance in a Thermally Loaded Reservoir". Symposium on Innovations in Thermal Research and Ecological Effects from Thermal Discharges at the 142nd Annual Meeting of the American Fisheries Society, Minneapolis – St. Paul, MN. 19 – 23 August.

Dargahi, B. and V. Cvetkovic. 2014. Hydrodynamic and Transport Characterization of the Baltic Sea 2000-2009. TRITA-LWR.REPORT 2014:03, ISSN 1650-8610, ISBN: 978-91-7595-215-4. KTH Royal Institute of Technology, Stockholm, Sweden. July.

Edinger, J. E. and E. M. Buchak. 1980. Numerical Hydrodynamics of Estuaries in Estuarine and Wetland Processes with Emphasis on Modelling, (P. Hamilton and K. B. Macdonald, eds.). Plenum Press, New York, New York, pp. 115 146.

Edinger, J. E. and E. M. Buchak. 1985. Numerical Waterbody Dynamics and Small Computers. Proceedings of ASCE 1985 Hydraulic Division Specialty Conference on Hydraulics and Hydrology in the Small Computer Age. American Society of Civil Engineers, Lake Buena Vista, FL. Aug. 13-16.

Edinger, J. E. and E. M. Buchak. 1995. Numerical Intermediate and Far Field Dilution Modelling. Journal Water, Air and Soil Pollution 83: 147-160, 1995. Kluwer Academic Publishers, The Netherlands.

Edinger, J. E., E. M. Buchak, and M. D. McGurk. 1994. Analyzing Larval Distributions Using Hydrodynamic and Transport Modelling. Estuarine and Coastal Modelling III. American Society of Civil Engineers, New York.

Edinger J.E., J. Wu and E.M. Buchak. 1997. Hydrodynamic and Hydrothermal Analyses of the Once-through Cooling Water System at Hudson Generating Station. Prepared for Public Service Electric and Gas (PSE&G). Prepared by J. E. Edinger Associates, Inc., June 1997.

Edinger, J. E., V. S. Kolluru. 1999. "Implementation of Vertical Acceleration and Dispersion Terms in an Otherwise Hydrostatically Approximated Three-Dimensional Model." In Spaulding,

M.L, H. L. Butler (eds.). Proceedings of the 6th International Conference on Estuarine and Coastal Modelling. pp. 1019 – 1034.

Febbo E., V. Kolluru, S. Prakash, A. Adenekan. 2012. "Numerical Modelling of Thermal Plume and Residual Chlorine Fate in Coastal Waters of the Arabian Gulf". SPE-156813-PP. Presented at the SPE/APPEA International Conference on Health, Safety, and Environment in Oil and Gas Exploration and Production. Perth, Western Australia. 11–13 September 2012.

Fichera, M.J., V.S. Kolluru, C. Buahin, C. Daviau, and C.A. Reid. 2013. "Comprehensive Modeling Approach for EIA Studies in the Oil and Gas Industry." IAIA 2013.

HGL and Aqua Terra. 1999. Selection of Water Quality Components for Eutrophication-Related Total Maximum Daily Load Assessments. Task 4: Documentation of Review and Evaluation of Eutrophication Models and Components EPA Contract Number 68-C6-0020 Work Assignment No. 2-04. Prepared by HydroGeoLogic, Inc. Herndon, VA 20170, and AQUA TERRA Consultants, Mountain View, CA. June.

Kim, E.J. and S.S. Park. 2012a. "Multidimensional Dynamic Water Quality Modeling of Organic Matter and Trophic State in the Han River System." J. Kor.Soc.Environ.Eng.. 35(3), 141-164, 2013.

Kim, E.J. and S.S. Park. 2012b. "Multidimensional Hydrodynamic and Water Temperature Modeling of Han River System." Journal of Korean Society on Water Environment, Vol. 28, No 6, pp. 866-881 (2012).

Kolluru, V.S. and M. Fichera, 2003. "Development and Application of Combined 1-D and 3-D Modelling System for TMDL Studies." Proceedings of the Eighth International Conference on Estuarine and Coastal Modelling. American Society of Civil Engineers. pp. 108-127, 2003.

Kolluru, V.S. and S. Prakash. 2012. "Source Water Protection: Protecting our drinking waters". India Water Week 2012. April 10-14. New Delhi, India.

Kolluru, V. S., E. M. Buchak and J. E. Edinger. 1998. "Integrated Model to Simulate the Transport and Fate of Mine Tailings in Deep Waters," in the Proceedings of the Tailings and Mine Waste '98 Conference, Fort Collins, Colorado, USA, January 26-29.

Kolluru, V. S., E. M. Buchak, J. Wu. 1999. "Use of Membrane Boundaries to Simulate Fixed and Floating Structures in GLLVHT." In Spaulding, M.L, H.L. Butler (eds.). Proceedings of the 6th International Conference on Estuarine and Coastal Modelling. pp. 485 – 500.

Kolluru, V. S., J. E. Edinger, E. M. Buchak and P. Brinkmann. 2003. "Hydrodynamic Modelling of Coastal LNG Cooling Water Discharge." Journal of Energy Engineering. Vol. 129, No. 1, April 1, 2003. pp 16 – 31.

Kolluru, V.S., E. Buchak, J.E. Edinger, and P.E. Brinkmann. 2005. "Three-Dimensional Thermal Modelling of the RasGas Cooling Water Outfall." 2005.

Kolluru, V.S., M.J. Fichera, S. Prakash. 2006. Multipurpose modelling tool for aquatic and sediment contaminant fate and effect assessments. SETAC North America 27th Annual Meeting. Montreal, Canada. November 2006.

Kolluru, V.S., S. R. Chitikela and M. J. Fichera. 2009. "Watershed Water Quality Attainment Using TMDL – A Delaware USA Review." International Conference "Water, Environment, Energy and Society" (WEES-2009), New Delhi. 12-16 January.

Kolluru, V.S., S. Prakash and E. Febbo. 2012. "Modelling the Fate and Transport of Residual Chlorine and Chlorine By-Products (CBP) in Coastal Waters of the Arabian Gulf". The Sixth International Conference on Environmental Science and Technology 2012. June 25-29. Houston, Texas, USA.

Kruk, M., M. Kempa, T. Tjomsland, D. Durand. 2011. "Vistula Water Quality Modeling." pp. 165-180.

Long, K., R.M. Matty, D. Mathur, D. R. Royer, T. Sullivan, S. Prakash and E. Buchak. 2011. "Assessment of effects of the interaction of pumped storage station operations and thermal plume on the migration of American Shad (Alosa Sapisissuma) in the Lower Susquehanna River." EPRI 2011. Third Thermal Ecology and Regulation Workshop. October 11-12, 2011. Maple Grove, Minnesota.

Na, E.H. and Park, S.S. 2005. "A Hydrodynamic Modeling Study to Determine the Optimum Water Intake Location in Lake Paldang, Korea." Journal of the American Water Resources Association (JAWRA) 41(6), 1315-1332.

Na, E.H. and Park, S.S. 2006. "A Hydrodynamic and Water Quality Modeling Study of Spatial and Temporal Patterns of Phytoplankton Growth in a Stratified Lake with Buoyant Incoming Flow." Ecological Modeling 199 (2006) 298-314.

Prakash, S. and V.S. Kolluru. 2006. "Implementation of higher order transport schemes with explicit and implicit formulations in a 3-D hydrodynamic and transport model." Published in the 7th International Conference on Hydroscience and Engineering (ICHE 2006), Sep 10–Sep 13, Philadelphia, USA

Prakash, S., J.A. Vandenberg and E. Buchak. 2011. "The Oil Sands Pit Lake Model - Sediment Diagenesis Module." MODSIM 2011. Modelling and Simulation Society of Australia and New Zealand, December 12-16, 2011. Perth, Australia.

Prakash, S., J.A. Vandenberg and E. Buchak. 2012. "CEMA Oil Sands Pit Lake Model". CONRAD 2012 Water Conference. April 20-22. Edmonton, Alberta.

Prakash, S., V. S. Kolluru, and P. Tutton. 2012. "Semi-Lagrangian Approach to Studying Grassing Issue on a Nuclear Power Plant Cooling Water Intake." Proceedings of the 10th Intl. Conf. on Hydroscience & Engineering, Nov. 4-7, 2012, Orlando, Florida, U.S.A.

Tryland, I., Tjomsland, T., Berge, D., Kempa, M., and Kolluru, V. S. 2012. "Modeling the Transport of Fecal Microorganisms in Norwegian Drinking Water Sources (Lakes)." The Sixth International Conference on Environmental Science and Technology, Houston, Texas, USA. June.

U. S. Army Engineer Waterways Experiment Station, Environmental Laboratory, Hydraulics Laboratory. 1986. CE-QUAL-W2: A Numerical Two-Dimensional, Laterally Averaged Model of Hydrodynamics and Water Quality; User's Manual. Instruction Report E-86-5. Prepared

for Department of the Army, U.S. Army Corps of Engineers, Washington, DC. Final Report. August.

Vandenberg, J.A., S. Prakash, N. Lauzon and K. Salzsauler. 2011. "Use of water quality models for design and evaluation of pit lakes." Australian Center for Geomechanics. Mine Pit Lakes: Closure and Management. Page 63-81.

Water Environment Federation. 2001. Water Quality Models: A Survey and Assessment. Order No.: D13209WW (Electronic Media).

ERM HAS OVER 160 OFFICES ACROSS THE FOLLOWING COUNTRIES AND TERRITORIES WORLDWIDE

Argentina
Australia
Belgium
Brazil
Canada
China
Colombia
France
Germany
Ghana
Guyana
Hong Kong
India
Indonesia
Ireland
Italy
Japan
Kazakhstan
Kenya
Malaysia
Mexico
Mozambique
The Netherlands
New Zealand
Peru
Poland
Portugal
Romania
Senegal
Singapore
South Africa
South Korea
Spain
Switzerland
Taiwan
Tanzania
Thailand
UAE
UK
US
Vietnam

Environmental Resources Management (ERM)

1340 Treat Boulevard
Suite 550
Walnut Creek, CA 94597
T +1 650 704 9378

www.erm.com